International Journal of Bifurcation and Chaos, Vol. 17, No. 7 (2007) 2215–2255


# OPTIMAL PATH AND MINIMAL SPANNING TREES IN RANDOM WEIGHTED NETWORKS

LIDIA A. BRAUNSTEIN[*,†], ZHENHUA WU[†], YIPING CHEN[†], SERGEY V. BULDYREV[†,‡], TOMER KALISKY[§], SAMEET SREENIVASAN[†], REUVEN COHEN[§,¶], EDUARDO LÓPEZ[†,**], SHLOMO HAVLIN[†,§] and H. EUGENE STANLEY[†]

[*]*Departamento de Física, Facultad de Ciencias Exactas y Naturales, Universidad Nacional de Mar del Plata, Funes 3350, 7600 Mar del Plata, Argentina*

[†]*Center for Polymer Studies, Boston University, Boston, MA 02215, USA*

[‡]*Department of Physics Yeshiva University, 500 West 185th Street Room 1112, NY 10033, USA*

[§]*Minerva Center and Department of Physics, Bar-Ilan University, 52900 Ramat-Gan, Israel*

[¶]*Department of Electrical and Computer Engineering, Boston University, Boston, MA 02215, USA*

[**]*Theoretical Division, Los Alamos National Laboratory, Mail Stop B258, Los Alamos, NM 87545, USA*

[*]*lbrauns@mdp.edu.ar*

Received May 20, 2006; Revised September 22, 2006

We review results on the scaling of the optimal path length $\ell_{\rm opt}$ in random networks with weighted links or nodes. We refer to such networks as "weighted" or "disordered" networks. The optimal path is the path with minimum sum of the weights. In strong disorder, where the maximal weight along the path dominates the sum, we find that $\ell_{\rm opt}$ increases dramatically compared to the known small-world result for the minimum distance $\ell_{\rm min} \sim \log N$, where $N$ is the number of nodes. For Erdős–Rényi (ER) networks $\ell_{\rm opt} \sim N^{1/3}$, while for scale free (SF) networks, with degree distribution $P(k) \sim k^{-\lambda}$, we find that $\ell_{\rm opt}$ scales as $N^{(\lambda-3)/(\lambda-1)}$ for $3 < \lambda < 4$ and as $N^{1/3}$ for $\lambda \geq 4$. Thus, for these networks, the small-world nature is destroyed. For $2 < \lambda < 3$ in contrary, our numerical results suggest that $\ell_{\rm opt}$ scales as $\ln^{\lambda-1} N$, representing still a small world. We also find numerically that for weak disorder $\ell_{\rm opt} \sim \ln N$ for ER models as well as for SF networks. We also review the transition between the strong and weak disorder regimes in the scaling properties of $\ell_{\rm opt}$ for ER and SF networks and for a general distribution of weights $\tau$, $P(\tau)$. For a weight distribution of the form $P(\tau) = 1/(a\tau)$ with $(\tau_{\rm min} < \tau < \tau_{\rm max})$ and $a = \ln \tau_{\rm max}/\tau_{\rm min}$, we find that there is a crossover network size $N^* = N^*(a)$ at which the transition occurs. For $N \ll N^*$ the scaling behavior of $\ell_{\rm opt}$ is in the strong disorder regime, while for $N \gg N^*$ the scaling behavior is in the weak disorder regime. The value of $N^*$ can be determined from the expression $\ell_\infty(N^*) = ap_c$, where $\ell_\infty$ is the optimal path length in the limit of strong disorder, $A \equiv ap_c \to \infty$ and $p_c$ is the percolation threshold of the network. We suggest that for any $P(\tau)$ the distribution of optimal path lengths has a universal form which is controlled by the scaling parameter $Z = \ell_\infty/A$ where $A \equiv p_c\tau_c/\int_0^{\tau_c} \tau P(\tau) d\tau$ plays the role of the

disorder strength and $\tau_c$ is defined by $\int_0^{\tau_c} P(\tau)d\tau = p_c$. In case $P(\tau) \sim 1/(a\tau)$, the equation for $A$ is reduced to $A = ap_c$. The relation for $A$ is derived analytically and supported by numerical simulations for Erdős–Rényi and scale-free graphs. We also determine which form of $P(\tau)$ can lead to strong disorder $A \to \infty$. We then study the minimum spanning tree (MST), which is the subset of links of the network connecting all nodes of the network such that it minimizes the sum of their weights. We show that the minimum spanning tree (MST) in the strong disorder limit is composed of percolation clusters, which we regard as "super-nodes", interconnected by a scale-free tree. The MST is also considered to be the skeleton of the network where the main transport occurs. We furthermore show that the MST can be partitioned into two distinct components, having significantly different transport properties, characterized by centrality — number of times a node (or link) is used by transport paths. One component the *superhighways*, for which the nodes (or links) with high centrality dominate, corresponds to the largest cluster at the percolation threshold (incipient infinite percolation cluster) which is a subset of the MST. The other component, *roads*, includes the remaining nodes, low centrality nodes dominate. We find also that the distribution of the centrality for the incipient infinite percolation cluster satisfies a power law, with an exponent smaller than that for the entire MST. We demonstrate the significance identifying the superhighways by showing that one can improve significantly the global transport by improving a very small fraction of the network, the superhighways.

*Keywords*: Minimum spanning tree; percolation; scale-free; optimization.

## 1. Introduction

Recently much attention has been focused on the topic of complex networks which characterize many biological, social, and communication systems [Albert & Barabási, 2002; Mendes *et al.*, 2003; Pastor-Satorras & Vespignani, 2004]. The networks are represented by nodes associated to individuals, organizations, or computers and by links representing their interactions. The classical model for random networks is the Erdős–Rényi (ER) model [Erdős & Rényi, 1959, 1960; Bollobas, 1985]. An important quantity characterizing networks is the average distance (minimal hopping) $\ell_{\min}$ between two nodes in the network of total $N$ nodes. For the Erdős–Rényi network $\ell_{\min}$ scales as $\ln N$ [Bollobas, 1985], which leads to the concept of "small worlds" or "six degrees of separation". For scale-free (SF) [Albert & Barabási, 2002] networks $\ell_{\min}$ scales as $\ln \ln N$, this leads to the concept of ultra small worlds [Cohen *et al.*, 2002; Mendes *et al.*, 2003].

In most studies, all links in the network are regarded as identical and thus a crucial parameter for information flow including efficient routing, searching and transport is $\ell_{\min}$. In practice, however, the weights (e.g. the quality or cost) of links are usually not equal [Barrat *et al.*, 2004; Boccaletti *et al.*, 2006].

Thus the length of the optimal path $\ell_{\text{opt}}$, minimizing the sum of weights, is usually longer than $\ell_{\min}$. For example, the cost could be the time required to transit the link. There are often many traffic routes from site A to site B with a set of transit time $\tau_i$, associated with each link along the path. The fastest (optimal) path is the one for which $\sum_i \tau_i$ is a minimum, and often the optimal path has more links than the shortest path. In many cases, the selection of the path is controlled by most of the weights (e.g. total cost) contributing to the sum. This case corresponds to weak disorder (WD). However, in other cases, for example when the distribution of disorder is very broad a *single* weight dominates the sum. This situation — in which one link controls the selection of the path — is called the strong disorder limit (SD).

For a recent quantitative criterion for SD and WD, see [Chen *et al.*, 2006] and Sec. 4.2 in this article.

The strong disorder is relevant e.g. for computer and traffic networks, since the slowest link in communication networks determines the connection speed. An example for SD is when a transmission at a constant high rate is needed (e.g. in broadcasting video records over the Internet). In this case the narrowest band link in the path between the transmitter and receiver controls the rate of transmission. This limit is also called the "ultrametric" limit and we refer to the optimal path in this limit as the min-max path.

The SD limit is also related to the minimal spanning tree which includes all optimal paths between all pairs of sites in the network. The disorder on a network is usually implemented from a distribution $P(\tau) \sim 1/(a\tau)$, where $1 < \tau < e^a$ [Porto *et al.*, 1999; Braunstein *et al.*, 2001; Cieplak *et al.*, 1996; Braunstein *et al.*, 2003]. We assign to each link of the network a random number $r$, uniformly distributed between 0 and 1. The cost associated with link $i$ is then $\tau_i \equiv \exp(ar_i)$ where $a$ is the parameter which controls the broadness of the distribution of link costs. The parameter $a$ represents the strength of disorder. The limit $a \to \infty$ is the strong disorder limit, since for this case clearly only one link dominates the cost of the path. The strong disorder limit (SD) can be implemented in a disordered media by assigning to each link a potential barrier $\epsilon_i$ so that $\tau_i$ is the time to cross this barrier in a thermal activation process. Thus $\tau_i = e^{\epsilon_i/KT}$, where $K$ is the Boltzmann constant and $T$ is absolute temperature. The optimal path corresponds to the minimum $(\sum_i \tau_i)$ over all possible paths. We can define disorder strength $a = 1/KT$. When $a \to \infty$, only the largest $\tau_i$ dominates the sum. Thus, $T \to 0$ (very low temperature) corresponds to the strong disorder limit.

There are distinct scaling relationships between the length of the average optimal path $\ell_{\text{opt}}$ and the network size (number of nodes) $N$ depending on whether the network is strongly or weakly disordered [Porto *et al.*, 1999; Braunstein *et al.*, 2003]. It was shown using percolation arguments (see Sec. 4) that for strong disorder [Braunstein *et al.*, 2003], $\ell_{\text{opt}} \sim N^{\nu_{\text{opt}}}$, where $\nu_{\text{opt}} = 1/3$ for Erdős–Rényi (ER) random networks [Erdős & Rényi, 1959] and for scale-free (SF) [Albert & Barabási, 2002] networks with $\lambda > 4$, where $\lambda$ is the exponent characterizing the power law decay of the degree distribution. For SF networks with $3 < \lambda < 4$, $\nu_{\text{opt}} = (\lambda - 3)/(\lambda - 1)$. For $2 < \lambda < 3$, percolation arguments do not work, but the numerical results suggest $\ell_{\text{opt}} \sim \ln^{\lambda-1} N$, which is again much larger than the ultra small result for the shortest path $\ell_{\min} \sim \ln\ln N$ found for $2 < \lambda < 3$ in [Cohen & Havlin, 2003]. When the weights are taken from a uniform distribution we are in the weak disorder limit. In this case $\ell_{\text{opt}} \sim \ln N$ for both ER and SF for all values of $\lambda$ [Braunstein *et al.*, 2003]. For $2 < \lambda < 3$, this result is significantly different from the ultra small-world result found for unweighed networks.

Porto [Porto *et al.*, 1999] considered the optimal path transition from weak to strong disorder for 2-D and 3-D lattices, and found a crossover in the scaling properties of the optimal path that depends on the disorder strength $a$, as well as the lattice size $L$ (see also [Buldyrev *et al.*, 2006]). Similar to regular lattices, there exists for any finite $a$, a crossover network size $N^*(a)$ such that for $N \ll N^*(a)$, the scaling properties of the optimal path are in the strong disorder regime while for $N \gg N^*(a)$, the network is in the weak disorder regime. The function $N^*(a)$ was evaluated. Moreover, a general criterion to determine which form of $P(\tau)$ can lead to strong disorder, and a general condition when strong or weak disorder occurs was found analytically [Chen *et al.*, 2006]. The derivation was supported by extensive simulations.

The study of the distribution of the length of the optimal paths in a network was reported in [Kalisky *et al.*, 2005]. It was found that the distribution has the scaling form $P(\ell_{\text{opt}}, N, a) \sim (1/\ell_\infty)G(\ell_{\text{opt}}/\ell_\infty, (1/p_c)(\ell_\infty/a))$, where $\ell_\infty$ is $\ell_{\text{opt}}$ for $a \to \infty$ and $p_c$ is the percolation threshold. It was also shown that a single parameter $Z \equiv (1/p_c)(\ell_\infty/a)$ determines the functional form of the distribution. Importantly, it was found [Chen *et al.*, 2006] that for all $P(\tau)$ that possess a strong-weak disorder crossover, the distributions $P(\ell_{\text{opt}})$ of the optimal path lengths display the same universal behavior.

Another interesting question is about a possible origin of scale-free degree distribution with $\lambda = 2.5$ in some real world networks. Kalisky [Kalisky *et al.*, 2006] introduced a simple process that generates random scale-free networks with $\lambda = 2.5$ from weighted Erdös–Rényi graphs [Erdős & Rényi, 1960]. They found that the minimum spanning tree (MST) on an Erdös–Rényi graph is composed of percolation clusters, which we regard as "super nodes", interconnected by a scale-free tree with $\lambda = 2.5$.

Known as the tree with the minimum weight among all possible spanning tree, the MST is also the union of all "strong disorder" optimal paths between any two nodes [Barabási, 1996; Dobrin & Duxbury, 2001; Cieplak *et al.*, 1996; Porto *et al.*, 1999; Braunstein *et al.*, 2003; Wu *et al.*, 2005]. As the global optimal tree, the MST plays a major role for transport process, which is widely used in different fields, such as the design and operation of communication networks, the traveling salesman problem, the protein interaction problem,

optimal traffic flow, and economic networks [Khan *et al.*, 2003; Skiena, 1990; Fredman & Tarjan, 1987; Kruskal, 1956; Macdonald *et al.*, 2005; Bonanno *et al.*, 2003; Onnela *et al.*, 2003]. One important question in network transport is how to identify the nodes or links that are more important than others. A relevant quantity that characterizes transport in networks is the betweenness centrality, $C$, which is the number of times a node (or link) used by all optimal paths between all pairs of nodes [Newman, 2001a, 2001b; Goh *et al.*, 2001; Kim *et al.*, 2004]. For simplicity we call the "betweenness centrality" here "centrality" and we use the notation "nodes" but similar results have been obtained for links. The centrality, $C$, quantifies the "importance" of a node for transport in the network. Moreover, identifying the nodes with high $C$ enables us to improve their transport capacity and thus improve the global transport in the network. The probability density function (pdf) of $C$ was studied on the MST for both SF [Barabási & Albert, 1999] and ER [Erdős & Rényi, 1959, 1960] networks and found to satisfy a power law, $\mathcal{P}_{\rm MST}(C) \sim C^{-\delta_{\rm MST}}$, with $\delta_{\rm MST}$ close to 2 [Goh *et al.*, 2005; Kim *et al.*, 2004]. However, [Wu *et al.*, 2006] found that a sub-network of the MST,[1] the infinite incipient percolation cluster (IIC) has a significantly higher average $C$ than the entire MST — i.e. the set of nodes inside the IIC are typically used by transport paths more often than other nodes in the MST (see Sec. 9). In this sense the IIC can be viewed as a set of *superhighways* (SHW) in the MST. The nodes on the MST which are not in the IIC are called *roads*, due to their analogy with roads which are not superhighways (usually used by local residents). Wu *et al.* [2006] demonstrated the impact of this finding by showing that improving the capacity of the superhighways (IIC) is significantly a better strategy to enhance global transport compared to improving the same number of links of the highest $C$ in the MST, although they have higher $C$.[2] This counterintuitive result shows the advantage of identifying the IIC subsystem, which is very small and of order zero compared to the full network.[3]

## 2. Algorithms

### 2.1. *Construction of the networks*

To construct an ER network of size $N$ with average node degree $\langle k\rangle$, we start with $\langle k\rangle N/2$ edges and randomly pick a pair of nodes from the total possible $N(N-1)/2$ pairs to connect with an edge. The only condition we impose is that there cannot be multiple edges between two nodes. When $\langle k\rangle > 1$ almost all nodes of the network will be connected with high probability.

To generate scale-free (SF) graphs of size $N$, we employ the Molloy–Reed algorithm [Molloy & Reed, 1998]. Initially the degree of each node is chosen according to a scale-free distribution, where each node is given a number of open links or "stubs" according to its degree. Then, stubs from all nodes of the network are interconnected randomly to each other with two constraints that there are no multiple edges between two nodes and that there are no looped edges with identical ends. The exact form of the degree distribution is usually taken to be

$$P(k) = ck^{-\lambda} \quad k = m, \ldots, K \tag{1}$$

where $m$ and $K$ are the minimal and maximal degrees, and $c \approx (\lambda-1)m^{\lambda-1}$ is a normalization constant. For real networks with finite size, the highest degree $K$ depends on network size $N$: $K \approx mN^{1/(\lambda-1)}$, thus creating a "natural" cutoff for the highest possible degree. When $m > 1$ there is a high probability that the network is fully connected.

### 2.2. *Dijkstra's algorithm*

The Dijkstra's algorithm [Cormen *et al.*, 1990] is used in general to find the optimal path, when the weights are drawn from an arbitrary distribution. The search for the optimal path follows a procedure akin to "burning" where the "fire" starts from our chosen origin. At the beginning, all nodes are given a distance $\infty$ except the origin which is given a distance 0. At each step we choose the next unburned

[1]The IIC contains loops in lattices in dimension $d$ below 6. However, for networks ($d = \infty$), in the IIC loops can be neglegted and in this case for large $N$ the IIC must be a subset of the MST. In our simulations, we found that more than 99% links of IIC belong to MST. For lattices, we only choose the part of the IIC that belongs to the MST.

[2]The overlap between the two groups is about 30% for ER networks of size $N = 8192$.

[3]The ratio $\langle N_{\rm IIC}/N_{\rm MST}\rangle$ approaches zero for large $N_{\rm MST} \equiv N$ due to the fractal nature of the IIC. Indeed, $N_{\rm IIC} \sim N^{2/3}$ both for ER [Erdős & Rényi, 1959] and for SF with $\lambda > 4$ [Cohen]. For SF with $\lambda = 3.5$, $N_{\rm IIC} \sim N^{0.6}$ [Cohen] and for the $L \times L$ square lattice $N_{\rm IIC} \sim L^{91/48} \sim N^{91/96}$ [Bunde & Havlin, 1996].

node which is nearest to the origin, and "burn" it, while updating the optimal distance to all its neighbors. The optimal distance of a neighbor is updated only if reaching it from the current burning node gives a total path length that is shorter than its current distance.

### 2.3. *Ultrametric optimization*

Next, we describe a numerical method for computing $\ell_{\text{opt}}$ between any two nodes in strong disorder [Dobrin & Duxbury, 2001; Braunstein *et al.*, 2001]. In this case the sum of the weights must be completely dominated by the largest weight. Sometimes this condition is referred to as ultrametric. We can satisfy this condition assigning weights to all the links $\tau_i = \exp(ar_i)$ choosing $a$ to be so large, that any two links will have different binary orders of magnitude. For example, if we can select $0 \leq r_i < 1$ from a uniform distribution, using a 48-bit random number generator, there will be no two identical values of $r_i$ in a system of any size that we study. In this case $\Delta r_i \geq 2^{-48}$ and we can select $a \geq 2^{48} \ln 2$ to guarantee the strong disorder limit. To find the optimal paths under the ultrametric condition, we start from one node (the origin — see Fig. 1) and visit all the other nodes connected to the origin using a burning algorithm. If a node at distance $\ell_0$ (from the origin) is being visited for the first time, this node will be assigned a list $S_0$ of weights $\tau_{0i}$, $i = 1 \cdots \ell_0$ of the links by which we reach that node sorted in descending order. Since $\tau_{0i} = \exp(ar_{0i})$, we can use a list of random numbers $r_{0i}$ instead.

$$S_0 = \{r_{01}, r_{02}, r_{03}, \ldots, r_{0l_0}\}, \tag{2}$$

with $r_{0j} > r_{0j+1}$ for all $j$. If we reach a node for a second time by another path of length $\ell_1$, we define for this path a new list $S_1$,

$$S_1 = \{r_{11}, r_{12}, r_{13}, \ldots, r_{1l_1}\}, \tag{3}$$

and compare it with $S_0$ previously defined for this node.

Different sequences can have weights in common because some paths have links in common because of the loops, so it is not enough to identify

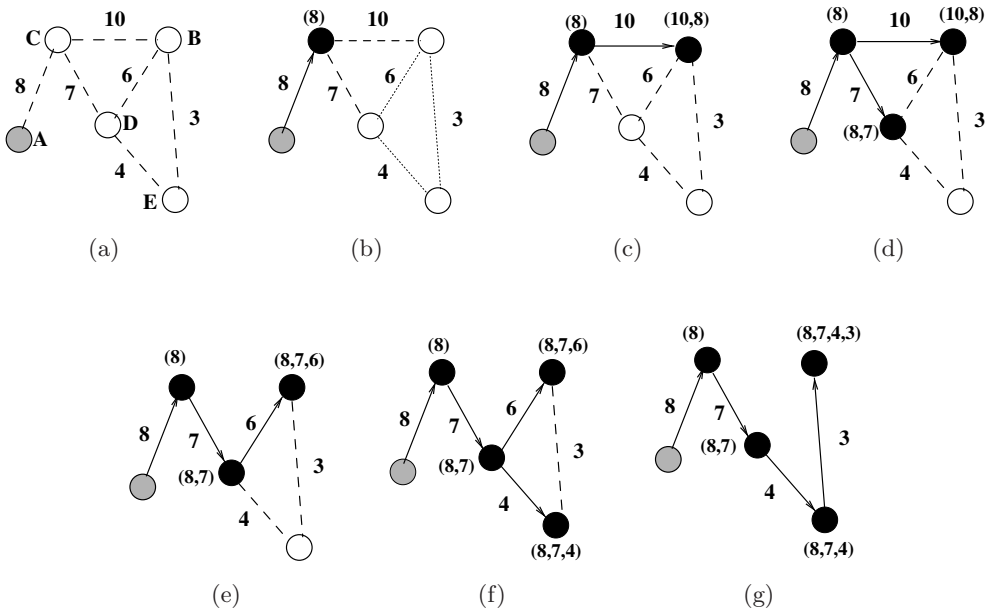


Fig. 1. In (a) we show schematically a network consisting of five nodes (A, B, C, D and E). The links between them are shown in dashed lines. The origin (A) is marked in gray. All links were assigned random weights, shown beside the links. In (b) one node (C) has been visited for the first time (marked in black) and assigned the sequence (8) of length $\ell = 1$. The path is marked by a solid arrow. Notice that there is no other path going from the origin (A) to this node (C) so $\ell_{\text{opt}} = 1$ for that path. In (c) another node (B) is visited for the first time (marked in black) and assigned the sequence $(10, 8)$ of length 2. The sequence has the information of all the weights of that path arranged in decreasing order. In (d) another node (D) is visited for the first time and assigned the sequence $(8, 7)$ of length 2. In (e), node (B) visited in (c) with sequence $(10, 8)$ is visited again with sequence $(8, 7, 6)$. The last sequence is smaller than the previous sequence $(10, 8)$ so that node (B) is reassigned the sequence $(8, 7, 6)$ of length 3 [see Eq. (4)]. The new path is shown as a solid line. In (f) a new node (E) is assigned with sequence $(8, 7, 4)$. In (g) node (B) is reached for the third time and reassigned the sequence $(8, 7, 4, 3)$ of length 4. The optimal path for this configuration from A to B is denoted by the solid arrows in (g) (after [Havlin *et al.*, 2005]).

the sequence by its maximum weight; in this case it must also be compared with the second maximum, the third maximum, etc. We define $S_p < S_q$ if there exists a value $m$, $1 \leq m \leq \min(\ell_p, \ell_q)$ such that

$$\begin{aligned} r_{pj} &= r_{qj} \quad \text{for } 1 \leq j < m \quad \text{and} \\ r_{pj} &< r_{qj} \quad \text{for } j = m, \end{aligned} \tag{4}$$

or if $\ell_q > \ell_p$ and $r_{pj} = r_{qj}$ for all $j \leq \ell_p$. If $S_1 < S_0$, we replace $S_0$ by $S_1$. The procedure continues until all paths have been explored and compared. At this point, $S_0 = S_{\text{opt}}$, where $S_{\text{opt}}$ is the sequence of weights for the optimal path of length $\ell_{\text{opt}}$. A schematic representation of this ultrametric algorithm is presented in Fig. 1. This algorithm is slow and memory consuming since we have to keep track of a sequence of values and the rank. Using this method, we obtain systems of sizes up to $2^{12}$ nodes, typically $10^5$ realizations of disorder.

### 2.4. *Bombing optimization*

This algorithm allows to compute $\ell_{\text{opt}}$ (and other relevant quantities) between any two nodes in strong disorder limit and was introduced by Cieplak *et al.* [1996]. Basically the algorithm does the following

1. Sort the edges by descending weight.
2. If the removal of the highest weight edge will not disconnect $A$ from $B$ — remove it.
3. Go back to step 2 until all edges have been processed.

Since the edge weights are random, so is the ordering. Therefore, in fact, one does not need even to select edge weights and "bombing" algorithm can be simplified by removing randomly chosen edges one at a time, provided that their removal does not break the connectivity between the two nodes. The bottleneck of this algorithm is checking the connectivity after each removal. To speed it up, we first compute the minimal path between nodes A and B using Dijkstra's algorithm. Then we must check the connectivity only if the removed bond belongs to this path. In this case, we attempt to compute a new minimal path between A and B on the subset of remaining bonds. If our attempt fails, it means that the removal of this bond would destroy the connectivity between A and B. Therefore, we restore this bond and exclude it from the list of bonds subject to random removal. With this improvement we could reach systems of sizes up to $2^{16}$ nodes and $10^5$ realizations of weight disorder.

### 2.5. *The minimum spanning tree (MST)*

The MST on a weighted graph is a tree that reaches all nodes of the graph and for which the sum of the weights of all the links or nodes (total weight) is minimal. Also, in the "strong disorder" limit, each path between two sites on the MST is the optimal path [Cieplak *et al.*, 1996; Dobrin & Duxbury, 2001], meaning that along this path the maximum *barrier* (weight) is the smallest possible [Dobrin & Duxbury, 2001; Braunstein *et al.*, 2003; Sreenivasan *et al.*, 2004]. Standard algorithms for finding the MST are Prim's algorithm [Cormen *et al.*, 1990] which resembles invasion percolation [Bunde & Havlin, 1996] and Kruskal's algorithm [Cormen *et al.*, 1990]. First we explain the Prim's algorithm.

(a) Create a tree containing a single vertex, chosen arbitrarily from the graph.
(b) Create a set containing all the edges in the graph.
(c) Remove from the set an edge with minimum weight that connects a vertex in the tree with a vertex not in the tree.
(d) Add that edge to the tree.
(e) Repeat steps (c–d) until every edge in the set connects two vertices in the tree.

Note that two nodes in the tree cannot be connected again by a link, thus forbidding loops to be formed. Prim's algorithm essentially starts by choosing a random node in the network, and then growing outward to the "cheapest" link which is adjacent to the starting node. Each link which is "invaded" is added to the growing cluster (tree), and the process is iterated until every site has been reached. Bonds can only be invaded if they do not produce a loop, so that the tree structure is maintained [20]. This process resembles invasion percolation with trapping studied in the physics literature [Barabási, 1996; Porto *et al.*, 1997]. A direct consequence of the invasion process is that a path between two sites A and B on the MST is the path whose maximum weight is minimal, i.e. the minimal-barrier path. This is because if there were another path with a smaller barrier (i.e. maximal weight link) connecting A and B, the invasion process would have chosen that path to be on the MST instead. The minimal-barrier path is important in cases where the "bottleneck" link is important. For example, in streaming video

broadcast on the Internet, it is important that each link along the path to the client will have enough capacity to support the transmission rate, and even one link with not enough bandwidth can become a bottleneck and block the transmission. In this case we will choose the minimal-barrier path rather than the optimal path. An equivalent algorithm for generating the MST is the Kruskal's algorithm:

(a) Create a forest F (a set of trees), where each vertex in the graph is a separate tree.
(b) Create a set S containing all the edges in the graph.
(c) While S is nonempty: "Remove an edge with minimum weight from S." If that edge connects two different trees, then add it to the forest, combining two trees into a single tree." Otherwise discard that edge. Note that an edge cannot connect a tree to itself, thus forbidding loops to be formed.

Kruskal's algorithm resembles the percolation process because we add links to the forest according to increasing order of weights. The forest is actually the set of percolation clusters growing as the occupation probability is increasing. It was noted by Dobrin *et al.* [Dobrin & Duxbury, 2001] that the geometry of the MST depends only on the unique ordering of the links of the network according to their weights. It does not matter if the weights are nearly the same or wildly different, it is only their ordering that matters. Given a network with weights on the links, any transformation which preserves the ordering of the weights (e.g. the link which has the fiftieth largest energy is the same before and after the transformation) leaves the MST geometry unaltered. This property is termed "universality" of the MST. Thus, given a network with weights, represented by a random variable distributed uniformly, a monotonic transformation of the weights will leave the MST unchanged.

Another equivalent algorithm to find the MST is the "bombing optimization algorithm" [Braunstein *et al.*, 2003]. Similar to the one explained in Sec. 2.4, we start with the full network and remove links in order of descending weights. If the removal of a link disconnects the graph, we restore the link [Ioselevich & Lyubshin, 2004]; otherwise the link is removed. The algorithm ends and the MST is obtained when no more links can be removed without disconnecting the graph.

### 2.6. *The incipient infinite cluster (IIC)*

To find the IIC of ER and SF in uncorrelated weighted networks,[4] we start with the fully connected network and remove links in descending order of their weights. After each removal of a link, we calculate the weighted average degree $\kappa \equiv \langle k^2 \rangle / \langle k \rangle$, which decreases with link removals. When $\kappa < 2$, we stop the process [Cohen *et al.*, 2000]. The meaning of this criterion is explained in the next section, where its connection with the percolation threshold $p_c$ is established. The largest remaining component is the IIC. For the two-dimensional (2D) square lattice we cut the links (bonds) in descending order of their weights until we reach the percolation threshold $p_c$ ($= 0.5$). At that point the largest remaining component is the IIC [Bunde & Havlin, 1996].

## 3. Optimal Path in Strong Disorder and Percolation on the Cayley Tree

In this section we review classical analytical methods for exploring random networks based on percolation theory on a Cayley tree [Stauffer & Aharony, 1994; Bunde & Havlin, 1996], or branching processes [Harris, 1989]. To obtain the optimal path in the strong disorder limit, we present the following theoretical argument. It has been shown [Braunstein *et al.*, 2001; Cieplak *et al.*, 1996] that the optimal path in the SD limit between two nodes A and B on the network can be obtained by the bombing algorithm described in Sec. 2.4. This algorithm is based on randomly removing links. Since randomly removing links is a percolation process, the optimal path must be on the percolation backbone connecting A and B. We can explore the network starting with node A by Dijkstra's algorithm, sequentially creating burning shells of chemical distance $n$ from the node A. Alternatively we can think of the $n$th shell as of $n$th generation of descendants of a parent A in a branching process. The random network consisting of a large number of nodes $N \to \infty$ and small average degree $\langle k \rangle \ll N$, has a tree-like local structure with no loops, since the probability that a node we randomly chose by an outgoing link

[4]By uncorrelated we mean that the weights are not correlated with the topology, such as the degree of nodes.

has been already visited is less than $\langle k\rangle^n/N$, which remains negligible for $n < \ln N/\ln\langle k\rangle$.

As we remove links by the bombing algorithm, the average degree of remaining nodes decreases, and the role of loops decreases. Thus finite loops play no role in determining the properties of the optimal path. In fact, connecting the nodes A and B by an optimal path is equivalent to connecting each of them to a very distant shell on a corresponding Cayley tree. As the fraction $q = 1 - p$ of remaining links decreases, we reach the percolation threshold at which removal of a next link destroys the connectivity with a very high probability. Note that if we select weights of the links $\tau_i = \exp(ar_i)$, where $r_i$ is uniformly distributed on $[0, 1]$, the fraction of remaining bonds, $p$, is equal to $r_i$ of the next link, we will remove.

### 3.1. *Distribution of the maximal weight on the optimal path*

In order to further develop this analogy, we will show that the distribution of the maximal random number $r_{\max}$ along the optimal path[5] can be expressed in terms of the order parameter $P_\infty(p)$ in the percolation problem on the Cayley tree, where $P_\infty(p)$ is the probability that a randomly chosen site on the Cayley tree has infinite number of generations of descendants or, in other words, belongs to the infinite cluster.

If the original graph has a degree distribution $P(k)$, the probability that we reach a node with a degree $k$ by following a randomly chosen link on the graph, is equal to $kP(k)/\langle k\rangle$, where $\langle k\rangle$ is the average degree. This is because the probability of reaching a given node by following a randomly chosen link is proportional to the number of links, $k$, of that node and $\langle k\rangle$ comes from normalization. Also, if we arrive at a node with degree $k$, the total number of outgoing branches is $k - 1$. Therefore, from the point of view of the Cayley tree, the probability $p_{k-1}$ to arrive at a node with $k - 1$ outgoing branches by following a randomly chosen link is

$$p_{k-1} = \frac{kP(k)}{\langle k\rangle}. \tag{5}$$

In the asymptotic limit, $N \to \infty$, when the optimal path between the two nodes is very long, the probability distribution for the maximal weight link can be obtained from the following analysis. Let us assume that the probability of *not* reaching $n$th generation starting from a randomly chosen link of the Cayley tree whose links exist with a probability $p$, is $Q_n$. Suppose this link leads to a node whose outgoing degree is 2. Then the probability that starting from this link, we will not reach $n$ generations of its descendants is the sum of three terms:

1. The probability that both outgoing links do not exist is equal to $(1 - p)^2$.
2. The probability that both outgoing links exist, but they do not have $n-1$ generations of descendants is equal to $p^2Q_{n-1}^2$.
3. The probability that only one of the two outgoing links exist but it does not have $n - 1$ generations of descendants is equal to $2(1 - p)pQ_{n-1}$.

Therefore, in this case

$$Q_n = (1 - p)^2 + p^2Q_{n-1}^2 + 2(1 - p)pQ_{n-1}, \tag{6}$$

which on simplification becomes

$$Q_n = ((1 - p) + pQ_{n-1})^2. \tag{7}$$

Following this argument for the case when our link leads to a node with $m$ outgoing links, the probability that starting from this node, we cannot reach $n$ generations, is

$$Q_n = ((1 - p) + pQ_{n-1})^m. \tag{8}$$

In the case of a Cayley tree with a variable degree, we must incorporate a factor $p_{k-1}$ given by Eq. (5) which accounts for the probability that the node under consideration has $k - 1$ outgoing edges and sum up over all possible values of $k$. Thus for a existing link on the Cayley tree, the probability that it does not have descendants in generation $n$ can be obtained by applying a recursion relation

$$Q_l = \sum_{k=1}^{\infty} \frac{P(k)k((1 - p) + pQ_{l-1})^{k-1}}{\langle k\rangle} \tag{9}$$

for $l = 1, 2, \ldots, n$ with the initial condition $Q_0 = 0$, which indicates that a given link is always present in generation zero of its descendants.

For a random graph, a randomly chosen node has $k$ outgoing edges with the original probability $P(k)$. Thus it has a slightly different

[5]The maximal random number, is the first random number in the bombing process that we cannot remove without breaking the connection between a pair of nodes. In other words, it is the value that dominates the sum of the costs in the SD limit (see [Braunstein *et al.*, 2003, 2004]).

probability $Q_n(p)$ of not having descendants in its $n$th generation:

$$\tilde{Q}_n = \sum_{k=0}^{\infty} P(k)((1-p)+pQ_{n-1})^k. \tag{10}$$

It is convenient to introduce the generating function of the original degree distribution

$$\tilde{G}(x) \equiv \sum_{k=1}^{\infty} P(k)x^k \tag{11}$$

and the generating function of the degree distribution of the Cayley tree

$$G(x) \equiv \sum_{k=1}^{\infty} \frac{kP(k)}{\langle k\rangle} x^{k-1}, \tag{12}$$

where $x$ is an arbitrary complex variable. Using the normalization conditions for the probabilities $\sum_{k=0}^{\infty} P(k) = 1$, it is easy to see that $\tilde{G}(1) = 1$. Taking into account that $\langle k\rangle = \sum_{k=0}^{\infty} kP(k)$ we have $\langle k\rangle = d\tilde{G}/dx|_{x=1} = \tilde{G}'(1)$ and hence $\tilde{G}(x)$ and $G(x)$ are connected by a relation

$$G(x) = \frac{\tilde{G}'(x)}{\tilde{G}'(1)}. \tag{13}$$

For any degree distribution $P(k) \to 0$, as $k \to \infty$ and thus both functions are analytic functions of $x$ and have a convergence radius $R \geq 1$. Since $P(k) > 0$, these functions and all their derivatives are monotonically increasing functions on an interval $[0, 1)$. For the ER networks, the degree distribution is Poisson given by: $P(k) = \langle k\rangle^k \exp^{-\langle k\rangle}/k!$, hence $\tilde{G}(x) = G(x) = \exp[\langle k\rangle(x-1)]$. For scale free distribution, $P(k) \sim k^{-\lambda}$, hence $\tilde{G}(x)$ is proportional to Riemann $\zeta$-function, $\zeta_\lambda(x)$.

If we denote by $f_n(p)$, the probability that starting at a randomly chosen existing link we can reach, or survive up to, the $n$th generation, then

$$f_n = 1 - Q_n(p) \tag{14}$$

and by $\tilde{f}_n(p)$, the probability that a randomly chosen node has at least $n$ generation of descendants,

$$\tilde{f}_n = 1 - \tilde{Q}_n(p) \tag{15}$$

then

$$f_n = 1 - G(1 - pf_{n-1}) \tag{16}$$

and

$$\tilde{f}_n = 1 - \tilde{G}(1 - pf_{n-1}). \tag{17}$$

The sequence of iterations (16) is visualized (see Fig. 2) as a process of solving the equation

$$x = 1 - G(1 - px) \tag{18}$$

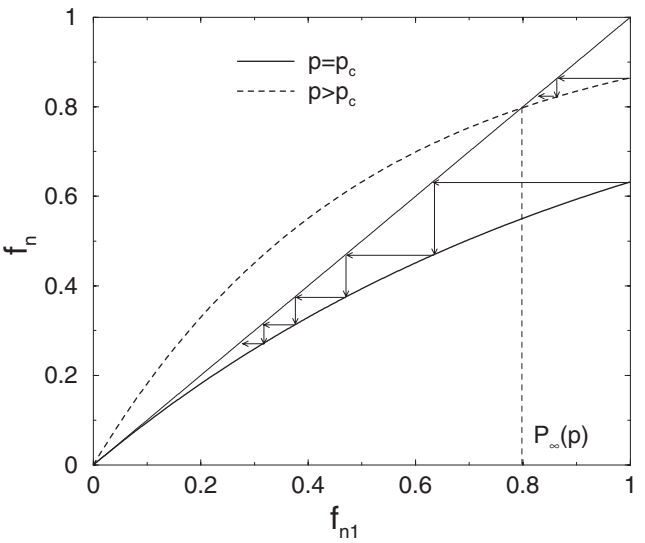


Fig. 2. The iterative process of solving Eq. (18). The thin straight line $y = x$ represents the left-hand side. The bold curve represents the right-hand side (r.h.s) for $p = p_c$, at which the r.h.s. is tangential to $y = x$ at the origin. The dashed curve represents r.h.s. for $p > p_c$. Both cases are computed for the Poisson degree distribution with $\langle k\rangle = 2$, so r.h.s of Eq. (18) is given by $1 - \exp(-2px)$. The arrows represent iterations starting from $f_0 = 1$ (the starting link belongs to generation 0). It is clear that the convergence of the iterations is very fast (exponential) for $p \neq p_c$, while it is very slow (power law) for $p = p_c$.

by an iteration method. Obviously, this equation has at least one root $x_0 = 1$. But if the derivative of the right-hand side, $[1 - G(1 - px)]'|_{x=0} = pG'(1) > 1$, we will have another root $0 < x_1 \leq 1$. This root has a physical meaning of a probability $P_\infty(p)$ that a randomly selected existing link is connected to infinity (see also [Cohen *et al.*, 2000]). For $p > 1/G'(1)$, the iterations will converge to this root, while for $p \leq 1/G'(1)$, the iterations will converge to $P_\infty(p) = 0$. Thus

$$p_c \equiv \frac{1}{G'(1)} = \frac{\langle k\rangle}{\langle k^2\rangle - \langle k\rangle} = \frac{1}{\kappa - 1} \tag{19}$$

has a meaning of the percolation threshold above which there is a finite probability to reach the infinity. Using this equation we can derive the condition $\kappa < 2$ to stop bombing in the process of obtaining IIC. Indeed $\kappa < 2$ indicates that Eq. (18) has only one trivial solution $x_0 = 0$ even for $p = 1$. This means that all the clusters in this network are finite. If $\kappa > 2$, $p_c < 1$ accordingly $P_\infty(1) > 0$, i.e. the infinite cluster does exist. The condition $\kappa = 2$ corresponds to $p_c = 1$ which means that any further link removal will produce a network in which

$P_\infty(1) = 0$, i.e. the network with only finite clusters, while at $p = 1$, the infinite cluster is incipient.

The probability that a randomly chosen node is connected to infinity can be determined as

$$\tilde{P}_\infty(p) = 1 - \tilde{G}(1 - pP_\infty(p)), \tag{20}$$

where $P_\infty(p)$ is a nontrivial solution of Eq. (18). For some degree distributions including Poisson distribution, $\tilde{P}_\infty(1) < 1$. This indicates that a randomly chosen node on the original network may not belong to the giant component of the network. In fact, the optimal path between nodes A and B exists if both belong to the giant component. Provided that A and B both belong to the giant component, the probability that they are still connected when the fraction $1 - p$ of bonds is removed is

$$\Pi(p) = \left(\frac{\tilde{P}_\infty(p)}{\tilde{P}_\infty(1)}\right)^2. \tag{21}$$

Translating this condition to the bombing algorithm of generating an optimal path, $\Pi(p)$ is the probability that the maximum random number along the optimal path $r_{\max} \leq p$. Indeed, $\Pi(p)$ is the probability that when only a fraction $p$ of links remains, the connectivity between A and B still exists. Hence $r_{\max} \leq p$. Thus, $\Pi(r_{\max})$ is the cumulative distribution of $r_{\max}$. The probability density of $r_{\max}$ is thus equal to the derivative of $\Pi(p)$ with respect to $p$:

$$P(r_{\max}) = \frac{d}{dp}\Pi(p)\Big|_{p=r_{\max}}. \tag{22}$$

In Fig. 3 we plot two curves. The curve with symbols is the probability distribution of $r_{\max}$ in a strongly disordered ER graph with $\langle k\rangle = 4$ obtained by simulations. The line shows the same probability distribution obtained using [Eq. (22)] for a Poisson degree distribution with $\langle k\rangle = 4$. The curves coincide very well, indicating the excellent agreement between the theoretical analysis and simulations.

### 3.2. *Distribution of the cluster chemical length at percolation threshold*

Figure 2 illustrates the convergence of the probability of the random link to have descendants in the $n$th generations. The difference $P(n) = f_n - f_{n+1}$ is the probability that the last generation of the descendants of this link is $n$. In percolation language, it is the probability distribution of the cluster chemical length $\ell = n$. In order to find, how $f_n \to 0$ when $p = p_c$, we can expand Eq. (16) in

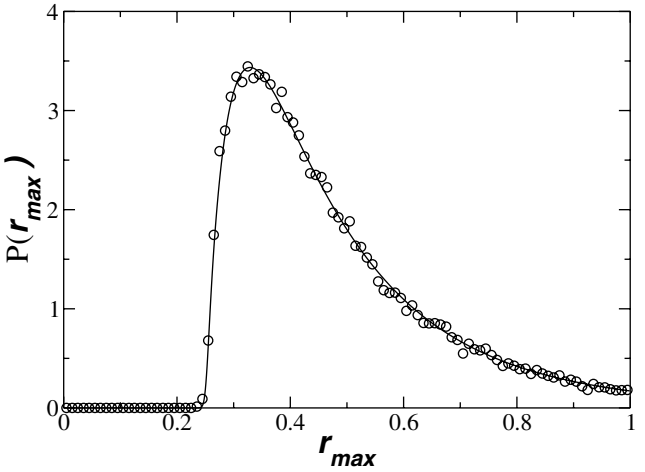


Fig. 3. The probability distribution of the maximal random number $r_{\max}$ along the optimal path obtained using simulations on a random graph with $\langle k\rangle = 4$ and using the analytical method on a Cayley tree with Poisson degree distribution and $\langle k\rangle = 4$. The simulations involve 100000 network realizations and are carried out on a network of 65536 nodes. The values of $l_{\rm opt}$ for this network lie in the range $40 < l_{\rm opt} < 120$ (after [Braunstein *et al.*, 2004]).

Taylor series at $f_n = 0$. For ER networks, $G(x)$ has all the derivatives at $x = 1$, thus (16) can be presented as

$$f_n = pG'(1)f_{n-1} - \frac{1}{2}p^2G''(1)f_{n-1}^2 + O(f_{n-1}^2). \tag{23}$$

For SF graphs with $\lambda > 4$, $G''(1)$ also exists, thus the above equation holds. For $3 < \lambda < 4$ the second derivative does not exist, however using the Tauberian theorem which relates the speed of the decay of the coefficients $P(k) \sim k^{-\mu}$ of the power series and the behavior of its singularity at the convergence radius: $G_s(x) \sim (1 - x)^{\mu-1}$ we can write:

$$f_n = pG'(1)f_{n-1} - cf_{n-1}^{\lambda-2} + O(f_{n-1}^{\lambda-2}), \tag{24}$$

where $c$ is some positive coefficient.

As $\lambda \to 3$, $G'(1) \to \infty$ and hence, according to Eq. (19) $p_c \to 0$. This means that for SF networks with $\lambda \leq 3$, percolation approach breaks down. However, for finite networks, it is unlikely to have a degree larger than $N^{1/(\lambda-1)}$. This fact is obvious since when one generates random degrees with probability distribution $P(k)$, one produces random numbers $x$ uniformly distributed on a interval between 0 and 1, and compute $k = f(x)$, where $f(x)$ satisfies the equation $x = \sum_{f(x)}^{\infty} P(k) \sim f(x)^{-\lambda+1}$. Thus the largest $k$ corresponds to the smallest $x$. Generating $N$ random numbers is equivalent to throwing $N$ points on an interval $[0, 1]$ which divide

this interval into $N+1$ segments whose lengths are identically distributed with an exponential distribution. Thus the average value of the smallest $x$ is equal to $1/(N+1)$. Accordingly, the average value of the largest $k$ can be approximated as $k_{\max} = f(1/(N+1)) \sim N^{1/(\lambda-1)}$ [Cohen *et al.*, 2000]. Thus replacing summation by integration up to $k_{\max}$ in the expression for $G'(1) \approx \int^{k_{\max}} k^{-\lambda+2} dk \sim k_{\max}^{3-\lambda} = N^{(3-\lambda)/(\lambda-1)}$. Hence for $2 < \lambda < 3$ [Cohen *et al.*, 2000].

$$p_c \sim N^{(\lambda-3)/(\lambda-1)}. \tag{25}$$

When $p < p_c$, $f_n \sim (p/p_c)^n$, i.e. the convergence is exponential. When $p = p_c$, we will seek the solution of the above recursion relations in a power law form: $f_n \sim n^{-\theta}$. Expanding them in powers of $n^{-1}$, and equating the leading powers, we have $\theta + 1 = \theta(\lambda - 2)$, from which we obtain

$$f_n \sim n^{-1/(\lambda-3)}, \tag{26}$$

or

$$P(\ell) = f_\ell - f_{\ell+1} \sim \ell^{-\tau_\ell}, \tag{27}$$

where [Cohen *et al.*, 2002; Cohen *et al.*, 2002]

$$\tau_\ell = \begin{cases} 2, \lambda > 4 & \text{ER} \\ \dfrac{1}{(\lambda-3)} + 1, 3 < \lambda \le 4 & \end{cases}. \tag{28}$$

The probability that a randomly selected *node* has exactly $\ell$ generations of descendants is equal to

$$\tilde{P}(\ell) = \tilde{f}_\ell - \tilde{f}_{\ell+1} = \tilde{G}(1 - pf_\ell) - \tilde{G}(1 - pf_{\ell-1}) \sim \langle k \rangle p(f_\ell - f_{\ell-1}). \tag{29}$$

Thus it is characterized by the same $\tau_\ell$ as $P(\ell)$.

Taylor expansions (23) and (24) can be used to derive the behavior of $P_\infty(p)$ as $p \to p_c$ by letting $f_n = f_{n-1} = P_\infty(p)$ and solving the resulting equations with a leading term accuracy:

$$P_\infty(p) = (p - p_c)^\beta, \tag{30}$$

where [Cohen *et al.*, 2000]

$$\beta = \begin{cases} 1, \lambda > 4 & \text{ER} \\ \lambda - 3, 3 < \lambda \le 4 & \end{cases}. \tag{31}$$

### 3.3. *Distribution of the cluster sizes at percolation threshold*

Using the generating functions [Cohen *et al.*, 2002; Cohen *et al.*, 2002; Callaway *et al.*, 2000], one can also find the distribution of the clusters sizes, $P(s)$, connected to a randomly selected *link*. For simplicity, let us again consider a link (conducting with probability $p$) leading to a node of a degree $k = 3$, so it has only two outgoing links. The probability that this link is connected to a cluster consisting of $s$ nodes obeys the following relations

$$P(s) = p \sum_{k+l=s-1} P(k)P(l) \tag{32}$$

for $s > 0$ and $P(0) = 1 - p$. Introducing the generating function of the cluster size distribution $H(x) = \sum_0^\infty P(s)x^s$, we have: $H(x) = 1 - p + xpH^2(x)$. In a general Cayley tree with an arbitrary degree distribution we have:

$$H(x) = 1 - p + xpG(H(x)). \tag{33}$$

This equation defines the behavior of $H(x)$ for $x \to 1$, and thus via the Tauberian theorem defines the asymptotic behavior of its coefficients $P(s)$. Note that $H(1)$ is the cumulative probability of all finite clusters. Thus $(1 - H(1)) = pP_\infty(p)$ is the probability that a randomly selected link conducting with probability $p$ is connected to infinity and Eq. (33) becomes equivalent to Eq. (18) for $P_\infty(p)$.

Introducing $\delta_x = 1 - x$ and $\delta_H = 1 - H(x)$ and expanding $G(x)$ around $x = 1$ at percolation threshold $p = 1/G'(1)$, we have $\delta_H \delta_x + p\delta_x = cx\delta_H^{\lambda-2} + O(\delta_H^{\lambda-2})$ which yields $\delta_H \sim \delta_x^{1/(\lambda-2)}$. Using the Tauberian theorem we conclude [Cohen *et al.*, 2002; Cohen *et al.*, 2002]:

$$P(s) \sim s^{-\tau_s}, \tag{34}$$

where

$$\tau_s = \begin{cases} \dfrac{3}{2}, \lambda > 4 & \text{ER} \\ \dfrac{1}{\lambda-2} + 1, 3 < \lambda \le 4 & \end{cases}. \tag{35}$$

Analogous considerations suggest that the probabilities $\tilde{P}(s)$ that a randomly selected *node* belongs to the cluster of size $s$ produce the generating function $\tilde{H}(x) = \tilde{G}(H(x))$. Since for $\lambda > 3$, $\tilde{G}''(1) < \infty$, the singularity of $\tilde{H}(x)$ for $x \to 1$ is of the same order as the singularity of $H(x)$ and thus its coefficients, $\tilde{P}(s)$, also decay as $s^{-\tau_s}$.

Following [Stauffer & Aharony, 1994], we will show that the distribution of all the disconnected clusters in a network scales as $P_{\text{all}}(s) = \tilde{P}(s)/s \sim s^{-\tau_s+1}$. Indeed, let us select a random node in this network. The number of nodes belonging to

the clusters of size $s$ is $NsP_{\rm all}(s)/\sum_1^\infty sP_{\rm all}(s) = NsP_{\rm all}(s)/\langle s\rangle$. Thus, $\tilde{P}(s) = sP_{\rm all}(s)/\langle s\rangle$.

If we have a network of $N$ nodes, the size of the largest cluster $S$ is determined by the relation $\sum_{s=S}^\infty P_{\rm all}(s) \sim 1/N$, which becomes clear if we describe a concrete realization of the cluster sizes by throwing $N/\langle s\rangle$ random points representing clusters under the curve $P_{\rm all}(s)$. The average area corresponding to each of these points is $1/N$ and the area corresponding to the rightmost point representing the largest cluster is $\sum_{s=S}^\infty P_{\rm all}(s) \sim S^{-\tau_s}$. Thus the largest cluster (which coincides with IIC) in the network of $N$ nodes scales as

$$S \sim N^{1/\tau_s}. \tag{36}$$

For ER graphs, the relation $S \sim N^{2/3}$ has been derived in a classical work [Erdős & Rényi, 1959].

## 4. Scaling of the Length of the Optimal Path in Strong Disorder

The relations obtained in the previous subsections allow us to determine the scaling of the average optimal path length in a network of $N$ nodes. During bombing, when we reach percolation threshold, we have targeted only a tiny fraction of links (or nodes) on the optimal path, with $r_{\max} > p_c$ which we have to restore, because their removal would destroy the connectivity. The majority of the links on the optimal path remains intact. All of them belong to the remaining percolation clusters which at percolation threshold has a tree-like structure with no loops. At this point, the optimal path coincides with the shortest path, which is uniquely determined. We will describe this situation in detail in Sec. 6. With high probability, the optimal path between any two nodes A and B goes through the largest cluster at the percolation threshold. Thus its length must scale as the chemical length of the largest percolation cluster [Braunstein *et al.*, 2003]. Assuming a power law relation between the cluster size $s$ and its chemical dimension $\ell$, $s = \ell^{d_\ell}$, and using the fact that both of the quantities have power law distributions $P(\ell)d\ell = \tilde{P}(s)ds$, we have $\ell^{-\tau_\ell} = \ell^{-d_\ell\tau_s + d_\ell - 1}$. Thus [Barrat *et al.*, 2004]

$$d_\ell = \frac{\tau_l - 1}{\tau_s - 1}. \tag{37}$$

Therefore, $S \sim \ell_{\rm opt}^{d_\ell}$ and using (36) we have $\ell_{\rm opt} \sim S^{1/d_\ell} \sim N^{\nu_{\rm opt}}$, where

$$\nu_{\rm opt} = \frac{1}{d_\ell\tau_s}. \tag{38}$$

Using Eqs. (35) and (28) for $\tau_s$ and $\tau_\ell$ respectively, we have

$$\nu_{\rm opt} = \begin{cases} \dfrac{1}{3}, \lambda > 4, & \text{ER} \\ \dfrac{\lambda-3}{\lambda-1}, 3 < \lambda \le 4 & \end{cases}. \tag{39}$$

Note that $\lambda = 4$ corresponds to the special case when $G''(1)$ diverges, in this case the Tauberian theorem predicts logarithmic corrections, and hence we expect $\ell_{\rm opt} \sim N^{1/3}/\ln N$ for $\lambda = 4$.

We review above the exact results for the Cayley tree, from which using heuristic arguments we have derived the scaling relation between the average length of the optimal path and the number of nodes in the network. Now we will show how the same predictions can be obtained using general percolation theory. We will also present numerical data supporting our heuristic arguments. We begin by considering the ER graph. At criticality, it is equivalent to percolation on the Cayley tree or percolation at the upper critical dimension $d_c = 6$. For the ER graph, we derived above that the mass of the IIC, $S$, scales as $N^{2/3}$ [Erdős & Rényi, 1959]. This result can also be obtained in the framework of percolation theory for $d_c = 6$. Since $S \sim R^{d_f}$ and $N \sim R^d$ (where $d_f$ is the fractal dimension and $R$ the spatial diameter of the cluster), it follows that $S \sim N^{d_f/d}$ and for $d_c = 6$, $d_f = 4$ [Bunde & Havlin, 1996] we obtain $S \sim N^{2/3}$ [Watts, 2003].

It is also known [Bunde & Havlin, 1996] that, at criticality, at the upper critical dimension, the average shortest path length $\ell_{\min} \sim R^2$, like a random walk and therefore $S \sim \ell_{\min}^{d_\ell}$ with $d_\ell = 2$. Thus

$$\ell_{\min} \sim \ell_{\rm opt} \sim S^{1/d_\ell} \sim N^{2/3d_\ell} \sim N^{\nu_{\rm opt}}, \tag{40}$$

where $\nu_{\rm opt} = 2/3d_\ell = 1/3$.

For SF networks, we can also use the percolation results at criticality. It was found [Cohen *et al.*, 2002; Cohen *et al.*, 2002] (see Sec. 3) that $d_\ell = 2$ for $\lambda > 4$, $d_\ell = (\lambda-2)/(\lambda-3)$ for $3 < \lambda < 4$, $S \sim N^{2/3}$ for $\lambda > 4$, and $S \sim N^{(\lambda-2)/(\lambda-1)}$ for $3 < \lambda \le 4$. Hence, we conclude that

$$\ell_{\min} \sim \ell_{\rm opt} \sim \begin{cases} N^{1/3} & \lambda > 4 \\ N^{(\lambda-3)/(\lambda-1)} & 3 < \lambda \le 4 \end{cases}. \tag{41}$$

Thus $\nu_{\rm opt} = 1/3$ for ER and SF with $\lambda > 4$, and $\nu_{\rm opt} = (\lambda-3)/(\lambda-1)$ for SF with $3 < \lambda < 4$. Since for SF networks with $\lambda > 4$ the scaling behavior of $\ell_{\rm opt}$ is the same as for ER graphs and for $\lambda < 4$ the

scaling is different, we can regard SF networks as a generalization of ER graphs.

Next, we describe the details of the numerical simulations and show that the results agree with the above theoretical predictions. We perform numerical simulations in the strong disorder limit by the method described in Sec. 2.4 for ER and SF networks. We also perform additional simulations for the case of strong disorder on ER networks using the ultrametric optimization algorithm (see Sec. 2.3) and find results identical to the results obtained by randomly removing links. In Fig. 4(a) we show a double logarithmic plot of $\ell_{\rm opt}$ as a function of $N$ for ER graphs. To evaluate the asymptotic value for $\nu_{\rm opt}$ we use successive slopes for both approaches, defined as the successive slopes

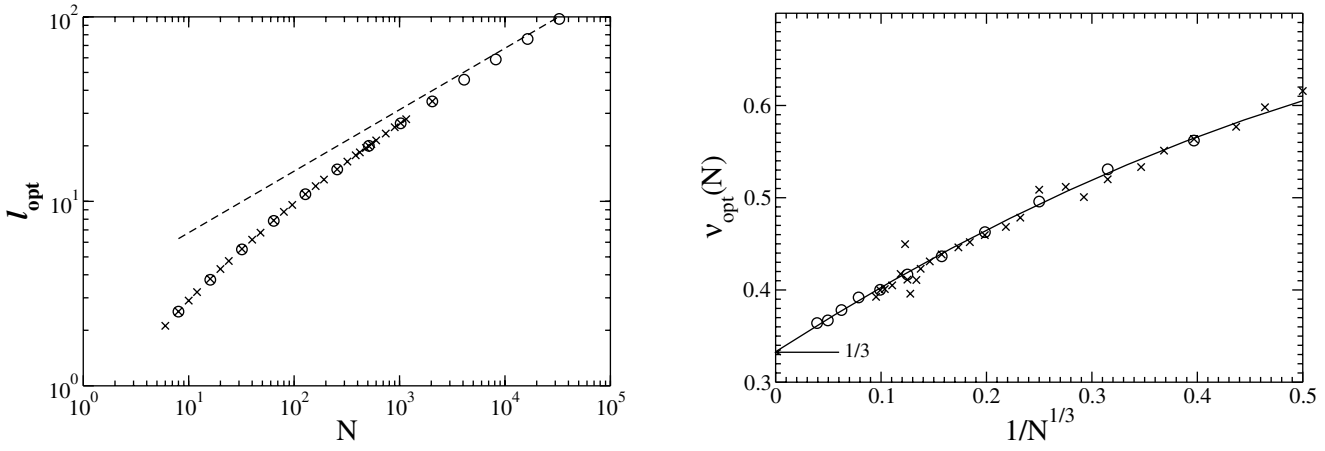


(a) (b)

Fig. 4. (a) Plot of $\ell_{\rm opt}$ as a function of $N$ in double logarithmic scale for the optimal path length in strong disorder using the two numerical methods discussed in the text: (i) results obtained using the "bombing" approach (○) and (ii) results obtained using the ultrametric approach (×). The dashed line shows the slope 1/3. (b) Successive slopes $\nu_{\rm opt}(N)$ as a function of $1/N^{1/3}$ for the optimal path length in strong disorder using the two methods described in the text. The symbols denote the same as in (a). The dashed line is the quadratic fitting of the results showing that the extrapolated value of the effective exponent in the limit $N \to \infty$ approaches 1/3. This result coincides with our theoretical value $\nu_{\rm opt} = 1/3$ asymptotically (after [Braunstein *et al.*, 2003; Havlin *et al.*, 2005]).

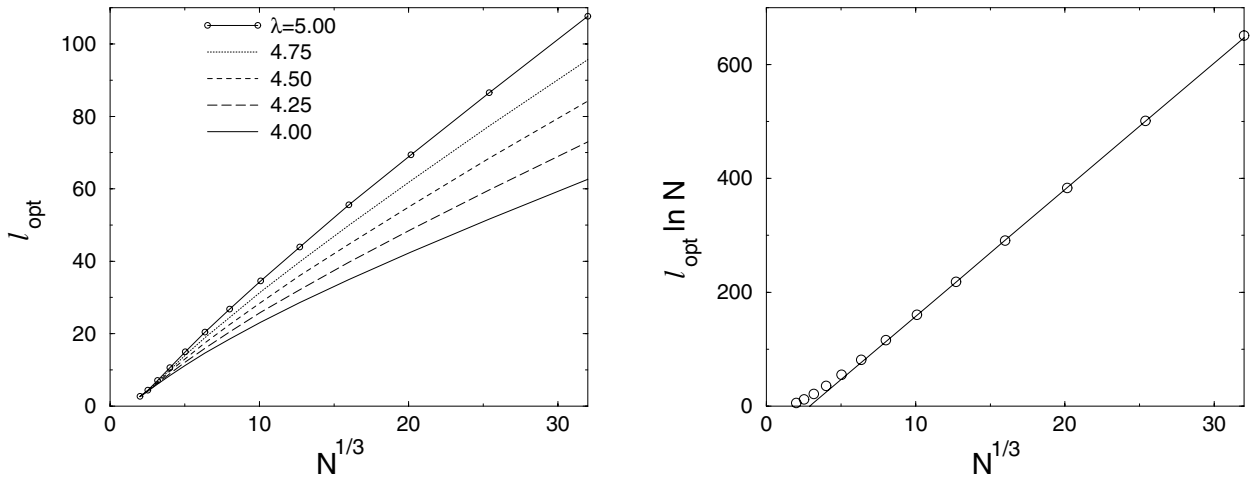


(a) (b)

Fig. 5. Results of numerical simulations. (a) The dependence of $\ell_{\rm opt}$ on $N^{1/3}$ for $\lambda \geq 4$. (b) The dependence of $\ell_{\rm opt}/\ln N$ on $N^{1/3}$ for $\lambda = 4$. (c) The dependence of $\ell_{\rm opt}$ on $N^{(\lambda-3)/(\lambda-1)}$ for $3 < \lambda < 4$. (d) The dependence of $\ell_{\rm opt}$ on $\ln N$ for $\lambda \leq 3$ (after [Braunstein *et al.*, 2003; Havlin *et al.*, 2005]).

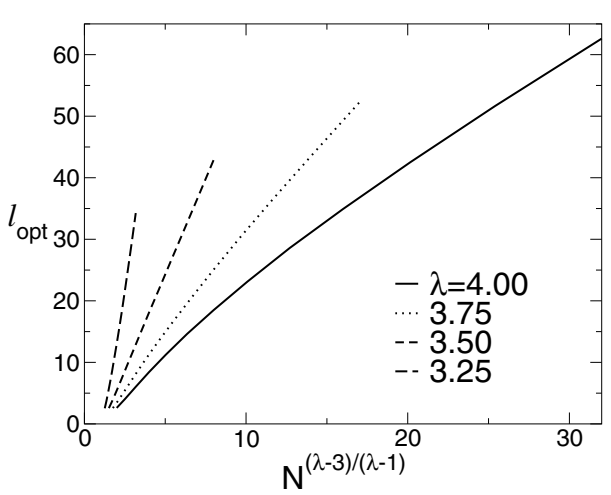


(c)

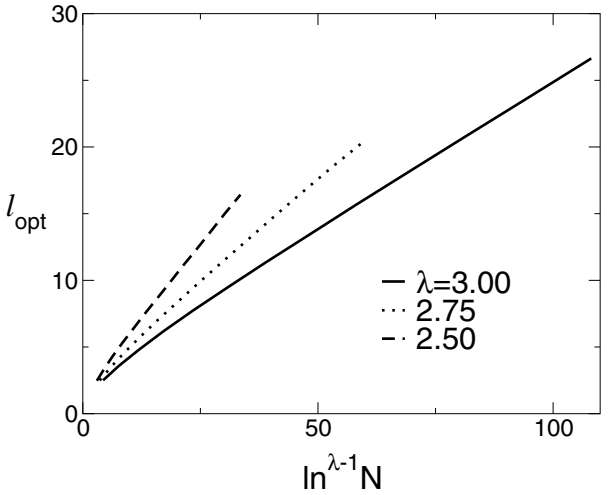


(d)

Fig. 5. (*Continued*)

[Braunstein *et al.*, 2001] of the values in Fig. 4. One can see from Fig. 4(b) that their value approaches 1/3 when $N \gg 1$, supporting Eq. (40).

The theoretical considerations [Eqs. (40) and (41)] predict that SF graphs with $\lambda > 4$, are similar to ER with $\ell_{\text{opt}} \sim N^{1/3}$, while for SF graphs with $3 < \lambda < 4$, $\ell_{\text{opt}} \sim N^{(\lambda-3)/(\lambda-1)}$. Figure 5(a) shows data from numerical simulations supporting the linear behavior of $\ell_{\text{opt}}$ versus $N^{1/3}$ for $\lambda \geq 4$. The quality of the linear fit becomes poor for $\lambda \to 4$. At this value, there are corrections probably due to logarithmic divergence of the second moment of the degree distribution, i.e. $\ell_{\text{opt}} \sim N^{1/3}/\ln N$ [see Fig. 5(b)]. Figure 5(c) shows results of simulations supporting the asymptotic linear behavior of $\ell_{\text{opt}}$ versus $N^{(\lambda-3)/(\lambda-1)}$ for $3 < \lambda \leq 4$. Theoretically, as $\lambda \to 3$, $\nu_{\text{opt}} = (\lambda-3)/(\lambda-1) \to 0$, and thus one can expect for $\lambda = 3$ a logarithmic $N$ dependence of $\ell_{\text{opt}}$. Indeed, for $2 < \lambda < 3$ our numerical results for the strong disorder limit suggest that $\ell_{\text{opt}}$ scales slower than a power law with $N$ but slightly faster than $\ln N$. The numerical results can be fit to $\ell_{\text{opt}} \sim (\ln N)^{\lambda-1}$ [see Fig. 5(d)]. Note that the correct asymptotic behavior may be different and this result may represent only a crossover regime. The exact nature of the percolation cluster at $\lambda < 3$ is not clear yet, since in this regime the transition does not occur at a finite (nonzero) critical threshold [Cohen *et al.*, 2000]. We obtain similar results for SF networks where the weights are associated with nodes instead of links.

## 5. Scaling of the Length of the Optimal Path in Weak Disorder

When $a = 1/kT \to 0$, all the $\tau_i$ essentially contribute to the total cost. Thus $T \to \infty$ (very high temperatures) corresponds to weak disorder limit. We expect that the optimal path length in the weak disorder case will not be considerably different from the shortest path, as found also for regular lattices [Smailer *et al.*, 1993] and random graphs [van der Hofstad *et al.*, 2001]. Thus we expect that the scaling for the shortest path will also be valid for the optimal path in weak disorder, but with a different prefactor depending on the details of the graph and on the type of disorder. We simulate weak disorder by selecting $0 \leq \tau_i < 1$ from a uniform distribution. To compute $\ell_{\text{opt}}$, we use the Dijkstra algorithm (see Sec. 2.2) [Cormen *et al.*, 1990]. The scaling of the length of the optimal path in WD for ER, is shown in Fig. 6(a). Here we plot $\ell_{\text{opt}}$ as a function of $\ln N$ for $\langle k \rangle = 4$. The weak disorder does not change the scaling behavior of $\ell_{\text{opt}}$ on ER compared to $\ell_{\min}$, only the prefactor.

For SF networks, the behavior of the optimal path in the weak disorder limit is shown in Fig. 6(b) for different degree distribution exponents $\lambda$. Here we plot $\ell_{\text{opt}}$ as a function of $\ln N$. All the curves seem to have linear asymptotes. This result is analogous to the behavior of the shortest path $\ell_{\min} \sim \ln N$ for $3 < \lambda < 4$ and ER. Note, however, that for $2 < \lambda < 3$, $\ell_{\min}$ scale as $\ln \ln N$ [Cohen & Havlin, 2003]. Thus, $\ell_{\text{opt}}$ is significantly larger and scales as $\ln N$ [Fig. 3(b)]. Thus, weak disorder does

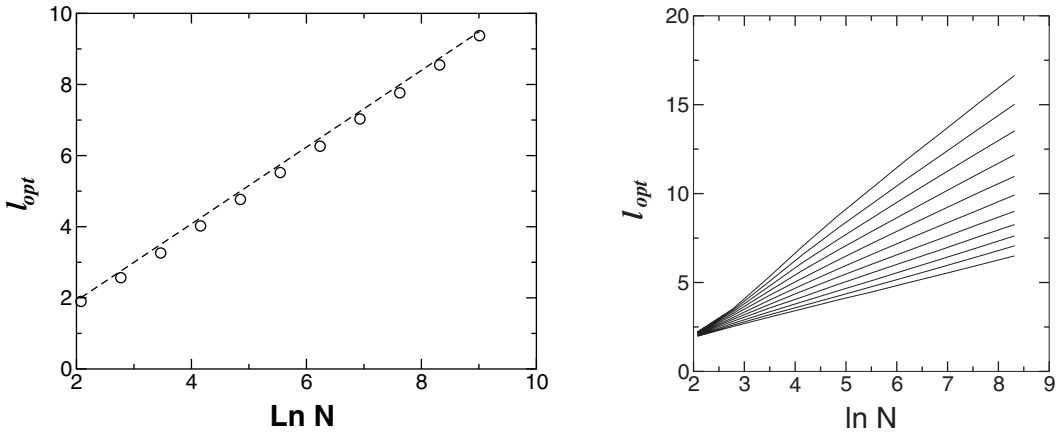


(a) (b)

Fig. 6. Results of numerical simulations. (a) The linear dependence of $\ell_{\rm opt}$ on $\ln N$ for ER graphs in the weak disorder case for $\langle k\rangle = 4$. The dashed line is used as a guide to show the linear dependence. (b) The dependence of $\ell_{\rm opt}$ on $\ln N$ for SF graphs in the weak disorder case for various values of $\lambda$. The different curves represent different values of $\lambda$ from 2.5 (bottom) to 5 (top) (after [Sreenivasan *et al.*, 2004; Sreenivasan *et al.*, 2005]).

not change the universality class of the length of the optimal path except in the case of "ultra-small" worlds $2 < \lambda < 3$, where $\ell_{\rm opt} \sim \exp(\ell_{\rm min})$, and the networks become small worlds.

## 6. Crossover from Weak to Strong Disorder

### 6.1. *Exponential disorder*

Consider the case of finite $a$ ($T > 0$). In this case we expect a crossover in the length of the optimal path (or the system size $N$) from strong disorder behavior to weak disorder depending on the value of $a$. In order to study this crossover we have to use an implementation of disorder that can be tuned to realize narrow distributions of link weights (WD) as well as broad distributions of link weights (SD). The procedure that we adopt to implement the disorder is as follows [Cieplak *et al.*, 1996; Porto *et al.*, 1999; Braunstein *et al.*, 2001; Braunstein *et al.*, 2003] (see Sec. 4.1). Assign to each link $i$ of the network a random number $r_i$, uniformly distributed between 0 and 1. For the analogy with the thermally activated process described in Sec. 4 the $r_i$ play the role of the energy barriers. The transit time or cost associated with link $i$ is then $\tau_i \equiv \exp(ar_i)$, where $a$ controls the strength of disorder i.e. the broadness of the distribution of link weights. The limit $a \to \infty$ is the strong disorder limit, where a single link dominates the cost of the path. For $d$-dimensional lattices of size $L$, the crossover is found [Cieplak *et al.*, 1996; Porto *et al.*, 1999] to behave as

$$\ell_{\rm opt} \sim \begin{cases} L^{d_{\rm opt}}, & L \ll a^{\nu}; \\ L, & L \gg a^{\nu}. \end{cases} \tag{42}$$

where $\nu$ is the percolation correlation exponent [Strelniker *et al.*, 2004; Wu *et al.*, 2005]. For $d = 2$, $d_{\rm opt} \approx 1.22$ and for $d = 3$, $d_{\rm opt} \approx 1.44$ [Cieplak *et al.*, 1996; Porto *et al.*, 1999]. Here we show [Sreenivasan *et al.*, 2004] that for any network of size $N$ and any finite $a$, there exists a crossover network size $N^*(a)$ such that for $N \ll N^*(a)$ the scaling properties of the optimal path are in the strong disorder regime, while for $N \gg N^*(a)$ the typical optimal paths are in the weak disorder regime. We evaluate below the function $N^*(a)$.

In general, the average optimal path length $\ell_{\rm opt}(a)$ in a weighted network depends on $a$ as well as on $N$. In the following, we use instead of $N$ the min-max path length $\ell_\infty$ which is related to $N$ as $\ell_\infty \equiv \ell_{\rm opt}(\infty) \sim N^{\nu_{\rm opt}}$ [Eqs. (40) and (41)] and hence $N$ can be expressed in terms of $\ell_\infty$,

$$N \sim \ell_\infty^{1/\nu_{\rm opt}}. \tag{43}$$

Thus, for finite $a$, $\ell_{\rm opt}(a)$ depends on both $a$ and $\ell_\infty$. We expect a crossover length $\ell^*(a)$, which corresponds to the crossover network size $N^*(a)$, such that (i) for $\ell_\infty \ll \ell^*(a)$, the scaling properties of $\ell_{\rm opt}(a)$ are of the strong disorder regime, and (ii) for $\ell_\infty \gg \ell^*(a)$, the scaling properties of $\ell_{\rm opt}(a)$ are of the weak disorder regime. In Fig. 7, we show a schematic representation of the changes of the optimal path as the network size increases.

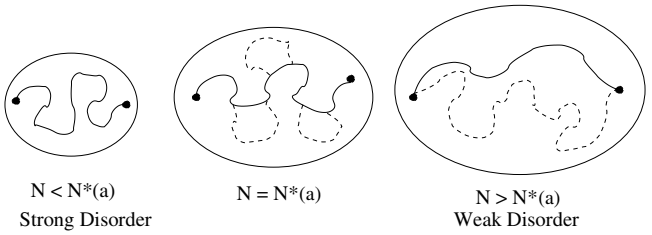


Fig. 7. Schematic representation of the transition in the topology of the optimal path with system size $N$ for a given disorder strength $a$. The solid line shows the optimal path at a finite value of $a$ connecting two nodes indicated by the filled circles. The portion of the min-max path that is distinct from the optimal path is indicated by the dashed line. (a) For $N \ll N^*(a)$ (i.e. $\ell_\infty \ll \ell^*(a)$), the optimal path coincides with the min-max path, and we expect the statistics of the SD limit. (b) For $N = N^*(a)$ (i.e. $\ell_\infty = \ell^*(a)$), the optimal path starts deviating from the min-max path. (c) For $N \gg N^*(a)$ (i.e. $\ell_\infty \gg \ell^*(a)$), the optimal path has almost no links in common with the min-max path, and we expect the statistics of the WD limit (after [Sreenivasan *et al.*, 2004; Sreenivasan *et al.*, 2005]).

In order to study the transition from strong to weak disorder, we introduce a measure which indicates how close or far the disordered network is from the limit of strong disorder. A natural measure is the ratio

$$W(a) \equiv \frac{\ell_{\rm opt}(a)}{\ell_\infty}. \tag{44}$$

Using the scaling relationships between $\ell_{\rm opt}(a)$ and $N$ in both regimes, and $\ell_\infty \sim N^{\nu_{\rm opt}}$, we get

$$\ell_{\rm opt}(a) \sim \begin{cases} \ell_\infty \sim N^{\nu_{\rm opt}} & [\text{SD}] \\ \ln \ell_\infty \sim \ln N & [\text{WD}] \end{cases}. \tag{45}$$

From Eqs. (44) and (45) it follows,

$$W(a) \sim \begin{cases} \text{const} & [\text{SD}] \\ \dfrac{\ln \ell_\infty}{\ell_\infty} & [\text{WD}] \end{cases}. \tag{46}$$

We propose the following scaling Ansatz for $W(a)$,

$$W(a) = F\left(\frac{\ell_\infty}{\ell^*(a)}\right), \tag{47}$$

where

$$F(u) \sim \begin{cases} \text{const} & u \ll 1 \\ \dfrac{\ln(u)}{u} & u \gg 1, \end{cases} \tag{48}$$

with

$$u \equiv \frac{\ell_\infty}{\ell^*(a)}. \tag{49}$$

We now develop analytic arguments [Sreenivasan *et al.*, 2004] to obtain the dependence of the crossover length $\ell^*$ on the disorder strength $a$. These arguments will also give a clearer picture about the nature of the transition of the optimal path with disorder strength.

We begin by making few observations about the min-max path. In Fig. 8, we plot the average value of the random numbers $r_n$ on the min-max path as a function of their rank $n$ ($1 \le n \le \ell_\infty$) for ER networks with $\langle k \rangle = 4$ and for SF networks with $\lambda = 3.5$. This can be done for a min-max path of any length but in order to get good statistics we use the most probable min-max path length. We call links with $r \le p_c$ "black" links, and links with $r > p_c$ "gray" links, following the terminology of Ioselevich and Lyubshin [2004] where $p_c$ is the percolation threshold of the network [Cohen *et al.*, 2000].

We make the following observations regarding the min-max path:

(i) For $r_n < p_c$, the values of $r_n$ decrease linearly with rank $n$, implying that the values of $r$ for black links are uniformly distributed between 0 and $p_c$, consistent with the results of [Szabó *et al.*, 2003]. This is shown in Fig. 8.
(ii) The average number of black links, $\langle \ell_b \rangle$, along the min-max path increases linearly with the average path length $\ell_\infty$. This is shown in Fig. 9(a).
(iii) The average number of gray links $\langle \ell_g \rangle$ along the min-max path increases logarithmically with the average path length $\ell_\infty$ or, equivalently, with the network size $N$. This is shown in Fig. 9(b).

The simulation results presented in Fig. 9 are for ER networks; however, we have confirmed that the observations (ii) and (iii) are also valid for SF networks with $\lambda > 3$ [Sreenivasan *et al.*, 2004; Kalisky *et al.*, 2006].

Next we discuss our observations using the concept of the MST. The path on the MST between any two nodes $A$ and $B$, is the optimal path between the nodes in the strong disorder limit — i.e. the min-max path.

In order to construct the MST we use the bombing algorithm (see Sec. 2.4). At the point that one cannot remove more links without disconnecting the

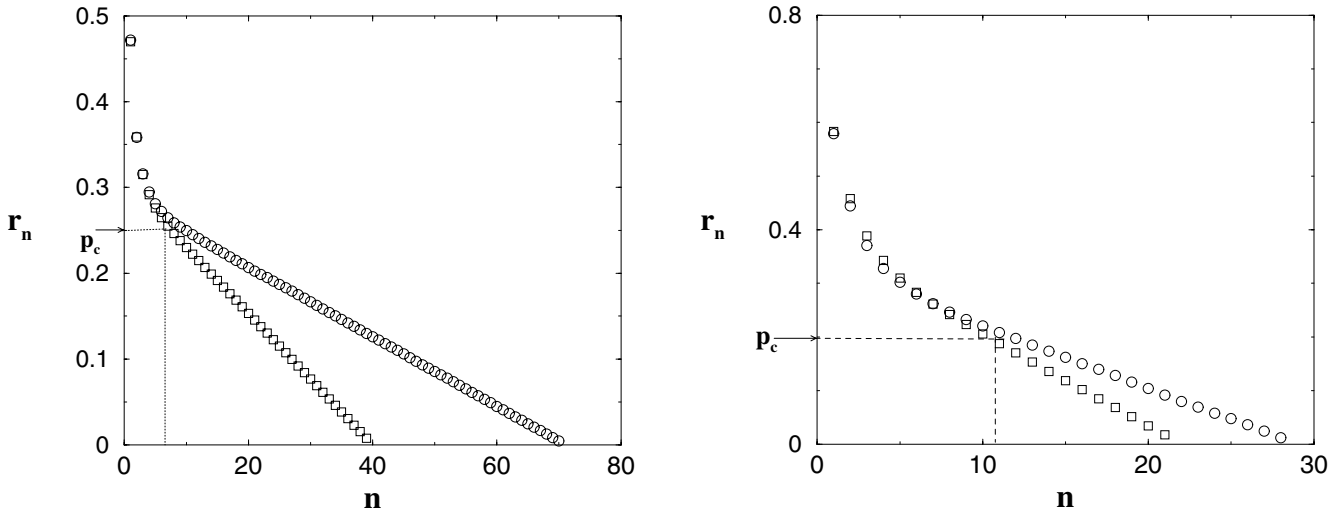


(a) ER (b) SF

Fig. 8. Dependence of rank $n$ on the average values of the random numbers $r_n$ along the most probable optimal path for (a) ER random networks of two different sizes $N = 4096$ (□) and $N = 16384$ (○) and, (b) SF random networks (after [Sreenivasan *et al.*, 2004; Sreenivasan *et al.*, 2005]).

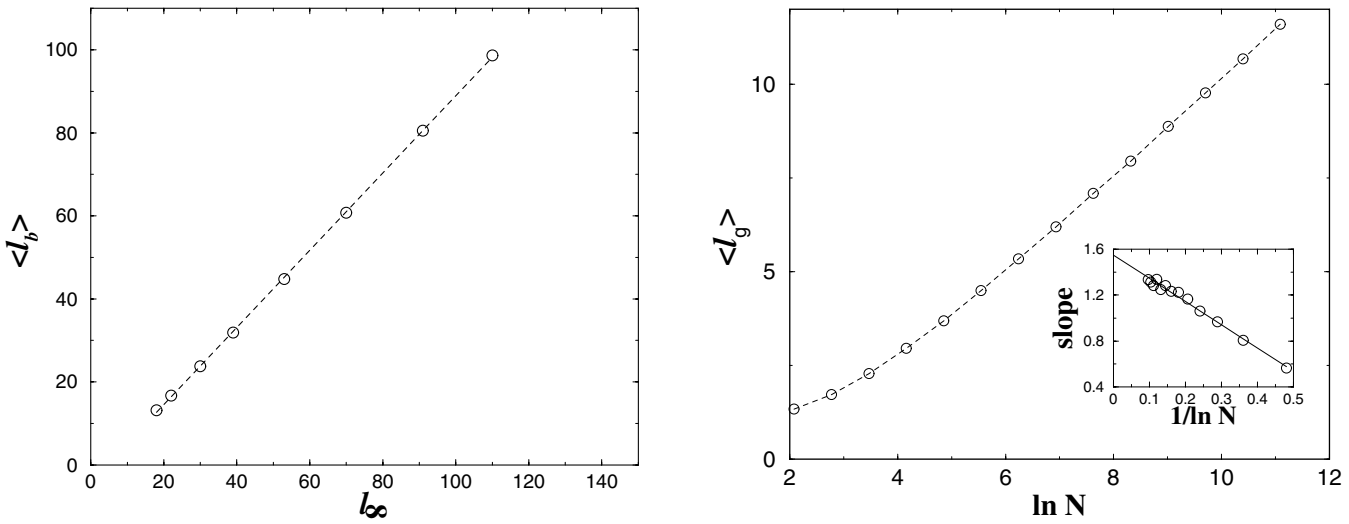


(a) (b)

Fig. 9. (a) The average number of links $\langle \ell_b \rangle$ with random number values $r \leq p_c$ on the min-max path plotted as a function of its length $\ell_\infty$ for an ER network, showing that $\langle \ell_b \rangle$ grows linearly with $\ell_\infty$. (b) The average number of links $\langle \ell_g \rangle$ with random number values $r > p_c$ on the min-max path versus $\ln N$ for an ER network, showing that $\langle \ell_g \rangle \sim \ln N$. The inset shows the successive slopes, indicating that in the asymptotic limit $\langle \ell_g \rangle \approx 1.55 \ln N$ (after [Sreenivasan *et al.*, 2004; Sreenivasan *et al.*, 2005]).

graph, the number of remaining black links is

$$N_b = \frac{N\langle k \rangle p_c}{2}, \tag{50}$$

where $\langle k \rangle$ is the average degree of the original graph and $p_c$ is given by [Cohen *et al.*, 2000]

$$p_c = \frac{\langle k \rangle}{\langle k^2 - k \rangle}. \tag{51}$$

The black links give rise to $N_c$ disconnected clusters. One of these is a spanning cluster, called the *giant component* or IIC (see Sec. 2.6). The $N_c$ clusters are linked together into a connected tree by exactly $N_c - 1$ gray links (see Fig. 10). Each of the $N_c$ clusters is itself a tree, since a random graph can be regarded as an infinite dimensional system, and at the percolation threshold in an infinite dimensional system the clusters can be regarded as trees.

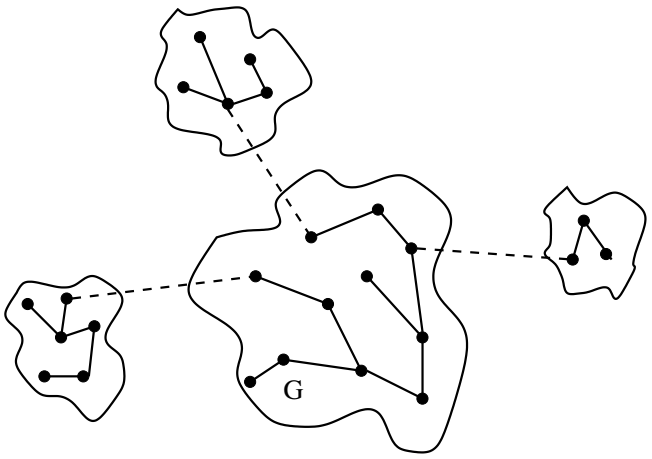


Fig. 10. Schematic representation of the structure of the minimal spanning tree, at the percolation threshold, with G being the giant component. Inside each cluster, the nodes are connected by black links to form a tree. The dotted lines represent the gray links which connect the finite clusters to form the gray tree. In this example $N_c = 4$ and the number of gray links equals $N_c - 1 = 3$ (after [Sreenivasan *et al.*, 2004; Sreenivasan *et al.*, 2005]).

Thus the $N_c$ clusters containing $N_b$ black links, together with $N_c - 1$ gray links form a spanning tree consisting of $N_b + N_c - 1$ links.

Thus the MST provides *all* min-max path between any two sites on the graph. Since the MST connects all $N$ nodes, the number of links on this tree must be $N - 1$, so

$$N_b + N_c = N. \tag{52}$$

From Eqs. (50) and (52) it follows that

$$N_c = N\left(1 - \frac{\langle k\rangle p_c}{2}\right). \tag{53}$$

Therefore $N_c$ is proportional to $N$.

A path between two nodes on the MST consists of $\ell_b$ black links. Since the black links are the links that remain after removing all links with $r > p_c$, the random number values $r$ on the black links are uniformly distributed between 0 and $p_c$ in agreement with observation (i) and [Szabó *et al.*, 2003].

Since there are $N_c$ clusters which include clusters of nodes connected by black links as well as isolated nodes, the MST can be described as an effective tree of $N_c$ "super" nodes, each representing a cluster, and $N_c - 1$ gray links. We call this tree the "gray tree" (see Fig. 10). This tree is in fact a scale free tree[6] [Kalisky *et al.*, 2006] with degree exponent $\lambda_g = 2.5$ for ER networks and scale for networks with $\lambda \geq 4$, and $\lambda_g = (2\lambda - 3)/(\lambda - 2)$ for SF networks with $3 < \lambda < 4$. If we take two nodes A and B on the original network, they will most likely lie on two distinct effective nodes of the gray tree. The number of gray links encountered on the min-max path connecting these two nodes will therefore equal the number of links separating the effective nodes on the gray tree. Hence, the average number of gray links $\langle \ell_g \rangle$ encountered on the min-max path between an arbitrary pair of nodes on the network is simply the average diameter of the gray tree. Our simulation results [see Fig. 9(b)] indicate that

$$\langle \ell_g \rangle \sim \ln N. \tag{54}$$

Since $\langle \ell_g \rangle \sim \ln \ell_\infty \ll \ell_\infty$, the average number of black links $\langle \ell_b \rangle$ on the min-max path scales as $\ell_\infty$ in the limit of large $\ell_\infty$ in agreement with observation (2) as shown in Fig. 9(a).

Next, we discuss the implications of our findings for the crossover from strong to weak disorder. From observations (i) and (ii), it follows that for the portion of the path belonging to the giant component, the distribution of random values $r$ is uniform. Hence we can approximate the sum of weights by [Kalisky *et al.*, 2005],

$$\begin{aligned}\sum_{k=1}^{\ell_b} \exp(ar_k) &\approx \frac{\ell_b}{p_c}\int_0^{p_c} \exp ar dr \\ &= \frac{\ell_b}{ap_c}(\exp(ap_c) - 1) \\ &\equiv \exp(ar^*),\end{aligned} \tag{55}$$

where $r^* \approx p_c + (1/a)\ln(\langle \ell_b \rangle / ap_c)$. Since $\langle \ell_b \rangle \approx \ell_\infty$,

$$r^* \approx p_c + \frac{1}{a}\ln\left(\frac{\ell_\infty}{ap_c}\right). \tag{56}$$

Thus restoring a short-cut link between two nodes on the optimal path with $p_c < r < r^*$ may drastically reduce the length of the optimal path. When $ap_c \gg \ell_\infty$, $r^* < p_c$ and such a link does not exist, if $\ell_\infty > ap_c$, the probability that such a link exists becomes positive. Hence when the min-max path is of length $\ell_\infty \approx ap_c$, the optimal path starts deviating from the min-max path. The length of the

[6]This is a consequence of the fact that for the original network the clusters at percolation have sizes $s$ distributed as $P(s) \sim s^{-\tau}$ [Cohen *et al.*, 2002], (with $\tau = 2.5$ for ER networks and for SF networks with $\lambda \geq 4$, and $\tau = (2\lambda - 3)/(\lambda - 2)$ for SF networks with $3 < \lambda < 4$) and each node within this cluster has a nonzero probability of connecting to a node outside the cluster.

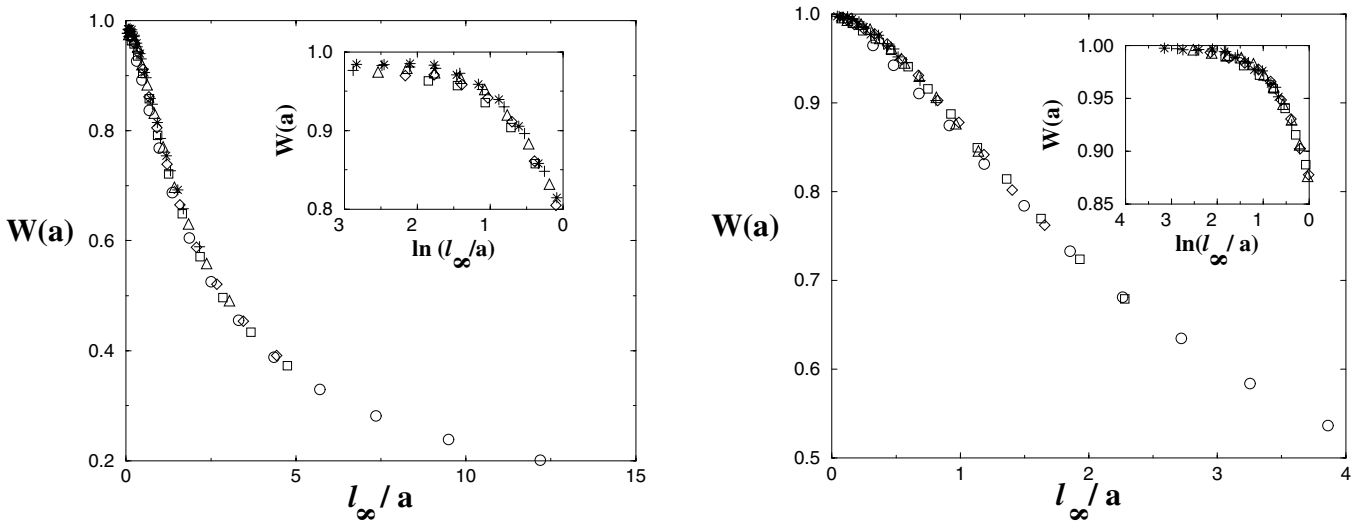


(a) ER (b) SF

Fig. 11. Test of Eqs. (47) and (48). (a) $W(a)$ plotted as a function of $\ell_\infty/a$ for different values of $a$ for ER networks with $\langle k\rangle = 4$. The different symbols represent different $a$ values: $a = 8(\bigcirc)$, $a = 16(\square)$, $a = 22(\diamond)$, $a = 32(\triangle)$, $a = 45(+)$ and $a = 64(*)$. (b) Same as SF networks with $\lambda = 3.5$. The symbols correspond to the same values of disorder as in (a). The insets show $W(a)$ plotted against $\log(l_\infty/a)$, and indicate for $\ell_\infty \ll a$, $W(a)$ approaches a constant in agreement with Eq. (48) (after [Sreenivasan *et al.*, 2004; Sreenivasan *et al.*, 2005]).

min-max path at which the deviation first occurs is precisely the crossover length $\ell^*(a)$, and therefore $\ell^*(a) \sim ap_c$. In the case of a network with an arbitrary degree distribution, we can write using Eq. (51), $\ell^*(a) \sim a(\langle k\rangle/\langle k^2 - k\rangle)$.

Note that in the case of SF networks, as $\lambda \to 3^+$, $p_c$ approaches zero and consequently $\ell^*(a) \to 0$. This suggests that for any finite value of disorder strength $a$, a SF network with $\lambda \leq 3$ is in the weak disorder regime. We perform numerical simulations and show that the results agree with our theoretical predictions. For the details of our simulation methods, see Sec. 2.

From our theoretical arguments, $\ell^*(a) \sim a$ and therefore, from Eq. (47), $W(a)$ must be a function of $\ell_\infty/a$. In Fig. 11 we show the ratio $W(a)$ for different values of $a$ plotted against $\ell_\infty/\ell^*(a) \equiv \ell_\infty/a$ for ER networks with $\langle k\rangle = 4$, and for SF networks with $\lambda = 3.5$. The excellent data collapse is consistent with the scaling relations Eq. (47). Figure 12 shows the scaled quantities $W(a)u = \ell_{\rm opt}(a)/\ell^*(a)$ versus $\ln u \equiv \ln(\ell_\infty/\ell^*(a)) \equiv \ln(\ell_\infty/a)$, for both ER networks with $\langle k\rangle = 4$ and for SF networks with $\lambda = 3.5$. The curves are linear at large $u \equiv \ell_\infty/\ell^*(a)$, supporting the validity of the logarithmic term in Eq. (48) for large $u$.

To summarize, for both ER random networks and SF networks we obtain a scaling function for the crossover from weak disorder characteristics to strong disorder characteristics. We show that the crossover occurs when the min-max path reaches a crossover length $\ell^*(a)$ and $\ell^*(a) \sim a$. Equivalently, the crossover occurs when the network size $N$ reaches a crossover size $N^*(a)$, where $N^*(a) \sim a^3$ for ER networks and for SF networks with $\lambda \geq 4$ and $N^*(a) \sim a^{(\lambda-1)/(\lambda-3)}$ for SF networks with $3 < \lambda < 4$.

### 6.2. *General disorder: Criterion for SD, WD crossovers*

Until now we considered a specific form of $P(\tau) \equiv P(\tau, a) = 1/(a\tau)$ with $1 < \tau < e^a$. The question is what happens for other distributions of weights and what is the general criterion to determine which form of $P(\tau)$ can lead to strong disorder, and what is the general condition for strong or weak disorder crossover. We present analytical results [Chen *et al.*, 2006] for such a criterion which are supported by extensive simulations. Using this criterion we show that certain power law distributions and log-normal distributions, $P(\tau, a)$, where $a$ is a parameter determining the broadness of the distribution, can lead to strong disorder and a weak-strong disorder crossover [Porto *et al.*, 1999; Braunstein *et al.*, 2003; Sreenivasan *et al.*, 2004]. We also show that for $P(\tau, a)$ uniform, Poisson or Gaussian, only weak disorder occurs regardless of the broadness

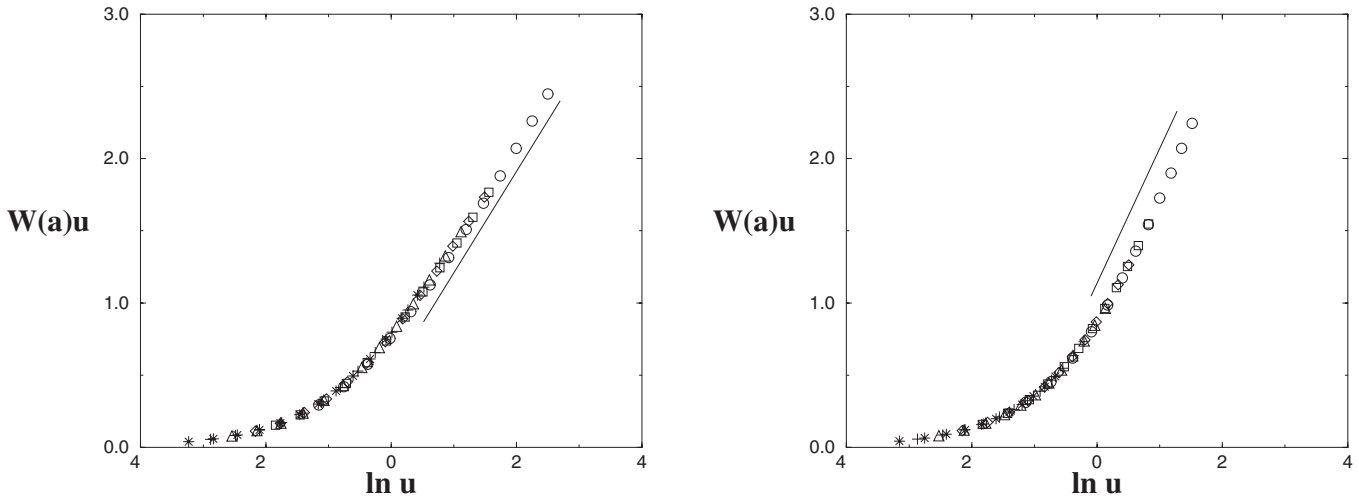


(a) ER (b) SF

Fig. 12. (a) Plot of $W(a)u = \ell_{\rm opt}(a)/\ell^*(a) = \ell_{\rm opt}(a)/a$ versus $\ln u \equiv \ln(\ell_\infty/\ell^*(a)) = \ln(\ell_\infty/a)$ for ER networks with $\langle k\rangle = 4$ for different values of $a$. (b) Plot of $W(a)u = \ell_{\rm opt}(a)/\ell^*(a) = \ell_{\rm opt}(a)/a$ versus $\ln u = \ln(\ell_\infty/\ell^*(a)) = \ln(\ell_\infty/a)$ for SF networks with $\lambda = 3.5$. The values of $a$ represented by the symbols in (a) and (b) are the same as in Fig. 8 (after [Sreenivasan *et al.*, 2004; Sreenivasan *et al.*, 2005]).

of $P(\tau, a)$. Importantly, we find that for all $P(\tau, a)$ that possess a strong-weak disorder crossover, the distributions of the optimal path lengths display the same universal behavior.

If we express $\tau$ in terms of a random variable $r$ uniformly distributed in $[0, 1]$, we can use the same gray and black link formalism as in the previous section. This can be achieved by defining $r(\tau)$ as a relation:

$$r(\tau) = \int_0^\tau P(\tau', a)d\tau'. \tag{57}$$

Solving this equation with respect to $\tau$ gives us $\tau(r, a) = f(r, a)$, where $f(r, a)$ satisfies the relation

$$r = \int_0^{f(r,a)} P(\tau', a)d\tau'. \tag{58}$$

For a strong disorder regime, the sum of the weights of the black links on the IIC must be smaller than the smallest weight of the removed link $\tau_c = f(p_c, a)$:

$$\sum_{i=1}^{\ell_b} \tau_i = \sum_{i=1}^{\ell_b} f(r_i, a) < \tau_c, \tag{59}$$

where $r_i$ are independent random variables uniformly distributed on $[0, p_c]$. As we have shown above, $\ell_b \approx \ell_\infty$ so in the following we will replace $\ell_b$ by the average path length in the strong disorder limit, $\ell_\infty$. The transition to weak disorder begins when the probability that this sum is greater than $\tau_c$ becomes substantial. The investigation of this condition belongs to the realm of pure mathematics and can be answered explicitly for any functional form $f(r, a)$. This condition is satisfied when the mathematical expectation of the sum is greater than $\tau_c$.

$$\frac{\ell_\infty}{p_c}\int_0^{p_c} f(r, a)dr > \tau_c. \tag{60}$$

Thus the crossover to weak disorder happens if

$$\ell_\infty > A \equiv \frac{f(p_c, a)p_c}{\displaystyle\int_0^{p_c} f(r, a)dr} = \frac{\tau_c p_c}{\displaystyle\int_0^{\tau_c} \tau P(\tau, a)d\tau}, \tag{61}$$

where $A$ plays the role of the disorder strength and $\tau_c$ satisfies the equation $p_c = \int_0^{\tau_c} P(\tau, a)d\tau$. In order for the strong disorder to exist for any network size $N$, the disorder strength must diverge together with the parameter $a$ of the weight distribution $a \to \infty$. In order to determine if a network exhibits a strong disorder behavior it is useful to introduce a scaling variable

$$Z \equiv \frac{\ell_\infty}{A}, \tag{62}$$

so that if $Z \gg 1$ the network is in the weak disorder regime and if $Z \ll 1$, the network is in the strong disorder regime.

Note that if $f'/f > A_0$ on the entire interval $[0, 1]$, then $A > A_0 p_c$. Thus, another sufficient

condition for a strong disorder to exist is

$$\frac{f'}{f} > \frac{\ell_\infty}{p_c}. \tag{63}$$

For the exponential disorder function $\tau = \exp(ar)$, we have $f'/f = a$ and thus Eq. (63) coincides with the condition of strong disorder $ap_c > \ell_\infty$ derived in the previous section.

In the following, we will show how the above condition is related to the strong to weak crossover condition for the optimal path on lattices [Cieplak *et al.*, 1996; Porto *et al.*, 1999; Buldyrev *et al.*, 2006]. For the optimal path in the strong disorder limit connecting the opposite sides of the lattice of linear size $L$, the largest random number $r_1$ follows a distribution characterized by a width which scales as $L^{-1/\nu}$, where $\nu$ is the percolation connectivity length exponent [Stauffer & Aharony, 1994; Bunde & Havlin, 1996; Coniglio, 1982; Kalisky & Cohen, 2006]. The transition to weak disorder starts when the optimal path may prefer to go through a slightly larger value $r_2$, taken from the same distribution and thus $r_2 - r_1 \sim p_c L^{-1/\nu}$. The condition for this to happen is $[f(r_2) - f(r_1)]/f(r_1) < 1$, which is equivalent to

$$\frac{f'}{f} < \frac{L^{1/\nu}}{p_c}. \tag{64}$$

Now we will show that this condition is equivalent to (63). Percolation on Erdős–Rényi (ER) networks is equivalent to percolation on a lattice at the upper critical dimension $d_c = 6$ [Bunde & Havlin, 1996; Cohen *et al.*, 2002]. For $d = 6$, $L \sim N^{1/6}$ and $\nu = 1/2$. Thus indeed $L^{1/\nu} \sim N^{1/(d_c\nu)} \sim \ell_\infty$ [Braunstein *et al.*, 2003].

Following similar arguments for a scale-free network with degree distribution $P(k) \sim k^{-\lambda}$ and $3 < \lambda < 4$, we can replace $L^{-1/\nu}$ by $N^{-(\lambda-3)/(\lambda-1)}$ since $d_c = 2(\lambda-1)/(\lambda-3)$ [Cohen *et al.*, 2002]. Thus, due to Eq. (38) $L^{1/\nu} \sim \ell_\infty$ and we can introduce the analogous scaling parameter $Z$ for lattices:

$$Z = \frac{L^{1/\nu}}{\dfrac{p_c f'}{f}}. \tag{65}$$

Next we calculate $A$ for several specific weight distributions $P(\tau)$ [Chen *et al.*, 2006]. We begin with the well-studied exponential disorder function $f(x) = e^{ar}$, where $r$ is a random number between 0 and 1 [Strelniker *et al.*, 2004; Cieplak *et al.*, 1996]. From Eq. (58) follows that $P(\tau, a) = 1/(a\tau)$, where $\tau \in [1, e^a]$. Using Eq. (61) we have

$$A = \frac{ap_c\tau_c}{\tau_c - 1} \sim ap_c; \tag{66}$$

For fixed $A$, but different $a$ and $p_c$, we expect to obtain the same optimal path behavior. Indeed, this has been shown to be valid [Wu *et al.*, 2005; Strelniker *et al.*, 2004; Kalisky *et al.*, 2005; Chen *et al.*, 2006].

Next we study $A$ for the disorder function $f(r, a) = r^a$, with $r$ between 0 and 1 where $a > 0$ [Hansen & Kertész, 2004]. For this case, the disorder distribution is a power law $P(\tau, a) = a^{-1}\tau^{1/a-1}$. Following Eq. (61) we obtain

$$A = a + 1 \sim a. \tag{67}$$

Note that here $a$ plays a similar role as $a$ in Eq. (66), but now $A$ is independent of $p_c$, which means that networks with different $p_c$, such as ER networks with different average degree $\langle k\rangle = 1/p_c$, yield the same optimal path behavior.

For the power law distribution with negative exponent $f(r) = (1-r)^{-a}$ $(a > 0)$, we have $P(\tau, a) = a^{-1}\tau^{-1-1/a}$ and

$$A = \frac{(a-1)p_c(1-p_c)^{-a}}{(1-p_c)^{1-a} - 1} \sim \frac{ap_c}{1-p_c}. \tag{68}$$

We further generalize the power law distribution with the disorder function $f(r, a) = r^a$ by introducing the parameter $0 \le \Delta \le 1$ which is defined as the lower bound of the uniformly distributed random number $r$, i.e. $1 - \Delta \le r \le 1$ [Hansen & Kertész, 2004]. Under this condition, the distribution becomes

$$P(\tau, a) = \frac{\tau^{1/a-1}}{|a|\Delta} \qquad \tau \in [(1-\Delta)^a, 1]. \tag{69}$$

Again using Eq. (61), we obtain

$$A = \frac{ap_c\Delta}{p_c\Delta + 1 - \Delta}. \tag{70}$$

Table 1 shows the results of similar analysis for the lognormal, Gaussian, uniform and exponential distributions $P(\tau, a)$. From Table 1, we see that for exponential function, power law and lognormal distributions, $A$ is proportional to $a$ and can thus become large. However for uniform, Gaussian and exponential distributions, $A$ is limited to a value of order 1, so $Z \gg 1$ for large $N$ and the optimal path is always in the weak disorder regime. Note that for these distributions, $A$ is independent of $a$.

In general, one can prove that $A \to \infty$ for a given distribution $P(\tau, a)$ as $a \to \infty$ if there exist

Table 1. Parameters controlling the optimal paths on networks for various distributions of disorder (after [Chen *et al.*, 2006]).

| Name | Function | Distribution | Domain | $A$ |
|---|---|---|---|---|
| Inverse | $e^{ax}$ | $\frac{1}{a\tau}$ | $\tau \in [1, e^a]$ | $ap_c$ |
| Power Law | $x^a$ | $\frac{\tau^{1/a-1}}{a}$ | $\tau \in (0, 1]$ | $a$ |
| Power Law | $(1-x)^a$ | $\frac{1}{a}\tau^{1+1/a}$ | $\tau \in [1, \infty]$ | $a\frac{p_c}{1-p_c}$ |
| Power Law | $x^a$ | $\frac{\tau^{1/a-1}}{\lvert a\rvert\Delta}$ | $\tau \in [(1-\Delta)^a, 1]$ | $a\frac{p_c\Delta}{1-(1-p_c)\Delta}$ |
| Lognormal | $e^{\sqrt{2}a\,\mathrm{erf}^{-1}(2x-1)}$ | $\frac{e^{-(\ln\tau)^2/2a^2}}{\tau a\sqrt{2\pi}}$ | $\tau \in (0, \infty)$ | $a\frac{\sqrt{2\pi}p_c}{e^{-[\mathrm{erf}^{-1}(2p_c-1)]^2}}$ |
| Uniform | $ax$ | $\frac{1}{a}$ | $\tau \in [0, a]$ | 2 |
| Gaussian | $\sqrt{2}a\,\mathrm{erf}^{-1}(x)$ | $\frac{2e^{-\tau^2/(2a^2)}}{a\sqrt{2\pi}}$ | $\tau \in [0, \infty)$ | $\frac{\sqrt{2\pi}p_c\mathrm{erf}^{-1}}{1-e^{-[\mathrm{erf}^{-1}(p_c)]^2}}$ |
| Exponential | $-a\ln(1-x)$ | $\frac{e^{-\tau/a}}{a}$ | $\tau \in [0, \infty)$ | $\frac{-p_c\ln(1-p_c)}{p_c+(1-p_c)\ln(1-p_c)}$ |

a normalization function $c(a)$ and a cutoff function $\tau(a)$ such that for $\forall\,\epsilon > 0, \forall\,\mathrm{E} > 0$, $\exists\,M > 0$ such that for $a > M$ and $\tau \in [\tau(a), \tau(a)\mathrm{E}]$, $|\tau P(\tau, a)c(a) - 1| < \epsilon$. We will call such functions $P(\tau, a)$ "quasi-$1/\tau$" distributions because they behave as $1/\tau$ in a wide range of $\tau$. Obviously the exponential, power-law and lognormal distributions are quasi-$1/\tau$ functions, so for them, for large enough $a$ we can observe a strong disorder.

To test the validity of our theory, we perform simulations of optimal paths in $2d$ square lattices and ER networks. Random weights from different disorder functions were assigned to the bonds. For an $L \times L$ square lattice, we calculate the average length $\ell_{\mathrm{opt}}$ of the optimal path from one lattice edge to the opposite. For an ER network of $N$ nodes, we calculate $\ell_{\mathrm{opt}}$ between two randomly selected nodes.

Simulations for optimal paths on ER networks are shown in Fig. 13. Here, we use the bombing algorithm (see Sec. 2.4 to determine the path length $\ell_\infty$ in the strong disorder limit, which is related to $N$ by $\ell_\infty \sim N^{\nu_{\mathrm{opt}}} = N^{1/3}$ [Braunstein *et al.*, 2003] (see Sec. 4). We see that for all disorder distributions studied, $\ell_{\mathrm{opt}}$ scales in the same universal way with $Z \equiv \ell_\infty/A$. For $Z \gg 1$, $\ell_{\mathrm{opt}}/A$ is linear with $\log(\ell_\infty/A)$ as expected [Fig. 3(a)]. For small $Z = \ell_\infty/A$ [Fig. 13(b)], $\ell_{\mathrm{opt}} \propto \ell_\infty \sim N^{1/3}$, which is the strong disorder behavior [Braunstein *et al.*, 2003]. Thus, we see that when $N$ increases, a crossover from strong to weak disorder occurs in the scaled optimal paths $\ell_{\mathrm{opt}}/A$ versus $Z$. Again, the collapse of all curves for different disorder distributions of ER networks supports the general condition of Eq. (62).

Next we use Eq. (62) to analyze the other types of disorder given in Table 1 that do not have strong disorder behavior. For a uniform distribution, $P(\tau) = 1/a$ and we obtain $A = 1$. The parameter $a$ cancels, so $Z = L^{1/\nu}$ for lattices, and $Z = N^{1/3}$ for ER networks. Hence for any value of $a$, $Z \ll 1$, and strong disorder behavior cannot occur for a uniform distribution.

Next we analyze the Gaussian distribution. We assume that all the weights $\tau_j$ are positive and thus we consider only the positive regime of the distribution. Using Eq. (61) we obtain

$$A = \frac{\sqrt{2\pi}p_c\mathrm{erf}^{-1}}{1-e^{-[\mathrm{erf}^{-1}(p_c)]^2}}. \tag{71}$$

The disorder is controlled solely by $p_c$ which is related only to the type of network, and $A$ cannot take on large values. Thus, also for the Gaussian $P(\tau, a)$, all optimal paths are in the weak disorder regime. Similar considerations lead to the same conclusion for the exponential distribution where $A = -p_c\ln(1-p_c)/(p_c + (1-p_c)\ln(1-p_c))$.

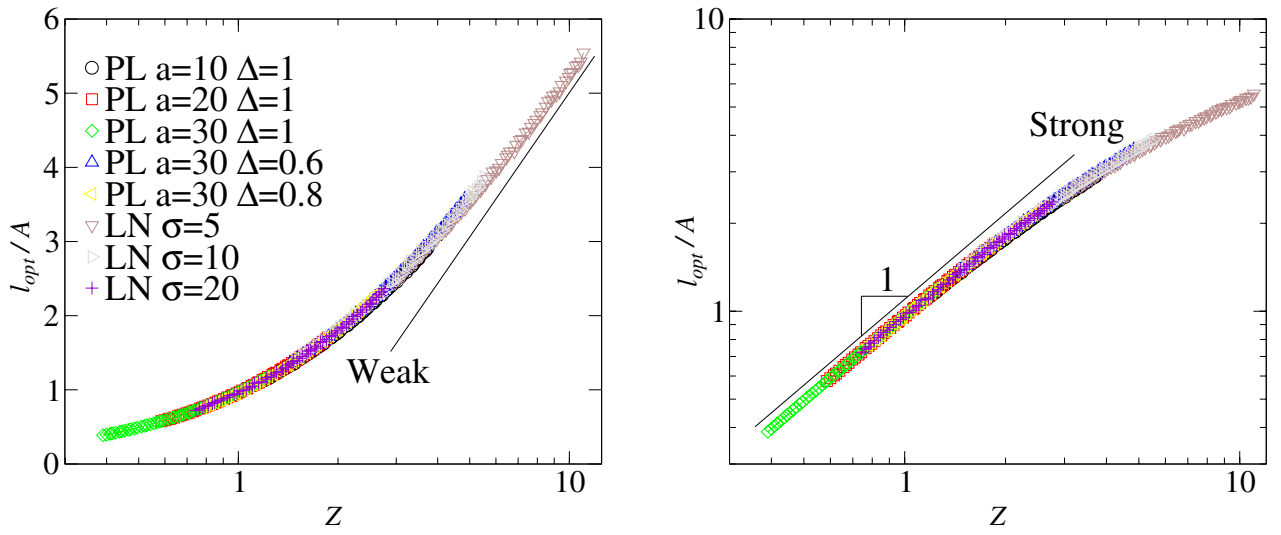


Fig. 13. The function $\ell_{\rm opt}/A$ for ER networks after scaling, where (a) is a linear-log plot and (b) is a log-log plot. Distributions used are power law $x^a$ with $10 \leq a \leq 30$ where $0 \leq x < 1$, $x^a$ with $a = 30$ and the range of $\Delta < x \leq 1$ with $\Delta = 0.6$ or 0.8, and lognormal distribution with $10 \leq a \leq 30$. The straight line in (a) indicates weak disorder and the straight line in (b) indicates strong disorder (after [Chen *et al.*, 2006]).

Simulation results for the Gaussian distribution shown in Fig. 14 display only weak disorder (i.e. no weak-strong disorder crossover), thus supporting the above conclusions.

To summarize, in this section we have presented a criterion for the inverse disorder strength $Z$ on the optimal path in weighted networks for general distributions $P(\tau, a)$. We show an analytical expression, Eq. (61), which fully characterizes the behavior of the optimal path. Simulation of several distributions support these analytical predictions. It is plausible that the criterion of Eq. (61) is valid also for other physical properties in weighted networks — such as conductivity and flow in random resistor networks — due to a recently-found close relation between the optimal path and flow [Strelniker *et al.*, 2004; Wu *et al.*, 2005].

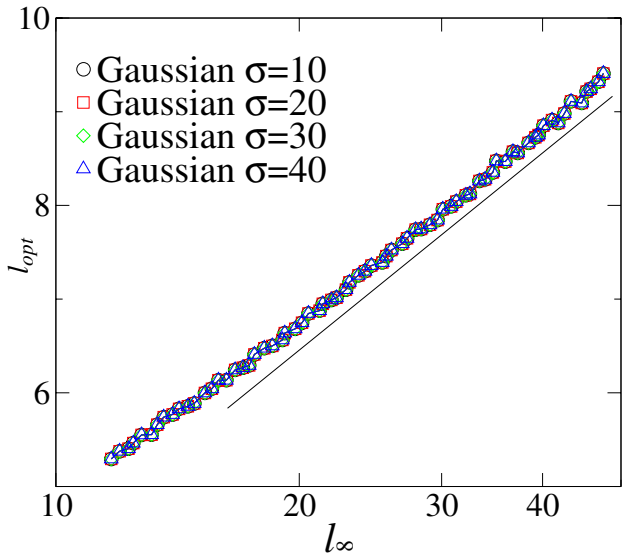


Fig. 14. The optimal path for Gaussian distribution of weights for ER networks. Note that these curves would collapse after scaling to the curves in Fig. 13 in the weak disorder tail of large $Z^{-1}$ (after [Chen *et al.*, 2006]).

## 7. Scaling of Optimal-Path-Lengths Distribution with Finite Disorder in Complex Networks

In this chapter we present further support [Kalisky *et al.*, 2005] for the general analytical results presented in Sec. 6.2. The question is how the different optimal paths in a network are distributed? The distribution of the optimal path lengths is especially important in communication networks, in which the overall network performance depends on the different path lengths between all nodes of the network, and not only the average. Sreenivasan *et al.* [2004] studied the probability distribution $P(\ell_{\rm opt})$ of optimal path lengths in an ER network in the SD limit. The scaled curve for $P(\ell_{\rm opt})$ for different network sizes is shown in Fig. 15 in a log-log plot. We find that similarly to the behavior of self-avoiding

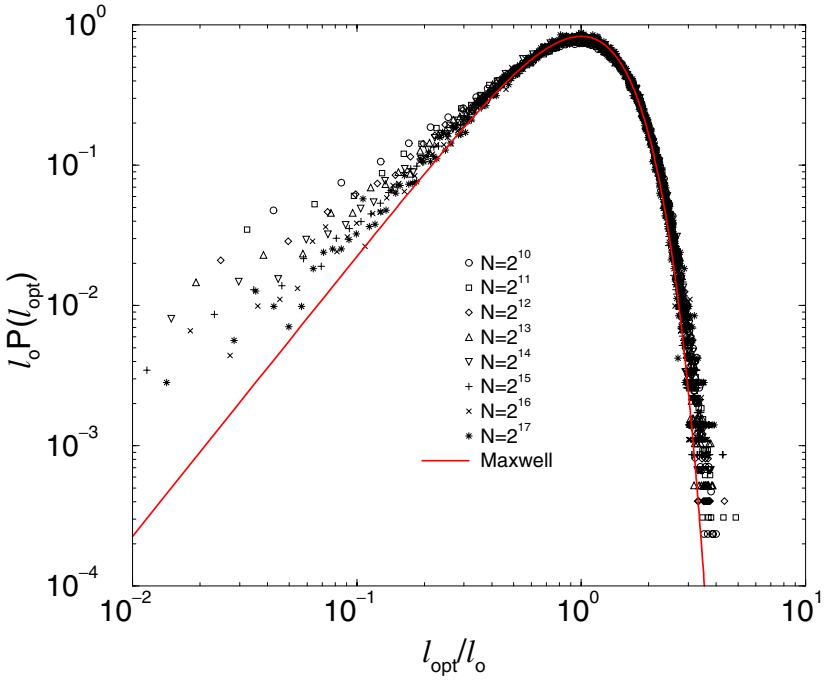


Fig. 15. Scaled curve for the probability distribution $P(\ell_{\rm opt})$ of optimal path lengths for network sizes $N = 1024, 2048, 4096, 8192, 16384, 32768, 65536$. The gray curve represents Maxwellian fit given by Eq. (72) (after [Buldyrev *et al.*, 2003]).

walks [de Gennes, 1979] there are two regimes in this distribution, the first one being a power law $P(\ell_{\rm opt}) \sim (\ell_{\rm opt})^g$ which is evident from the figure, with $g \approx 2$. The second regime is an exponential $P(\ell_{\rm opt}) \sim e^{-C\ell_{\rm opt}^{\delta}}$ where $C$ is a constant and $\delta$ is around 2. This leads us to the conjecture that the distribution may have a Maxwellian functional form:

$$P(\ell_{\rm opt}) = \frac{4\ell_{\rm opt}^2 e^{-(\ell_{\rm opt}/l_o)^2}}{\sqrt{\pi} l_o^3}, \qquad (72)$$

where $\ell_o = \sqrt{\pi}\langle \ell_{\rm opt}\rangle/2$ is the most probable value of $\ell_{\rm opt}$. The solid line in the figure is the plot of this function and as seen, it agrees with our numerical results.

The exponents $g$ and $\delta$ can be obtained from the following heuristic arguments. The right tail of the distribution $P(\ell_{\rm opt})$ is determined by the distribution of the IIC size in the network of $N$ nodes. At percolation threshold (Sec. 6), $N$ nodes are divided into $N/2$ clusters, obeying the power law distribution. However, the sum of all the cluster sizes is equal to $N$, thus the distribution of the largest cluster sizes must have a finite size exponential cutoff $P(S) \sim \exp(-CS)$, as for the distribution of the segments of an interval divided by random partitions. Since $S \sim \ell_{\rm opt}^{d_\ell}$, we have $\delta = d_\ell$.

To find the left tail distribution, we use the concept of MST. The chemical diameter of the MST is $\ell_{\rm opt}$ while its mass is $N \sim \ell_{\rm opt}^{1/\nu_{\rm opt}}$. Due to self-similarity of the MST the number of nodes $n(\ell)$ within a chemical distance $\ell$ also scales as $n(\ell) \sim \ell^{1/\nu_{\rm opt}}$. Thus the probability density of the of the optimal path for small values of $\ell$ scales as $dn(\ell)/d\ell = \ell^{1/\nu_{\rm opt}-1}$. Hence $g = 1/\nu_{\rm opt} - 1$. We expect that our conjecture is valid also for SF networks. Using Eqs. (37) and (38) we have:

$$\delta = d_\ell = \begin{cases} 2, \lambda > 4, & \text{ER} \\ \dfrac{\lambda - 2}{\lambda - 3}, 3 < \lambda \le 4 & \end{cases}, \qquad (73)$$

and

$$g = \begin{cases} 2, \lambda > 4, & \text{ER} \\ \dfrac{2}{\lambda - 3}, 3 < \lambda \le 4 & \end{cases}. \qquad (74)$$

A recent work has studied the distribution form of shortest path lengths on minimum spanning trees [Braunstein *et al.*, 2004], which corresponds to optimal paths on networks with large variation in link weights ($a \to \infty$).

Using the scaling derived in Sec. 6, more precisely:

$$\ell(a) \sim \ell_\infty F\left(\frac{\ell_\infty}{a p_c}\right), \tag{75}$$

where $p_c$ is the percolation threshold and $\ell_\infty \sim N^{\nu_{\rm opt}}$ is the optimal path length for strong disorder ($a \to \infty$). For Erdős–Rényi (ER) graphs $\nu_{\rm opt} = 1/3$. We generalize these results and suggest that the distribution of the optimal path lengths has the following scaling form:

$$P(\ell_{\rm opt}, N, a) \sim \frac{1}{\ell_\infty} G\left(\frac{\ell_{\rm opt}}{\ell_\infty}, \frac{1}{p_c}\frac{\ell_\infty}{a}\right). \tag{76}$$

The parameter $Z \equiv (1/p_c)(\ell_\infty/a)$, which is equivalent to $Z$ in Eq. (62), determines the functional form of the distribution. Relation (76) is supported by simulations [Kalisky *et al.*, 2005] for both ER and SF graphs, including SF graphs with $2 < \lambda < 3$, for which $p_c \to 0$ with system size $N$ [Cohen *et al.*, 2000].

We simulate ER graphs with weights on the links for different values of graph size $N$, control parameter $a$, and average degree $\langle k \rangle$ (which determines $p_c = 1/\langle k \rangle$). We then generate the shortest path tree (SPT) using Dijkstra's algorithm (see Sec. 2.2) from some randomly

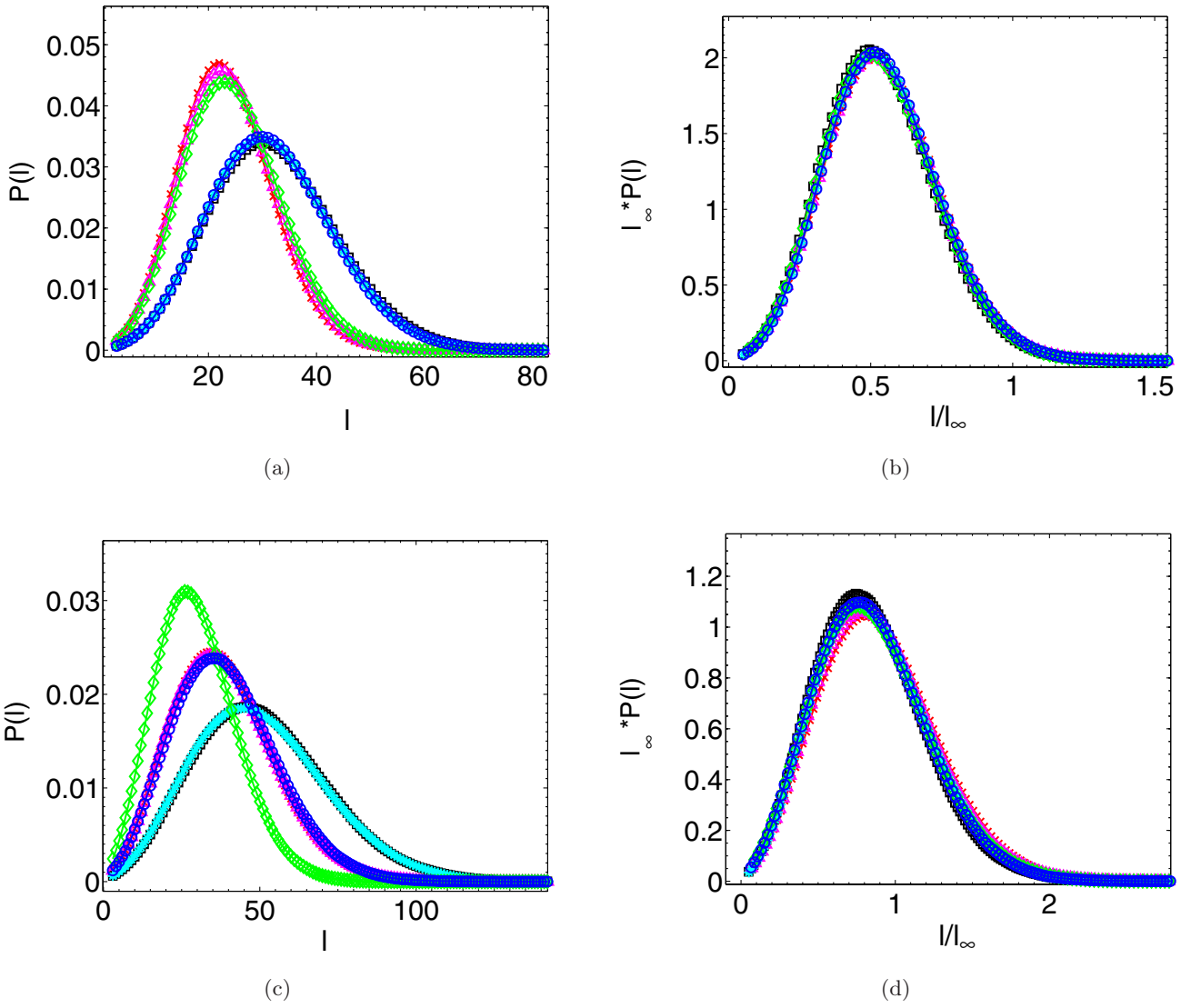


Fig. 16. Optimal path lengths distribution, $P(\ell_{\rm opt})$, for ER networks with (a,b) $Z \equiv (1/p_c)(\ell_\infty/a) = 10$ and (c,d) $Z = 3$. (a) and (c) represent the unscaled distributions for $Z = 10$ and $Z = 3$ respectively, while (b) and (d) are the scaled distribution. Different symbols represent networks with different characteristics such as size $N = 2000, 4000, 8000$ (which determines $\ell_\infty \sim N^{1/3}$), average degree $\langle k \rangle = 3, 5, 8$ (which determines $p_c = 1/\langle k \rangle$), and disorder strength $a = \ell_\infty/(p_c Z)$. Results were averaged over 1500 realizations (after [Kalisky *et al.*, 2005]).

chosen root node. Next, we calculate the probability distribution function of the optimal path lengths for all nodes in the graph [Kalisky *et al.*, 2005].

In Fig. 16 we plot $\ell_\infty P(\ell_{\rm opt}, N, a)$ versus $\ell_{\rm opt}/\ell_\infty$ for different values of $N$, $a$, and $\langle k\rangle$. A collapse of the curves is seen for all graphs with the same value of $Z = (1/p_c)(\ell_\infty/a)$.

Figure 17 shows similar plots for SF graphs — with a degree distribution of the form $P(k) \sim k^{-\lambda}$ and with a minimal degree $m$. Scale-free graphs were generated according to the "configuration model" or Molloy Reed algorithm (see Sec. 2.1) [Molloy & Reed, 1998].[7] A collapse is obtained for different values of $N$, $a$, $\lambda$ and $m$, with $\lambda > 3$ and for the same values of $Z$.

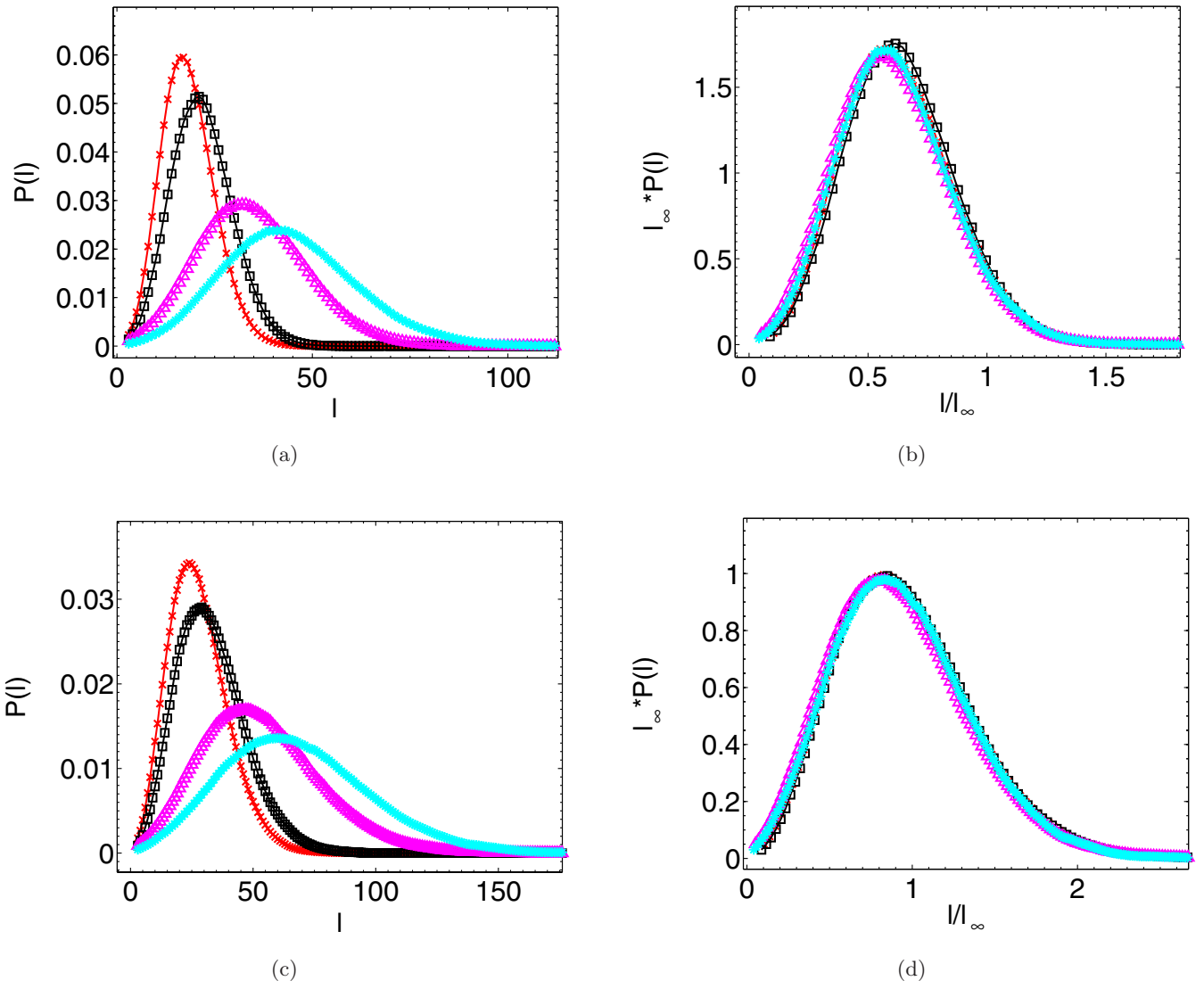


Fig. 17. Optimal path lengths distribution, $P(l)$, for SF networks with (a,b) $Z \equiv (1/p_c)(\ell_\infty/a) = 10$ and (c,d) $Z = 2$. (a) and (c) represent the unscaled distributions for $Z = 10$ and $Z = 2$ respectively, while (b) and (d) are the scaled distribution. Different symbols represent networks with different characteristics such as size $N = 4000, 8000$ (which determines $\ell_\infty \sim N^{\nu_{\rm opt}}$), $\lambda = 3.5, 5$ and $m = 2$ (which determine $p_c$), and disorder strength $a = \ell_\infty/(p_c Z)$. Results were averaged over 250 realizations (after [Kalisky *et al.*, 2005]).

[7]Note that the minimal degree is $m = 2$ thus ensuring that there exists an infinite cluster for any $\lambda$, and thus $0 < p_c < 1$. For the case of $m = 1$ there is almost surely no infinite cluster for $\lambda > \lambda_c \approx 4$ (or for a slightly different model, $\lambda_c = 3.47875$), resulting in an effective percolation threshold $p_c = \langle k\rangle/\langle k(k-1)\rangle > 1$.

Next, we study SF networks with $2 < \lambda < 3$. In this regime the second moment of the degree distribution $\langle k^2 \rangle$ diverges, leading to several anomalous properties [Cohen *et al.*, 2000; Cohen & Havlin, 2003; Callaway *et al.*, 2000]. For example, the percolation threshold approaches zero with system size according to Eq. (25): $p_c \sim N^{-\frac{3-\lambda}{\lambda-1}} \to 0$, and the optimal path length $\ell_\infty$ in SD was found numerically to scale logarithmically with $N$ compared to polynomially, in $\lambda > 3$ [Braunstein *et al.*, 2003]. Nevertheless, it seems from Fig. 18 that the optimal paths probability distribution for SF networks with $2 < \lambda < 3$ exhibits similar collapse for different values of $N$ and $a$ for the same $Z$ (although its functional form is different compared to the $\lambda > 3$ case) [Kalisky *et al.*, 2005].

We present evidence that the optimal path is related to percolation [Sreenivasan *et al.*, 2004]. The numerical results suggest that for a finite disorder parameter $a$, the optimal path (on average) follows the percolation cluster in the network (i.e. links with weight below $p_c$) up to a typical "characteristic length" $\xi = ap_c$, before deviating and making a "shortcut" (i.e. crossing a link with weight above $p_c$). For length scales below $\xi$ the optimal path behaves as in strong disorder and its length is relatively long. The shortcuts have an effect of shortening the optimal path length from a polynomial to logarithmic form according to the universal function $F(u)$ [Eq. (75)]. Thus, the optimal path for finite $a$ can be viewed as consisting of "blobs" of size $\xi$ in which strong disorder persists. These blobs are interconnected by shortcuts, which result in the total path being in weak disorder.

We next present direct simulations supporting this argument [Kalisky *et al.*, 2005]. We calculate the optimal path length $\ell(a)$ inside a single network of size $N$, for a given $a$, and find (Fig. 19) that it scales differently below and above the characteristic length $\xi = ap_c$. For each node in the graph we find $\ell_{\min}$, which is the number of links ("hopcounts") along the shortest path from the root to this node *without regarding the weight of the link*.

In Fig. 19 we plot the length of the optimal path $\ell(a)$, averaged over all nodes with the same value of $\ell_{\min}$ for different values of $a$. The figure strongly suggests that $l(a) \sim \exp(\ell_{\min})$ for length scales below the characteristic length $\xi = ap_c$ [see the linear regime in Fig. 19(b)], while for large length scales $\ell(a) \sim \ell_{\min}$.

For length scales smaller than $\xi$ we have $\ell_{\text{opt}} = AN^{1/3}$ and $\ell_{\min} = B \ln N$, where $A$ and $B$ are constants. Thus $N = \exp(\ell_{\min}/B)$ and $\ell_{\text{opt}} = A \exp(l_{\min}/3B)$. Consequently, we expect that: $\ell_{\text{opt}}/\xi = A \exp(\ell_{\min}/3B)/\xi = A \exp[(l_{\min} - 3B \ln \xi)/3B]$. We find the best scaling in Fig. 19 for $B = 2/3 \ln\langle k \rangle$.

This is consistent with our hypothesis that below the characteristic length ($\xi = ap_c$) $\ell_{\min} \sim \log N$ and $l(a) \sim N^{1/3}$, while $\ell_{\min} \sim \log N$ and $l(a) \sim \log N$ above.

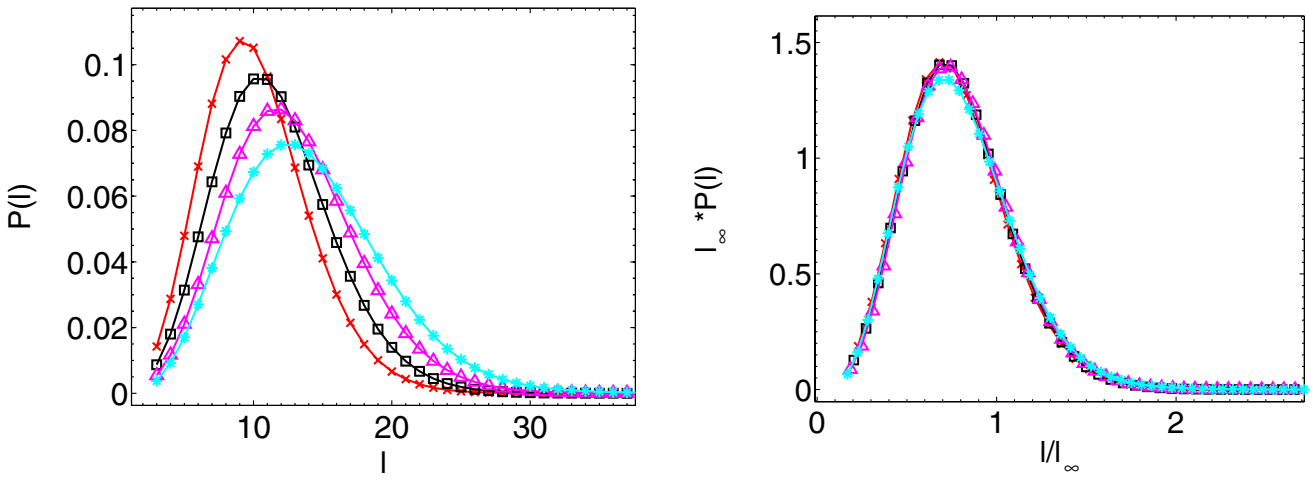


(a) (b)

Fig. 18. Optimal path lengths distribution function for SF graphs with $\lambda = 2.5$, $m = 2$ and with $Z \equiv (1/p_c)(\ell_\infty/a) = 10$. (a) Represents the unscaled distribution for $Z = 10$ while (b) shows the scaled distribution. Different symbols represent graphs with different characteristics such as size $N = 2000, 4000, 8000, 1600$ (which determines $\ell_\infty \sim \log(N)$ and $p_c \sim N^{-1/3}$), and disorder strength $a = \ell_\infty/(p_c Z)$. Results were averaged over 1500 realizations (after [Kalisky *et al.*, 2005]).

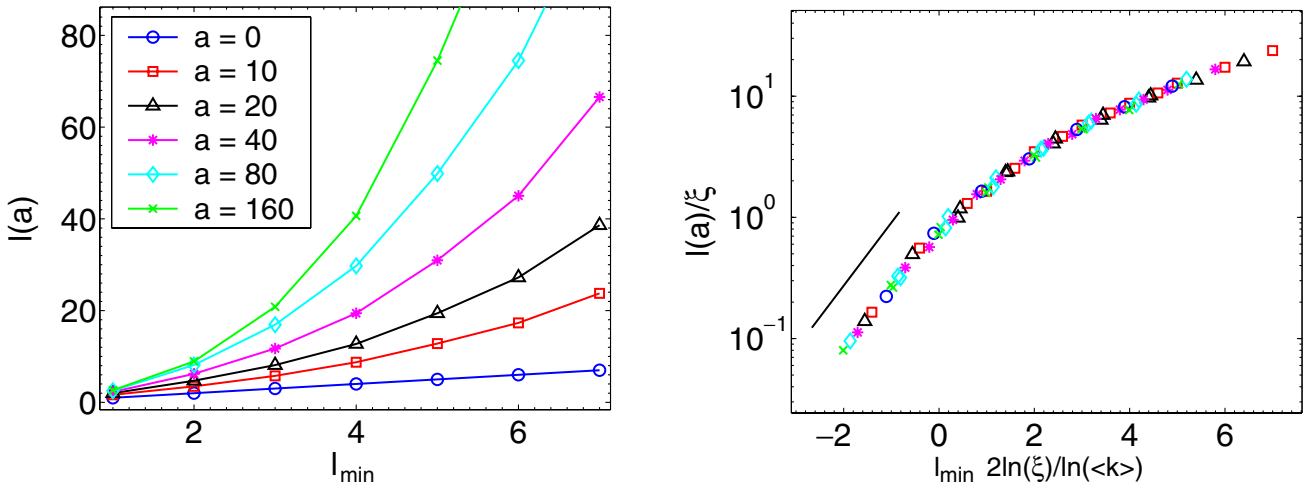


(a) (b)

Fig. 19. Transition between different scaling regimes for the optimal path length $l(a)$ inside an ER graph with $N = 128\,000$ nodes and $\langle k\rangle = 10$. (a) The unscaled, and (b) the scaled length of the optimal path $l(a)$ averaged over all nodes with same value of $\ell_{\min}$. Different symbols represent different values of the disorder strength $a$. For length scales $\ell(a)$ smaller than the "characteristic length", $\xi = ap_c$, $l(a)$ grows exponentially relative to the shortest hopcount path $\ell_{\min}$ (see solid line). This is consistent with $l(a) \sim N^{1/3}$ and $\ell_{\min} \sim \log N$ inside the range of size $\xi = ap_c$. For length scales above $\xi$ both quantities scale as $\log N$ (after [Kalisky *et al.*, 2005]).

In order to better understand why the distributions of $\ell_{\text{opt}}$ depend on $Z$ according to Eq. (76), we suggest the following argument. The optimal path for $a \to \infty$, was shown to be proportional to $N^{1/3}$ for ER graphs and $N^{(\lambda-3)/(\lambda-1)}$ for SF graphs with $3 < \lambda < 4$ [Braunstein *et al.*, 2003]. For finite $a$ the number of shortcuts, or number of blobs, is $Z = \ell_\infty/\xi = \ell_\infty/ap_c$. The deviation of the optimal path length for finite $a$ from the case of $a \to \infty$ is a function of the number of shortcuts. These results explain why the parameter $Z \equiv \ell_\infty/ap_c$ determines the functional form of the distribution function of the optimal paths (see also Sec. 6.2).

To summarize, we have shown that the optimal path length distribution in weighted random graphs has a universal scaling form according to Eq. (76). We explain this behavior and demonstrate the transition between polynomial and logarithmic behavior of the average optimal path in a single graph. Our results are consistent with results found for finite dimensional systems [Porto *et al.*, 1999; Wu *et al.*, 2005; Strelniker *et al.*, 2004]: In finite dimension the parameter controlling the transition is $Z = L^{1/\nu}/ap_c$, where $L$ is the system length and $\nu$ is the correlation length critical exponent as in Eq. (65). This is because only the "red bonds" — bonds that when cut would disconnect the percolation cluster [Stanley, 1977; Coniglio, 1982] — control the transition (see also Sec. 6.2).

## 8. Scale-Free Networks Emerging from Weighted Random Graphs

In this section we introduce a simple process that generates random scale-free networks with $\lambda = 2.5$ from weighted Erdös–Rényi graphs [Kalisky *et al.*, 2006]. We further show that the minimum spanning tree (MST) on an Erdös–Rényi graph is related to this network, and is composed of percolation clusters, which we regard as "super nodes", interconnected by a scale-free tree. We will see that due to optimization this scale-free tree is dominated by links having high weights — significantly higher than the percolation threshold $p_c$. Hence, the MST naturally distinguishes between links below and above the percolation threshold, leading to a scale-free "supernode network". Our results may explain the origin of scale-free degree distribution in some real world networks.

Consider an Erdös–Rényi (ER) graph with $N$ nodes and an average degree $\langle k\rangle$, thus having a total of $N\langle k\rangle/2$ links. To each link we assign a weight chosen randomly and uniformly from the range $[0, 1]$. We define black links to be those links with weights

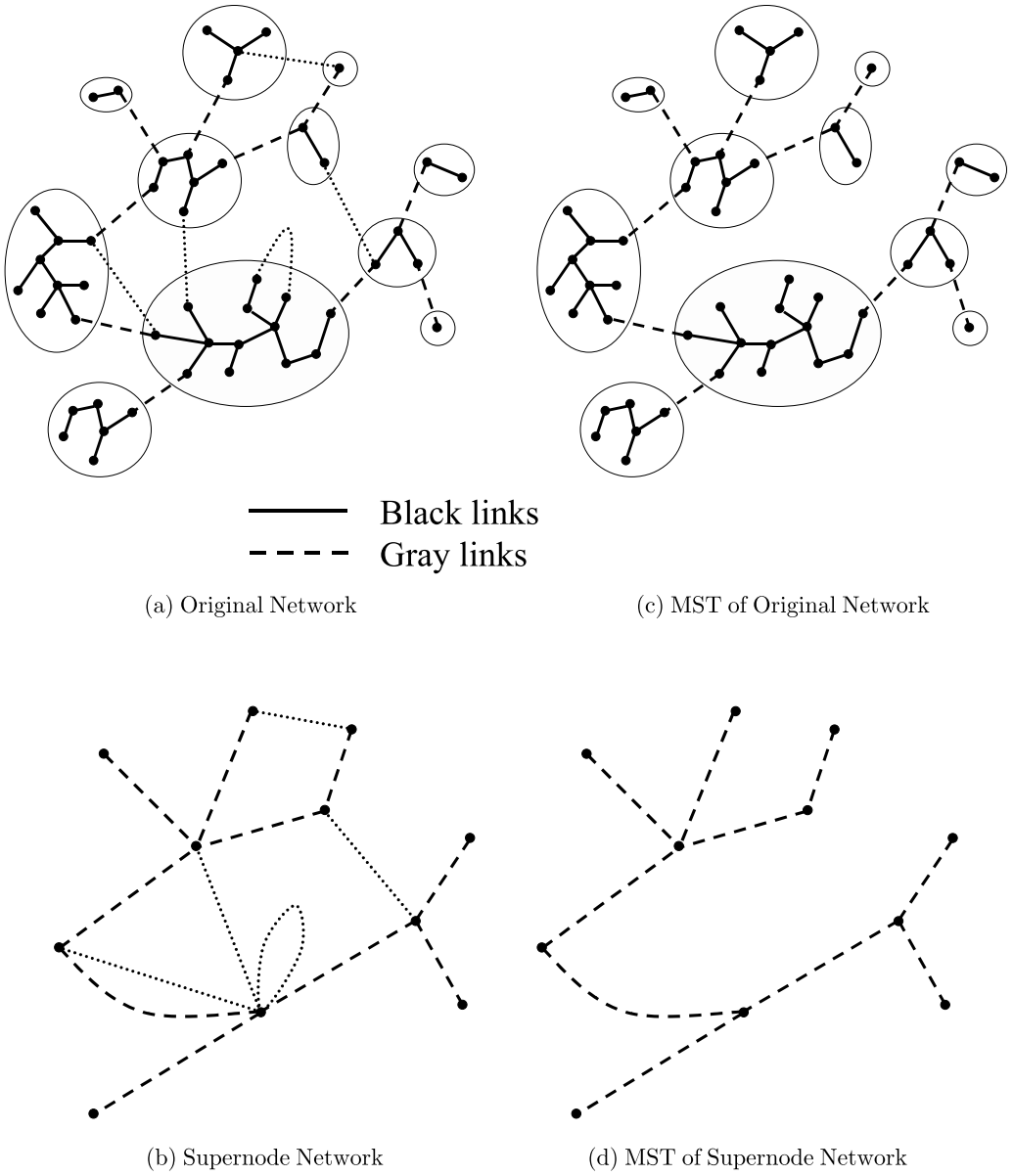


Fig. 20. Sketch of the "supernode network". (a) The original ER network, partitioned into percolation clusters whose sizes $s$ are power-law distributed, with $n_s \sim s^{-\tau}$ where $\tau = 2.5$ for ER graphs. The "black" links are the links with weights below $p_c$, the "dotted" links are the links that are removed by the bombing algorithm, and the "gray" links are the links whose removal will disconnect the network (and therefore are not removed even though their weight is above $p_c$). (b) The "supernode network": the nodes are the clusters in the original network and the links are the links connecting nodes in different clusters (i.e. "dotted" and "gray" links). The supernode network is scale-free with $P(k) \sim k^{-\lambda}$ and $\lambda = 2.5$. Notice the existence of self loops and of double connections between the same two supernodes. (c) The minimum spanning tree (MST), composed of black and gray links only. (d) The MST of the supernode network ("gray tree"), which is obtained by bombing the supernode network (thereby removing the "dotted" links), or equivalently, by merging the clusters in the MST to supernodes. The gray tree is scale-free, with $\lambda = 2.5$ (after [Kalisky *et al.*, 2006]).

below a threshold $p_c = 1/\langle k \rangle$. Two nodes belong to the same cluster if they are connected by black links [Fig. 20(a)].

From Sec. 6 follows that the number of clusters of $s$ nodes scales as a power law, $n_s \sim s^{-\tau}$, with $\tau = 2.5$ for ER networks. Next, we merge all nodes inside each cluster into a single "supernode". We define a new "supernode network" [Fig. 20(b)] of $N_{\rm sn}$ supernodes [Sreenivasan *et al.*, 2004]. The links between two supernodes [see Figs. 20(a) and 20(b)] have weights *larger* than $p_c$. The degree distribution $P(k)$ of the supernode network can be

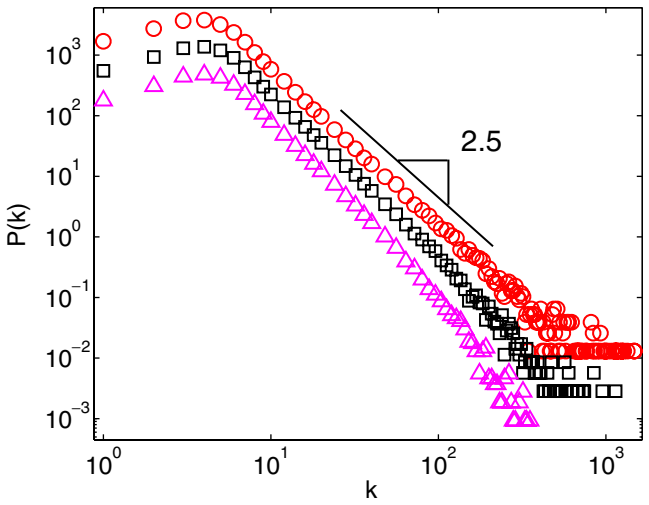


Fig. 21. The degree distribution of the supernode network of Fig. 1(b), where the supernodes are the percolation clusters, and the links are those with weights larger than $p_c$ (○). The distribution exhibits a scale-free tail with $\lambda \approx 2.5$. If we choose a threshold less than $p_c$, we obtain the same power law degree distribution with an exponential cutoff. The different symbols represent slightly different threshold values: $p_c - 0.03$ (□) and $p_c - 0.05$ (△). The original ER network has $N = 50\,000$ and $\langle k \rangle = 5$. Note that for $k \approx \langle k \rangle$ the degree distribution has a maximum (after [Kalisky *et al.*, 2006]).

obtained as follows. Every node in a supernode has the same (finite) probability to be connected to a node outside the supernode. Thus, we assume that the degree $k$ of each supernode is proportional to the cluster size $s$, which obeys $n_s \sim s^{-2.5}$. Hence $P(k) \sim k^{-\lambda}$, with $\lambda = 2.5$, as supported by simulations shown in Fig. 21. Furthermore, we also see that if the threshold for obtaining the clusters which are merged into supernodes is changed slightly, the degree distribution still remains scale free with $\lambda = 2.5$, but with an exponential cutoff. This is an indication of the fact that there are still supernodes of high degree which are connected to many other (small) supernodes by links with weights significantly higher than $p_c$; if this was not the case, a small change in the threshold would cause many clusters to merge and destroy the power law in the supernode network degree distribution.

We next show that the MST on an ER graph is related to the supernode network, and therefore also exhibits scale-free properties. In the MST each path between two sites on the MST is the optimal path in the "strong disorder" limit [Cieplak *et al.*, 1996; Dobrin & Duxbury, 2001], meaning that along this path the maximum *barrier* (weight) is the smallest possible [Dobrin & Duxbury, 2001; Braunstein *et al.*, 2003; Sreenivasan *et al.*, 2004].

Here we use the bombing algorithm (see Sec. 2.4). If the removal of a link disconnects the graph, we restore the link and mark it "gray"; otherwise the link [shown dotted in Fig. 20(a)] is removed. The links that are not bombed are marked as "black". In the bombing algorithm, only links that close a loop can be removed. Since below criticality loops are negligible [Erdős & Rényi, 1959; Albert & Barabási, 2002] for ER networks ($d \to \infty$), bombing does not modify the percolation clusters — where the links are black and have weights below $p_c$. Thus, bombing modifies only links *outside* the clusters, so actually it is only the links of the *supernode network* that are bombed. Hence the MST resulting from bombing is composed of percolation clusters (composed of black links) and connected by gray links [Fig. 20(c)].

From the MST of Fig. 20(c) we now generate a new tree, the MST of the supernode network, which we call the "gray tree", whose nodes are the supernodes and whose links are the gray links connecting them [see Fig. 20(d)]. Note that bombing the original ER network to obtain the MST of Fig. 20(c) is equivalent to bombing the supernode network of Fig. 20(b) to obtain the gray tree, because the links inside the clusters are not bombed. We find [Fig. 22(a)] that the gray tree has also a scale-free degree distribution $P(k)$, with $\lambda = 2.5$ — the same as the supernode network.[8] We also find [Fig. 22(b)] the average path length $\ell_{\text{gray}}$ scales as $\ell_{\text{gray}} \sim \log N_{\text{sn}} \sim \log N$ [Sreenivasan *et al.*, 2004].[9] Note that even though the gray tree is scale-free, it is not ultra-small [Cohen & Havlin, 2003], since the length does not scale as log-log N.

Next we show that the bombing optimization, which leads to the MST, yields a significant separation between the weights of the links inside the supernodes and the links connecting the supernodes. As explained above, the MST is optimal in two senses: (i) the total weight of all links is minimal, (ii) any path between any two nodes on the MST will encounter the smallest maximal *barrier* (weight) between these nodes. The last property is common to many physical systems (e.g. the protein folding

[8]MSTs on scale-free networks were found to retain the original network's degree distribution [Szabó *et al.*, 2003; Kim *et al.*, 2004; Macdonald *et al.*, 2005].

[9]MSTs on scale-free networks with $\lambda = 2.5$ were found to retain the original network's degree distribution.

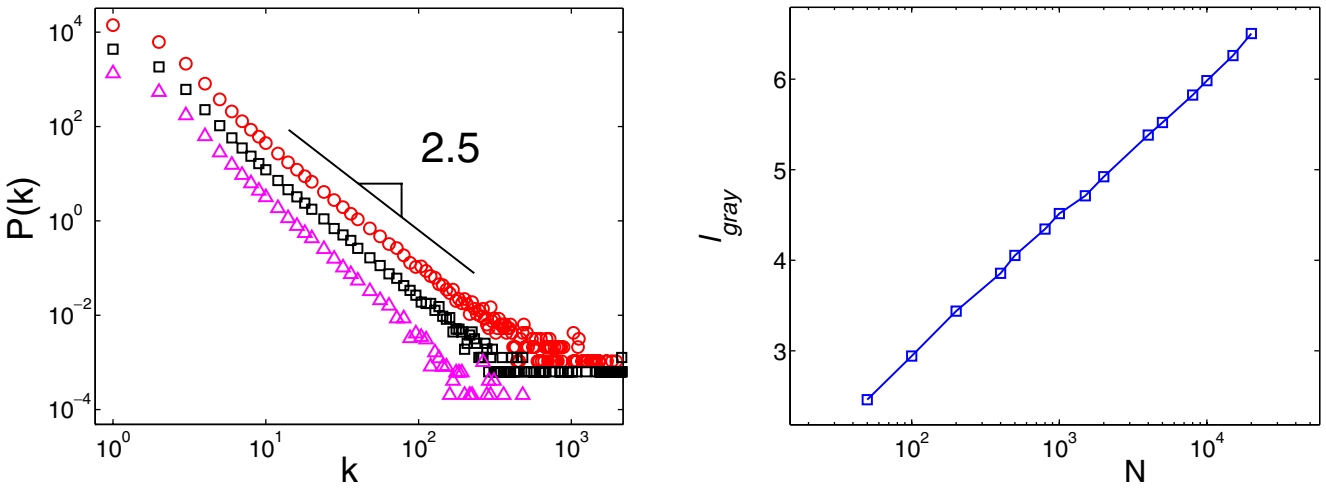


(a) (b)

Fig. 22. (a) The degree distribution of the "gray tree" (the MST of the supernode network, shown in Fig. 20(d)), in which the supernodes are percolation clusters and the links are the gray links. Different symbols represent different threshold values: $p_c$ (○), $p_c + 0.01$ (□) and $p_c + 0.02$ (△). The distribution exhibits a scale-free tail with $\lambda \approx 2.5$, and is relatively insensitive to changes in $p_c$. (b) The average path length $\ell_{\text{gray}}$ on the gray tree as a function of original network size. It is seen that $\ell_{\text{gray}} \sim \log N_{\text{sn}} \sim \log N$ (after [Kalisky *et al.*, 2006]).

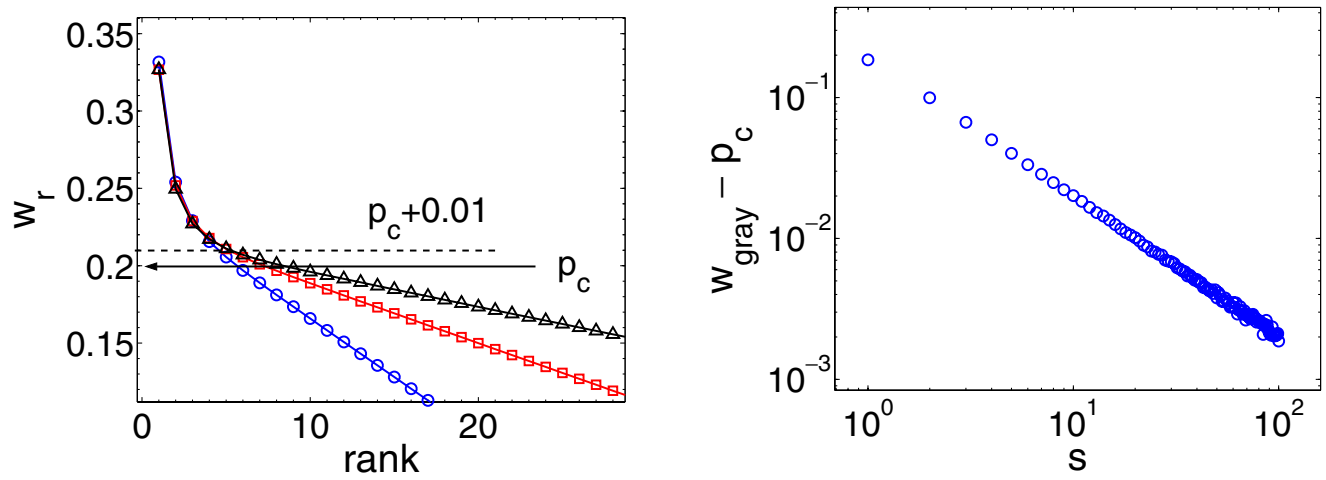


(a) (b)

Fig. 23. (a) The average weights $w_r$ along the optimal path of an ER graph with $\langle k \rangle = 5$, sorted according to their rank. Different symbols represent different system sizes: $N = 2000$ (○), $N = 8000$ (□) and $N = 32\,000$ (△). Below $p_c = 0.2$, the weights are uniformly distributed, while weights above $p_c$ are significantly higher and independent of $N$. (b) Cluster size versus the minimal gray link emerging from each cluster, for ER graphs with $\langle k \rangle = 5$ and $N = 10\,000$. Small clusters are associated with higher weights because they have a small number of exits and thus cannot be optimized (after [Kalisky *et al.*, 2006]).

network — see below). Accordingly, we study the weights encountered when traveling along a typical path on the MST.

We consider all pairs of nodes in the original MST of $N$ nodes [Fig. 20(c)] and calculate the typical path length $\ell_{\text{typ}}$, which is the most probable path length on the MST. For each path of length $\ell_{\text{typ}}$ we rank the weights on its links in descending order. For the largest weights ("rank 1 links"), we calculate the average weight $w_{r=1}$ over all paths. Similarly, for the next largest weights ("rank 2 links") we find the average $w_{r=2}$ over all paths, and so on up to $r = \ell_{\text{typ}}$. Figure 23(a) shows $w_r$ as a function of rank $r$ for three different network sizes $N = 2000$, 8000 and 32 000. It can be seen that weights below $p_c$ (black links inside the supernodes) are uniformly distributed and approach one another as $N$ increases. As opposed to this, weights above $p_c$

("gray links") are *not* uniformly distributed, due to the bombing algorithm, and are independent of $N$. Actually, weights above $p_c$ encountered along the optimal path (such as the largest weights $w_1$, $w_2$ and $w_3$) are significantly higher than those below $p_c$. Figure 23(b) shows that the links with the highest weights on the MST can be associated with gray links from very small clusters [Figs. 20(a) and 20(c)] (similar results have been obtained along the optimal path).

As mentioned earlier, this property is present also in the original supernode network and hence the change in the threshold used to obtain the supernodes does not destroy the power law degree distribution but only introduces an exponential cutoff. We thereby obtain a scale-free supernode network with $\lambda = 2.5$, which is not very sensitive to the precise value of the threshold used for defining the supernodes. For example, the scale-free degree distribution shown in Fig. 22(a) for a threshold of $p_c + 0.01$ corresponds to having only four largest weights on the optimal paths [see Fig. 23(a)]. However, even for $p_c + 0.02$ the degree distribution is well approximated by a scale-free distribution with $\lambda = 2.5$ [see Fig. 22(a)]. This means that mainly very small clusters, connected with high-weight links to large clusters, dominate the scale-free distribution $P(k)$ of the MST of the supernode network (gray tree). Hence, the bombing optimization process on an ER graph causes a significant separation between links below and above $p_c$ to emerge *spontaneously* in the system, and by merging nodes connected with links of low weights, a scale-free network can arise.

The process described above may be related to the evolution of some real world networks. Consider a homogeneous network with many components whose average degree $\langle k \rangle$ is well defined. Suppose that the links between the components have different weights, and that some optimization process separates the network into nodes which are well connected (i.e. connected by links with low weights) and nodes connected by links having much higher weights. If the well-connected components merge into a single node, this results in a new heterogeneous supernode network with scale free degree distribution.

An example of a real world network whose evolution may be related to this model is the protein folding network, which was found to be scale-free with $\lambda \approx 2.3$ [Rao, 2004]. The nodes are the possible physical configurations of the system and the links between them describe the possible transitions between the different configurations. We assume that this network is *optimal* because the system chooses the path with the smallest energy *barrier* from all possible trajectories in phase space. It is possible that the scale-free distribution evolves through a similar procedure as described above for random graphs: adjacent configurations with close energies (nodes in the same cluster) cannot be distinguished and are regarded as a single supernode, while configurations (clusters) with high barriers between them belong to different supernodes.

A second example is computer networks. Strongly interacting computers (such as computers belonging to researchers from the same company or research institution) are likely to converge into a single domain, and thus domains with various sizes and connectivities are formed. This network might be also optimal, because packets destined to an external domain are presumably routed through the router which has the best connection to the target domain.

To summarize, we have seen that any weighted random network hides an inherent scale-free "supernode network."[10] We showed that the minimum spanning tree, generated by the bombing algorithm, is composed of percolation clusters connected by a scale-free tree of "gray" links. Most of the gray links connect small clusters to large ones, thus having weights well above the percolation threshold that do not change with the original size of the network. Thus the optimization in the process of building the MST distinguishes between links with weights below and above the threshold, leading to a spontaneous emergence of a scale-free "supernode network". We raise the possibility that in some naturally optimal real-world networks, nodes connected well merge into one single node, and thus a scale-free network emerges.

## 9. Partition of the Minimum Spanning Tree into Superhighways and Roads

The centrality, $C$, quantifies the "importance" of a node for transport in the network. Moreover, identifying the nodes with high $C$ enables, as shown below, to improve their transport capacity and thus

[10]Similar results can also be obtained for graphs embedded in two or three dimensions, with different power law exponents.

improve the global transport in the network. Several definitions of centrality exists. Here we deal with the "betweenness centrality" which is defined as the relative number of shortest path in the network passing through a node (or a link). The probability density function (pdf) of $C$ was studied on the MST for both scale-free (SF) [Barabási & Albert, 1999] and Erdős–Rényi (ER) [Erdős & Rényi, 1959, 1960] networks and found to satisfy a power law,

$$\mathcal{P}_{\rm MST}(C) \sim C^{-\delta_{\rm MST}} \tag{77}$$

with $\delta_{\rm MST}$ close to 2 [Goh *et al.*, 2005; Kim *et al.*, 2004]. An important question is whether there are substructure of the MST which are more central and play a major role on the transport. Wu *et al.* [2006] showed that a sub-network of the MST, the infinite incipient percolation cluster (IIC) has a significantly higher average $C$ than the entire MST — i.e. the set of nodes inside the IIC are typically used by transport paths more often than other nodes in the MST [Wu *et al.*, 2006]. In this sense the IIC can be viewed as a set of *superhighways* (SHW) in the MST. The nodes on the MST which are not in the IIC are called *roads*, due to their analogy with roads of less traffic (usually used by local residents). We demonstrate the impact of this finding by showing that improving the capacity of the superhighways (IIC) is significantly a better strategy to enhance global transport compared to improving the same number of links with the highest $C$ in the MST, although they have higher $C$ [Wu *et al.*, 2006]. This counterintuitive result shows the advantage of identifying the IIC subsystem, which is very small compared to the full network. These results are based on extensive numerical studies for centrality of the IIC, and comparison with the centrality of the entire MST [Wu *et al.*, 2006; Newman, 2001], as described below. ER and SF network of size $N$ are generated by the methods explained in Sec. 2.1. Multiple connections between two nodes and self-loops in a single node are disallowed. To construct a *weighted* network, a weight $w_i$ is assigned to each link from a uniform distribution between 0 and 1. The MST is obtained from the weighted network using Prim's algorithm [Ahuja *et al.*, 1993] (see Sec. 2.5). Once the MST is built, one can compute the value of $C$ of each node by counting the number of paths between all possible pairs passing through that node and normalize $C$ by the total number of pairs in the MST, $N(N-1)/2$, which ensures that $C$ is between 0 and 1.[11] The IIC of ER and SF networks is simulated as explained in Sec. 2.6.

To quantitatively study the centrality of the nodes in the IIC, we calculate the pdf, $\mathcal{P}_{\rm IIC}(C)$ of $C$. Figure 24 shows that for all three cases studied, ER, SF and square lattice networks, $\mathcal{P}_{\rm IIC}(C)$ for nodes

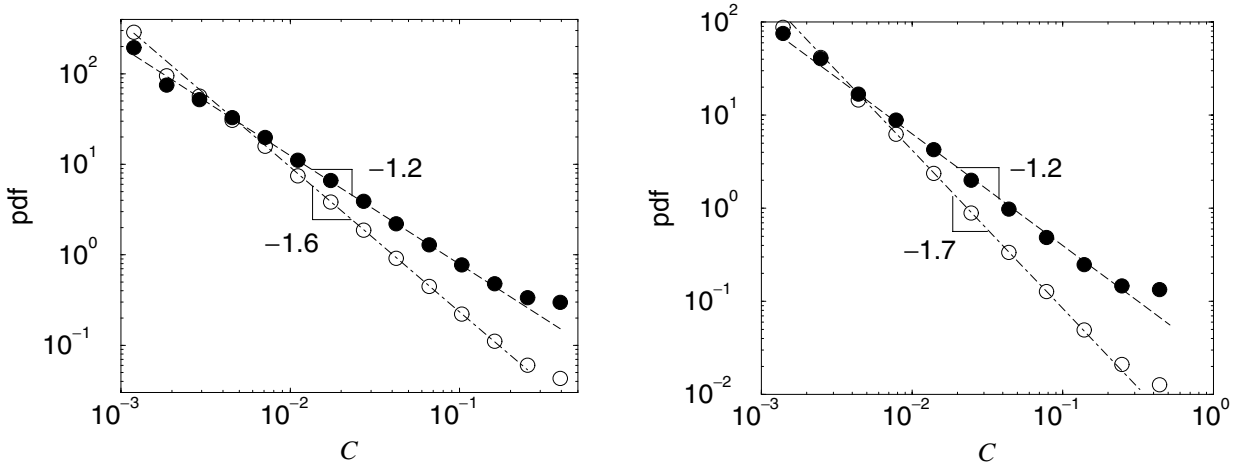


(a) ER Networks $\langle k\rangle = 4$ (b) SF Networks $\lambda = 4.5$

Fig. 24. The pdf of the centrality $C$ of nodes for (a) ER graph with $\langle k\rangle = 4$, (b) SF with $\lambda = 4.5$, (c) SF with $\lambda = 3.5$ and (d) $90 \times 90$ square lattice. For ER and SF, $N = 8192$ and for the square lattice $N = 8100$. We analyze $10^4$ realizations. For each graph, the full circles show $\mathcal{P}_{\rm IIC}$(C); the empty circles show $\mathcal{P}_{\rm MST}$(C) (after [Wu *et al.*, 2006]).

[11]This $C$ measurement is equivalent to counting the number of times a node (link) is used by the set of optimal paths linking all pairs of nodes, in the limit of strong disorder.

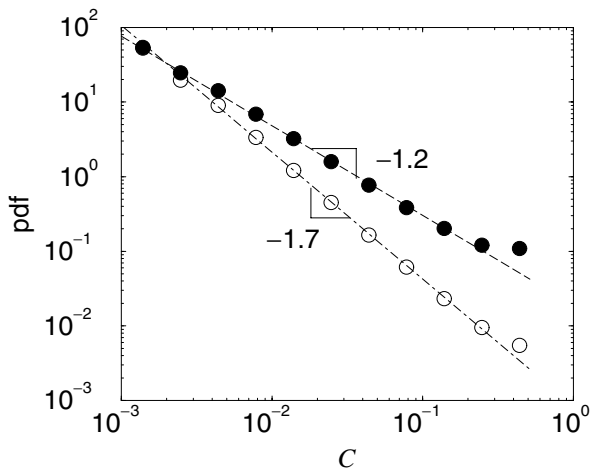


(c) SF Networks $\lambda = 3.5$

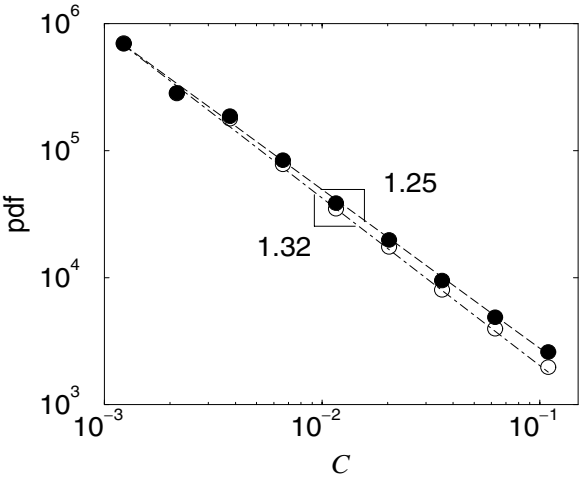


(d) Square Lattice

Fig. 24. (*Continued*)

satisfies a power law

$$\mathcal{P}_{\rm IIC}(C) \sim C^{-\delta_{\rm IIC}}, \tag{78}$$

where

$$\delta_{\rm IIC} \approx \begin{cases} 1.2 & [\text{ER, SF}] \\ 1.25 & [\text{square lattice}] \end{cases}. \tag{79}$$

Moreover, from Fig. 24, it is seen that $\delta_{\rm IIC} < \delta_{\rm MST}$, implying a larger probability to find a larger value of $C$ in the IIC compared to the entire MST. The values for $\delta_{\rm MST}$ are consistent with those found in [Goh *et al.*, 2005]. Similar results for the centrality of the links were obtained. The results thus show that the IIC is like a network of *superhighways* inside the MST. When we analyze centrality of the entire MST, the effect of the high $C$ of the IIC is not seen since the IIC is only a tiny fraction of the MST. Some results are summarized in Table 2.

The values of $\delta_{\rm MST}$ and $\delta_{\rm IIC}$ can be understood from the following scaling arguments, based on self-similarity properties of the MST and the IIC. Similar arguments are used in [Stauffer & Aharony, 1994; Bunde & Havlin, 1996] to express exponent $\tau_s$ describing the cluster size distribution at percolation threshold on a lattice in terms of the cluster fractal dimension and the dimension of the lattice. Indeed, the majority of nodes are connected through the superhighway links, whose centrality is proportional to $N^2$. The number of these links for the entire network scales as $\ell_\infty(N) \sim N^{1/\nu_{\rm opt}}$ [Braunstein *et al.*, 2003; Wu *et al.*, 2005]. Thus small regions of the MST of chemical diameter $\ell$ consists of $n^{1/\nu_{\rm opt}}$ nodes. These regions have length $\ell_\infty(n) \sim n^{1/\nu_{\rm opt}}$. These roads connect the nodes in this region with the rest of the nodes of the MST, and thus their centrality is at least $nN$. The total number of such links in all the regions of size $n$ is $m(n) = \ell_\infty(n)N/n \sim n^{\nu_{\rm opt}-1}$. This is the number of links with centrality larger than $nN$. Thus number of links with centrality exactly $nN$ is $m(n)-m(n+1) \sim n^{\nu_{\rm opt}-2} = n^{-\delta_{\rm MST}}$. Using Eq. (38) we have:

$$\delta_{\rm MST} = \begin{cases} \dfrac{5}{3}, \lambda > 4, & \text{ER} \\ \dfrac{\lambda+1}{\lambda-1}, 3 < \lambda \le 4 \end{cases}. \tag{80}$$

Table 2. Results for the IIC and the MST (after [Wu *et al.*, 2006]).

| | ER | SF ($\lambda = 4.5$) | SF ($\lambda = 3.5$) | Square Lattice |
|---|---|---|---|---|
| $\delta_{\rm IIC}$ | 1.2 | 1.2 | 1.2 | 1.25 |
| $\delta_{\rm MST}$ | 1.6 | 1.7 | 1.7 | 1.32 |
| $\nu_{\rm opt}$ | 1/3 | 1/3 | 0.2 | 0.61 |
| $\langle u \rangle$ | 0.29 | 0.20 | 0.13 | 0.64 |

Similar arguments lead to the centrality distribution of the nodes on the IIC. The small regions of chemical diameter $\ell$ have centrality larger or equal to $Nn(\ell)$. The number of links in the IIC belonging to these regions is $s(\ell) = \ell^{d_\ell}$ [Cohen *et al.*, 2002]. The total number of such regions is $S/s(\ell)$, thus the total number of the links of the IIC with centrality larger than $Nn(\ell)$ is $m[n(\ell)] = \ell/s(\ell) \sim \ell^{1-d_\ell} =$

$n^{(1-d_\ell)\,\nu_{\rm opt}}$. Accordingly

$$\delta_{\rm IIC} = 1 + (d_\ell - 1)\nu_{\rm opt} = \begin{cases} \dfrac{4}{3}, \lambda > 4, & \text{ER} \\ \dfrac{\lambda}{\lambda - 1}, 3 < \lambda \leq 4 & \end{cases} . \tag{81}$$

The values predicted by Eqs. (80) and (81) are in good agreement with the simulation results presented in Table 2.

To further demonstrate the significance of the IIC, we compute the average $\langle \mathrm{C} \rangle$ for each realization of the network over all nodes. Figure 27, shows the histograms of $\langle \mathrm{C} \rangle$ for both the IIC and for the other nodes on the MST. We see that the nodes on the IIC have significantly larger $\langle \mathrm{C} \rangle$ compared to the other nodes of the MST.

Figure 25 shows a schematic plot of the SHW inside the MST and demonstrates its use by the path between pairs of nodes. The MST is a "skeleton" subset of links inside the network, which plays a key role in transport between the nodes. However, the IIC in the MST is like the "spine in the skeleton", which plays the role of the superhighways inside a road transportation system. To illustrate our result a car can drive from the entry node A on roads until it reaches a superhighway, and finds the exit which is closest to node B. Thus those nodes which are far from each other in the MST use the IIC superhighways more than those nodes which are close to each other. In order to demonstrate this, we compute $f$, the average fraction of pairs of nodes using the shortest paths of the IIC, as a function of $\ell_{\rm MST}$, the distance between a pair of nodes on the MST (Fig. 26). We see that $f$ increases and

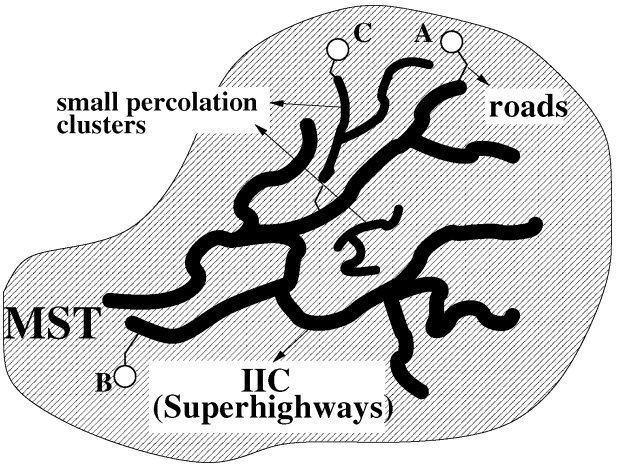


Fig. 25. Schematic graph of the network of connected superhighways (heavy lines) inside the MST (shaded). A, B and C are examples of possible entry and exit nodes, which connect to the network of superhighways by "roads" (thin lines). The middle size lines indicate other percolation clusters with much smaller size compared to the IIC (after [Wu *et al.*, 2006]).

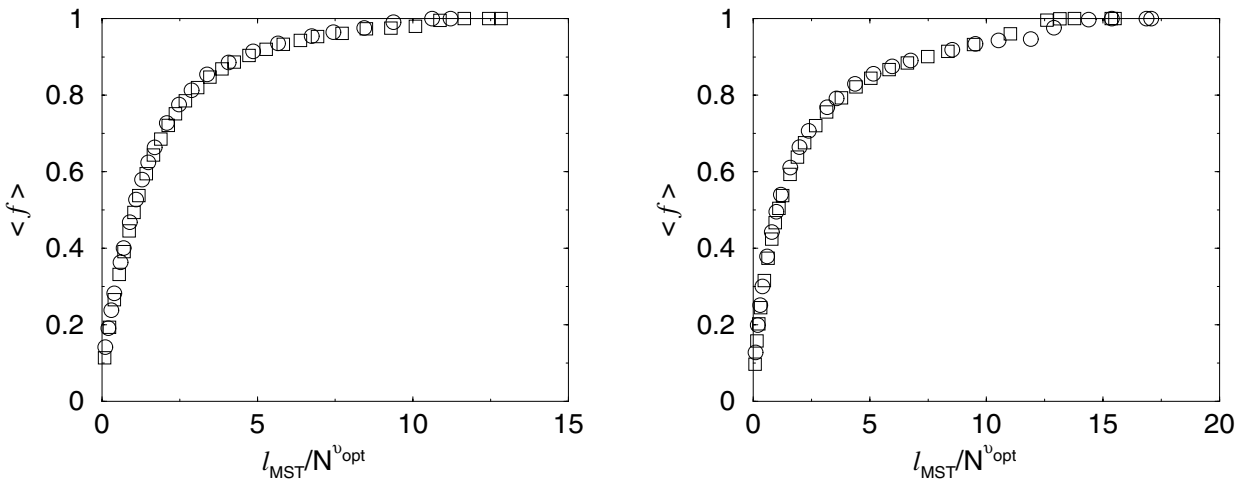


(a) ER Networks $\langle k \rangle = 4$

(b) SF Networks $\lambda = 4.5$

Fig. 26. The average fraction, $\langle f \rangle$, of pairs using the SHW, as a function of $\ell_{\rm MST}$, the distance between the pair on the MST. (a) ER graph with $\langle k \rangle = 4$, (b) SF with $\lambda = 4.5$, (c) SF with $\lambda = 3.5$ and (d) square lattice. For ER and SF: ($\bigcirc$)$N = 1024$ and ($\square$)$N = 2048$ with $10^4$ realizations. For square lattice: ($\bigcirc$)$N = 1024$ and ($\square$)$N = 2500$ with $10^3$ realizations. The $x$-axis is rescaled by $N^{\nu_{\rm opt}}$, where $\nu_{\rm opt} = 1/3$ for ER and for SF with $\lambda > 4$, and $\nu_{\rm opt} = (\lambda - 3)/(\lambda - 1)$ for SF networks with $3 < \lambda < 4$ [Braunstein *et al.*, 2003]. For the $L \times L$ square lattice, $\ell_{\rm MST} \sim L^{d_{\rm opt}}$ with $d_{\rm opt} = 1.22$ and since $L^2 = N$, $\nu_{\rm opt} = d_{\rm opt}/2 \approx 0.61$ [Cieplak *et al.*, 1996; Porto *et al.*, 1999] (after [Wu *et al.*, 2006]).

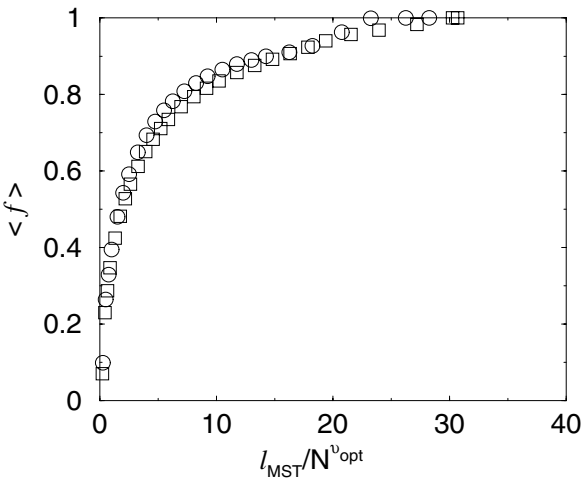


(c) SF Networks $\lambda = 3.5$

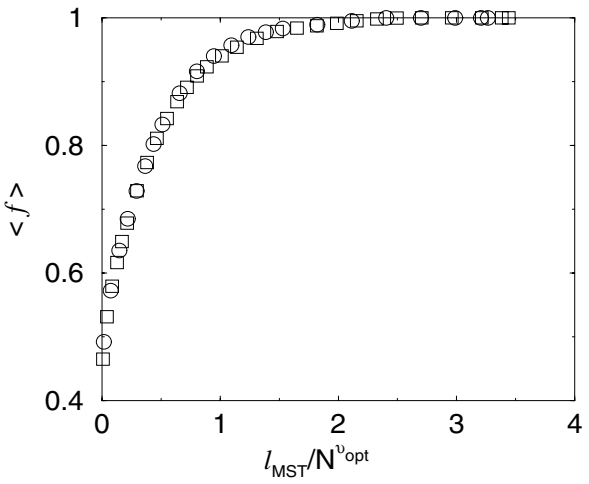


(d) L × L Square Lattice

Fig. 26. (*Continued*)

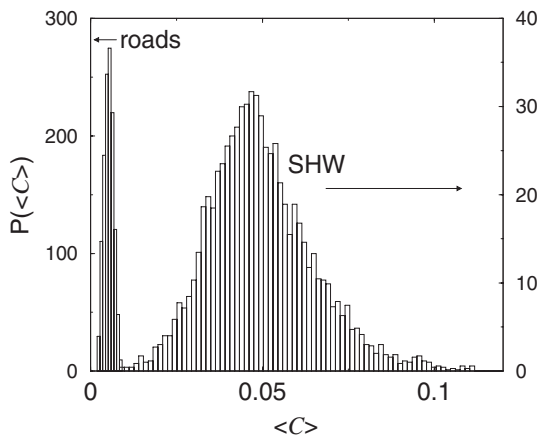


(a) ER Networks $\langle k \rangle = 4$

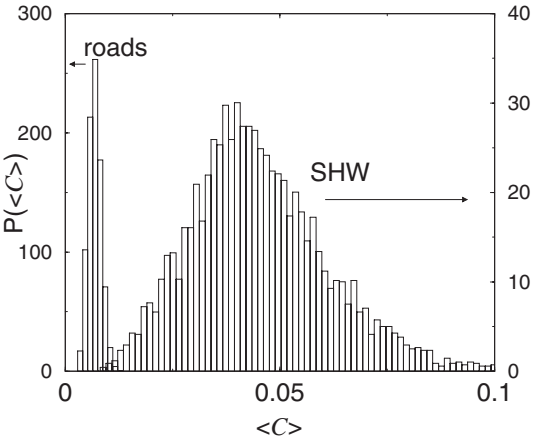


(b) SF Networks $\lambda = 4.5$

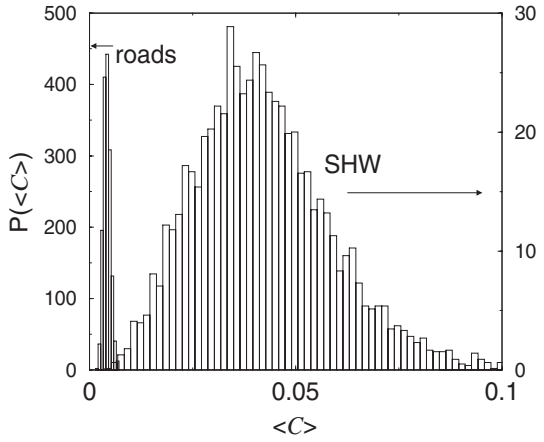


(c) SF Networks $\lambda = 3.5$

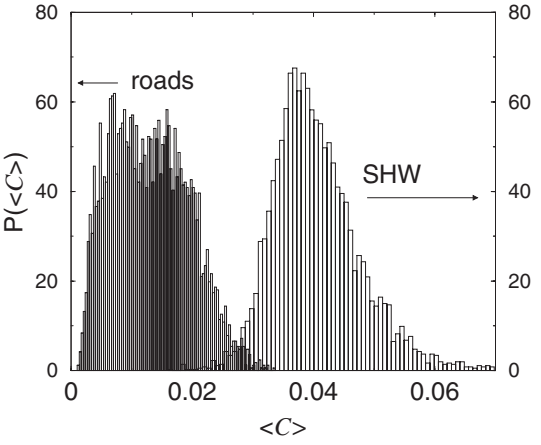


(d) 90 × 90 Square Lattice

Fig. 27. The normalized pdf for superhighway and roads of $\langle C \rangle$, the $C$ averaged over all nodes in one realization. (a) ER network, (b) SF network with $\lambda = 4.5$, (c) SF network with $\lambda = 3.5$ and (d) square lattice network. To make each histogram, we analyze 1000 network configurations (after [Wu *et al.*, 2006]).

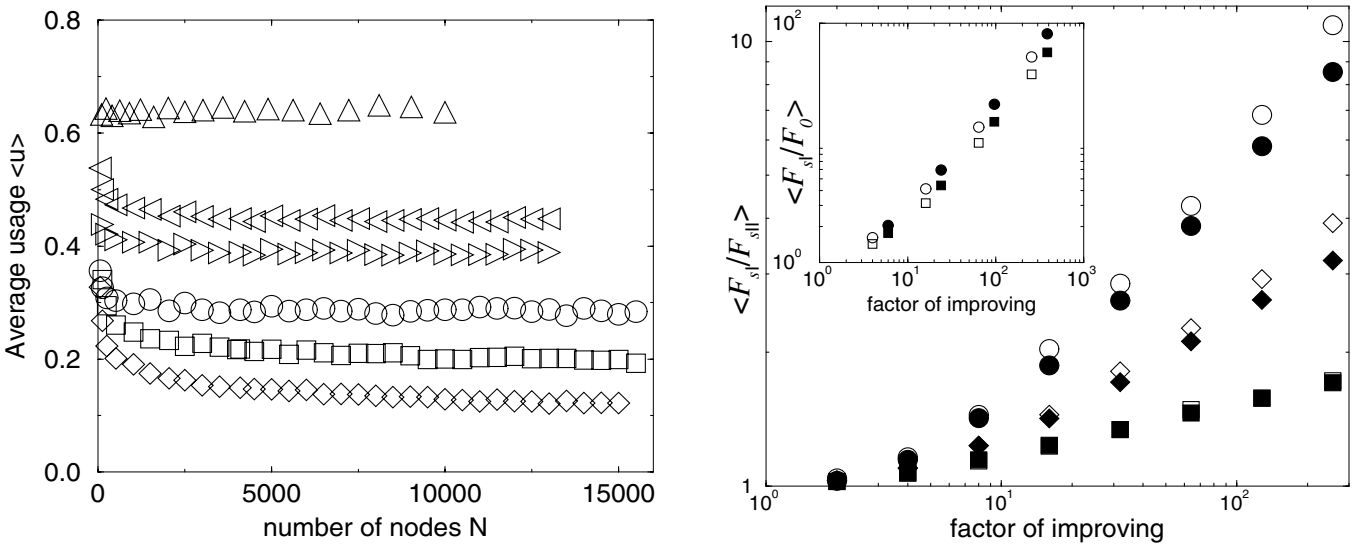


(a) (b)

Fig. 28. (a) The average usage $\langle u\rangle \equiv \langle \ell_{\rm IIC}/\ell_{\rm MST}\rangle$ for different networks, as a function of the number of nodes $N$. ○ (ER with $\langle k\rangle = 4$), □ (SF with $\lambda = 4.5$), ◊ (SF with $\lambda = 3.5$), △ ($L \times L$ square lattice). The symbols (▷) and (◁) represent the average usage for ER with $\langle k\rangle = 4$ when the two largest percolation clusters and the three largest percolation clusters are taken into account, respectively. (b) The ratio between the flow using strategy I, $F_{s\rm I}$, and that using strategy II, $F_{s\rm II}$, as a function of the factor of improving conductivity/capacity. The inset is the ratio between the flow using strategy I and the flow in the original network, $F_0$. The data are all for ER networks with $N = 2048$, $\langle k\rangle = 4$ and $n = 50(\bigcirc)$, $n = 250(\Diamond)$ and $n = 500(\square)$. The unfilled symbols are for current flow and the filled symbols are for maximum flow (after [Wu *et al.*, 2006]).

approaches one as $\ell_{\rm MST}$ grows. We also show that $f$ scales as $\ell_{\rm MST}/N^{\nu_{\rm opt}}$ for different system sizes, where $\nu_{\rm opt}$ is the percolation connectedness exponent [Braunstein *et al.*, 2003; Wu *et al.*, 2005].

The next question is how much the IIC is used in transport on the MST? We define the *IIC superhighway usage*,

$$u \equiv \frac{\ell_{\rm IIC}}{\ell_{\rm MST}}, \tag{82}$$

where $\ell_{\rm IIC}$ is the number of links in a given path of length $\ell_{\rm MST}$ belonging to the IIC superhighways. The average usage $\langle u\rangle$ quantifies what fraction of nodes/links of the IIC is used by the transport between all pairs of nodes. In Fig. 28(a), we show $\langle u\rangle$ as a function of the system size $N$. Our results suggest that $\langle u\rangle$ approaches a constant value and becomes independent of $N$ for large $N$. This is surprising since the average value of the ratio between the number of nodes on the IIC and on the MST, $\langle N_{\rm IIC}/N_{\rm MST}\rangle$, approaches zero as $N \to \infty$, showing that despite the although the IIC contains only a tiny fraction of the nodes in the entire network, its usage for the transport in the entire network is constant. We find that $\langle u\rangle \approx 0.3$ for ER networks, $\langle u\rangle \approx 0.2$ for SF networks with $\lambda = 4.5$, and $\langle u\rangle \approx 0.64$ for the square lattice. The reason why $\langle u\rangle$ is not close to 1.0 is that in addition to the IIC, the optimal path passes also through other percolation clusters, such as the second largest and the third largest percolation clusters. In Fig. 28, we also show for ER networks, the average usage of the two largest and the three largest percolation clusters for a path on the MST and we see that the average usage increases significantly and is also independent of $N$. However, the number of clusters used by a path on MST is relatively small and proportional to $\ln N$ [Sreenivasan *et al.*, 2004], suggesting that the path on the MST uses only few percolation clusters and few jumps between them (of order $\ln N$) when traveling from an entry node to an exit node on the network. When $N \to \infty$ the average usage of all percolation clusters should approach 1.

Can we use the above results to improve the transport in networks? It is clear that by improving the capacity or conductivity of the highest $C$ links one can improve the transport (see Fig. 28(b) inset). We hypothesize that improving the IIC links (strategy I), which represent the superhighways is more effective than improving the same number of links with the highest $C$ in the MST (strategy II), despite the higher centrality. To test the hypothesis, we study two transport problems: (i) current flow

in random resistor, networks, where each link of the network represents a resistor, and (ii) the maximum flow problem well known in computer science [Cormen *et al.*, 1990]. We assign to each link of the network a resistance/capacity, $e^{ax}$, where $x$ is an uniform random number between 0 and 1, with $a = 40$. The value of $a$ is chosen such as to have a broad distribution of disorder so that the MST carries most of the flow [Wu *et al.*, 2005; Sreenivasan *et al.*, 2004]. We randomly choose $n$ pairs of nodes as sources and other $n$ nodes as sinks and compute the flow between them. We compare the transport by improving the conductance/capacity of all links on the IIC (strategy I) by also improving the same number of links with the highest $C$ in the MST (strategy II). Since the two sets are not the same and therefore higher centrality links will be improved in II, it is tempting to suggest that the better strategy to improve the global flow is strategy II. However, here we demonstrate using ER networks as an example that counterintuitively strategy I is better. We also find similar advantage of strategy I compared to strategy II for SF networks with $\lambda = 3.5$.

In Fig. 28(b), we compute the ratio between the flow using strategy I ($F_{s\mathrm{I}}$) and the flow using strategy II ($F_{s\mathrm{II}}$) as a function of the factor of improving conductivity/capacity of the links. The figure clearly shows that strategy I is better than strategy II. Since the number of links in the IIC is relatively very small compared to the number of links in the whole network, it could prove to be a very efficient strategy.

In summary, we find that the centrality of the IIC for transport in networks is significantly larger than the centrality of the other nodes in the MST. Thus the IIC is a key component for transport in the MST. We demonstrate that improving the capacity/conductance of the links in the IIC is a useful strategy to improve transport.

## 10. Summary

We reviewed recent studies on the scaling of the average optimal path length $\ell_{\mathrm{opt}}$ in a disordered network. There are two scaling regimes of $\ell_{\mathrm{opt}}$ corresponding to the regimes of weak and strong disorder. For ER networks and SF networks with $\lambda > 4$, $\ell_{\mathrm{opt}} \sim \ln N$ in the weak disorder regime while $\ell_{\mathrm{opt}} \sim N^{1/3}$ in the strong disorder regime. For SF networks with $3 < \lambda < 4$, $\ell_{\mathrm{opt}} \sim \ln N$ in the weak disorder regime while $\ell_{\mathrm{opt}} \sim N^{\frac{\lambda-3}{\lambda-1}}$ in the strong disorder regime. For SF networks with $2 < \lambda < 3$, $\ell_{\mathrm{opt}} \sim \ln N$ in the weak disorder regime while $\ell_{\mathrm{opt}} \sim \ln^{\lambda-1} N$ in the strong disorder regime. The scaling behavior of $\ell_{\mathrm{opt}}$ in the strong disorder regime for ER and SF networks with $\lambda > 3$ is obtained analytically using percolation theory.[12] For exponential disorder, for both ER random networks and SF networks we obtain a scaling function for the crossover from weak disorder characteristics to strong disorder characteristics. We show that the crossover occurs when the min-max path reaches a crossover length $\ell^*(a)$ and $\ell^*(a) \sim a$. Equivalently, the crossover occurs when the network size $N$ reaches a crossover size $N^*(a)$, where $N^*(a) \sim a^3$ for ER networks and for SF networks with $\lambda \geq 4$ and $N^*(a) \sim a^{\frac{\lambda-1}{\lambda-3}}$ for SF networks with $3 < \lambda < 4$.

We have also shown that the optimal path length distribution in weighted random graphs has a universal scaling form according to Eq. (76). We explain this behavior and demonstrate the transition between polynomial to logarithmic behavior of the average optimal path in a single graph.

Our results are consistent with results found for finite dimensional systems [Porto *et al.*, 1999; Wu *et al.*, 2005; Strelniker *et al.*, 2005; Perlsman & Havlin, 2005]: In finite dimension the parameter controlling the transition is $L^{1/\nu}/ap_c$, where $L$ is the system length and $\nu$ is the correlation length critical exponent. This is because only the "red bonds" — bonds that when cut would disconnect the percolation cluster [Stanley, 1977; Coniglio, 1982] — control the transition.

We also show that any weighted random network hides an inherent scale-free "supernode network." We showed that the minimum spanning tree, generated by the bombing algorithm, is composed of percolation clusters connected by a scale-free tree of "gray" links. Most of the gray links connect small clusters to large ones, thus having weights well above the percolation threshold that do not change with the size of the network. Thus the optimization in the process of building the MST distinguishes between links with weights below and above the threshold, leading to a spontaneous emergence of a scale-free "supernode network" with $\lambda = 2.5$. We

[12]The results for SF networks with $2 < \lambda < 3$ have been obtained numerically and a theoretical explanation for these results is still pending.

raise the possibility that in some naturally optimal real-world networks, nodes connected well merge into one single node, and thus a scale-free network emerges.

The centrality in networks for transport on the MST is studied. We found that the centrality of the nodes in the IIC is significantly larger than the centrality of the other nodes in the MST. The analytical estimation for the exponents of the centrality distribution for both the MST and the IIC are provided. Thus the IIC is a key component for transport in the MST. As a result of this finding, we demonstrated that improving the capacity/conductance of the links in the IIC is a useful strategy to improve transport which is a better strategy compared to improving the same number of links with the highest centrality in the MST. This is probably due to the global nature of transport which prefer global improvement of the superhighways rather than local improvement of high centrality links.

## Acknowledgments

We thank ONR, Israel Science Foundation, European NEST project DYSONET, FONCyt (PICT-O 2004/370) and Israeli Center for Complexity Science for financial support.

## References

Albert, R. & Barabási, A.-L. [2002] "Statistical mechanics of complex networks," *Rev. Mod. Phys.* **74**, 47–97.

Ahuja, R. K., Magnanti, T. L. & Orlin, J. B. [1993] *Network Flows*: *Theory, Algorithms and Applications* (Prentice-Hall, Englewood Cliffs).

Barabási, A.-L. [1996] "Invasion percolation and global optimization," *Phys. Rev. Lett.* **76**, 3750–3753.

Barabási, A.-L. & Albert, R. [1999] "Emergence of scaling in random networks," *Science* **286**, 509–512.

Barabási, A.-L. [2002] *Linked*: *The New Science of Networks* (Perseus Publishing, Cambridge, MA).

Barrat, A. *et al.* [2004] "The architecture of complex weighted networks," *PNAS* **101**, 3747–3752.

Barthélémy, M. & Amaral, L. A. N. [1999] "Small-world networks: Evidence for a crossover picture," *Phys. Rev. Lett.* **82**, 3180–3183.

Boccaletti, S., Latora, V., Moreno, Y., Chavez, M. & Hwang, D.-U. [2006] "Complex networks: Structure and dynamics," *Phys. Rep.* **424**, 175–308.

Bollobas, B. [1985] *Random Graphs* (Academic, London).

Bonanno, G., Caldarelli, G., Lillo, F. & Mantegna, R. N. [2003] "Topology of correlation-based minimal spanning trees in real and model markets," *Phys. Rev. E* **68**, 046130-1–4.

Braunstein, L. A., Buldyrev, S. V., Havlin, S. & Stanley, H. E. [2001] "Universality classes for self-avoiding walks in a strongly disordered system," *Phys. Rev. E* **65**, 056128-1–6.

Braunstein, L. A., Buldyrev, S. V., Cohen, R., Havlin, S. & Stanley, H. E. [2003] "Optimal paths in disordered complex networks," *Phys. Rev. Lett.* **91**, 168701-1–4.

Braunstein, L. A., Buldyrev, S. V., Sreenivasan, S., Cohen, R., Havlin, S. & Stanley, H. E. [2004] "The optimal path in a random network," *Lecture Notes in Physics*: *Proc. 23rd CNLS Conf.*, "*Complex Networks*," *Santa Fe 2003*, eds. Ben-Naim, E., Frauenfelder, H. & Toroczkai, Z. (Springer, Berlin).

Buchanan, M. [2002] *Nexus*: *Small Worlds and the Groundbreaking Theory of Networks* (W. W. Norton, NY).

Buldyrev, S. V., Braunstein, L. A., Cohen, R., Havlin, S. & Stanley, H. E. [2003] "Length of optimal path in random networks with strong disorder," *Physica A* **330**, 246–252.

Buldyrev, S. V., Havlin, S. & Stanley, H. E. [2006] "Optimal paths in strong and weak disorder: A unified approach," *Phys. Rev. E* **73**, 036128-1–6.

Bunde, A. & Havlin, S. (eds.) [1996] *Fractals and Disordered Systems* (Springer, NY).

Callaway, D. S., Newman, M. E. J., Strogatz, S. H. & Watts, D. J. [2000] "Network robustness and fragility: Percolation on random graphs," *Phys. Rev. Lett.* **85**, 5468–5471.

Chen, Y. *et al.* [2006] "Universal behavior of optimal paths in weighted networks with general disorder," *Phys. Rev. Lett.* **96**, 068702-1–4.

Cieplak, M., Maritan, A. & Banavar, J. R. [1994] "Optimal paths and domain walls in the strong disorder limit," *Phys. Rev. Lett.* **72**, 2320–2323.

Cieplak, M., Maritan, A. & Banavar, J. R. [1996] "Invasion percolation and eden growth: Geometry and universality," *Phys. Rev. Lett.* **76**, 3754–3757.

Cohen, R., Erez, K., ben-Avraham, D. & Havlin, S. [2000] "Resilience of the Internet to random breakdowns," *Phys. Rev. Lett.* **85**, 4626–4628.

Cohen, R., ben-Avraham, D. & Havlin, S. [2002] "Percolation critical exponents in scale-free networks," *Phys. Rev. E* **66**, 036113-1–4.

Cohen, R., Havlin, S. & ben-Avraham, D. [2002] "Structural properties of scale free networks," in *Handbook of Graphs and Networks*, eds. Bornholdt, S. & Shuster, H. G. (Willey-VCH, NY), Chap. 4.

Cohen, R. & Havlin, S. [2003] "Scale free networks are ultrasmall," *Phys. Rev. Lett.* **90**, 058701-1–4.

Coniglio, A. [1982] "Cluster structure near the percolation threshold," *J. Phys. A* **15**, 3829–3844.

Cormen, T. H., Leiserson, C. E. & Rivest, R. L. [1990] *Introduction to Algorithms* (MIT Press, Cambridge, MA).

de Gennes, P.-G. [1979] *Scaling Concepts in Polymer Physics* (Cornell University Press, Ithaca).

Dobrin, R. & Duxbury, P. M. [2001] "Minimum spanning trees on random networks," *Phys. Rev. Lett.* **86**, 5076–5079.

Dorogovtsev, S. N. & Mendes, J. F. F. [2003] *Evolution of Networks: From Biological Nets to the Internet and WWW* (Oxford University Press, Oxford).

Erdős, P. & Rényi, A. [1959] "On random graphs," *Publ. Math.* **6**, 290–297.

Erdős, P. & Rényi, A. [1960] "On the evolution of random graphs," *Publ. Math. Inst. Hungarian Acad. Sci.* **5**, 17–61.

Fredman, M. L. & Tarjan, R. E. [1987] "Fibonacci heaps and their uses in improved network optimization algorithms," *J. ACM* **34**, 596–615.

Grassberger, P. & Zhang, Y. C. [1996] "Self-organized formulation of standard percolation phenomena," *Physica A* **224**, 169–179.

Goh, K.-I., Kahng, B. & Kim, D. [2001] "Universal behavior of load distribution in scale-free networks," *Phys. Rev. Lett.* **87**, 278701-1–4.

Goh, K.-I., Noh, J. D. Kahng, B. & Kim, D. [2005] "Load distribution in weighted complex networks," *Phys. Rev. E* **72**, 017102-1–4.

Hansen, A. & Kertész, J. [2004] "Phase diagram of optimal paths," *Phys. Rev. Lett.* **93**, 040601-1–4.

Harris, T. E. [1989] *The Theory of Branching Processes* (Dover Publication Inc., NY).

Havlin, S., Braunstein, L. A., Buldyrev, S. V., Cohen, R., Kalisky, T., Sreenivasan, S. & Stanley, H. E. [2005] "Optimal paths in random networks with disorder: A mini review," *Physica A* **346**, 82–92.

Ioselevich, A. S. & Lyubshin, D. S. [2004] "Phase transition in a self-repairing random network," *JETP Lett.* **79**, 231–235.

Kalisky, T., Braunstein, L. A., Buldyrev, S. V., Havlin, S. & Stanley, H. E. [2005] "Scaling of optimal-path-lengths distribution in complex networks," *Phys. Rev. E* **72**, 025102-1–4(R).

Kalisky, T. & Cohen, R. [2006] "Width of percolation transition in complex networks," *Phys. Rev. E* **73**, 035101-1–4(R).

Kalisky, T., Sreenivasan, S., Braunstein, L. A., Havlin, S. & Stanley, H. E. [2006] "Scale-free networks emerging from weighted random graphs," *Phys. Rev. E* **73**, 025103-1–4(R).

Khan, M., Pandurangan, G. & Bhargava, B. [2003] "Energy-efficient routing schemes for sensor networks," Tech. Rep. CSD TR 03-013, Dept. of Computer Science, Purdue University.

Kim, D.-H., Noh, J. D. & Jeong, H. [2004] "Scale-free trees: The skeletons of complex networks," *Phys. Rev. E* **70**, 046126-1–5.

Kruskal, J. B. [1956] "On the shortest spanning subtree and the traveling salesman problem," *Proc. Amer. Math. Soc.* **7**, 48–50.

Macdonald, P. J., Almaas, E. & Barabási, A.-L. [2005] "Minimum spanning trees of weighted scale-free networks," *Europhys. Lett.* **72**, 308–314.

Mendes, J. F. F., Dorogovtsev, S. N. & Ioffe, A. F. [2003] *Evolution of Networks: From Biological Nets to the Internet and the WWW* (Oxford University Press, Oxford).

Molloy, M. & Reed, B. [1995] "A critical-point for random graphs with a given degree sequence," *Rand. Struct. Algorith.* **6**, 161–179.

Molloy, M. & Reed, B. [1998] "The size of the giant component of a random graph with a given degree sequence ," *Combin. Probab. Comput.* **7**, 295–305.

Newman, M. E. J. [2001a] "Scientific collaboration networks. I. Network construction and fundamental results," *Phys. Rev. E* **64**, 016131-1–8.

Newman, M. E. J. [2001b] "Scientific collaboration networks. II. Shortest paths, weighted networks, and centrality," *Phys. Rev. E* **64**, 016132-1–7.

Onnela, J.-P. *et al.* [2003] "Dynamics of market correlations: Taxonomy and portfolio analysis," *Phys. Rev. E* **68**, 056110-1–12.

Pastor-Satorras, R. & Vespignani, A. [2004] *Structure and Evolution of the Internet: A Statistical Physics Approach* (Cambridge University Press, Cambridge).

Perlsman, E. & Havlin, S. [2005] "Directed polymer — directed percolation transition: The strong disorder case," *Eur. Phys. J. B* **43**, 517–520.

Perlsman, E. & Havlin, S. [2006] "Optimal paths as correlated random walks," *Europhys. Lett.* **73**, 178–182.

Porto, M., Havlin, S., Schwarzer, S. & Bunde, A. [1997] "Optimal path in strong disorder and shortest path in invasion percolation with trapping," *Phys. Rev. Lett.* **79**, 4060–4062.

Porto, M., Schwartz, N., Havlin, S. & Bunde, A. [1999] "Optimal paths in disordered media: Scaling of the crossover from self-similar to self-affine behavior," *Phys. Rev. E* **60**, R2448–R2451.

Rao, A. & Caflisch, F. [2004] "The protein folding network," *J. Mol. Biol.* **342**, 299–306.

Skiena, S. [1990] *Implementing Discrete Mathematics: Combinatorics and Graph Theory With Mathematica* (Addison-Wesley, NY).

Smailer, I., Machta, J. & Redner, S. [1993] "Exact enumeration of self-avoiding walks on lattices with random site energies," *Phys. Rev. E* **47**, 262–266.

Sreenivasan, S., Kalisky, T., Braunstein, L. A., Buldyrev, S. V., Havlin, S. & Stanley, H. E. [2004] "Effect of disorder strength on optimal paths in complex networks," *Phys. Rev. E* **70**, 046133-1–6.

Sreenivasan, S., Kalisky, T., Braunstein, L. A., Buldyrev, S. V., Havlin, S. & Stanley, H. E. [2005] "Transition between strong and weak disorder regimes on the optimal path," *Physica A* **346**, 174–182.

Stanley, H. E. [1977] "Cluster shapes at the percolation threshold: An effective cluster dimensionality and its

connection with critical-point exponents," *J. Phys. A* **10**, L211–L220.

Stauffer, D. & Aharony, A. [1994] *Introduction to Percolation Theory* (Taylor & Francis, London).

Strelniker, Y. M. *et al.* [2004] "Percolation transition in a two-dimensional system of Ni granular ferromagnets," *Phys. Rev. E* **69**, 065105-1–4(R).

Strelniker, Y. M., Havlin, S., Berkovits, R. & Frydman, A. [2005] "Resistance distribution in the hopping percolation model," *Phys. Rev. E* **72**, 016121-1–5.

Szabó, G. J., Alava, M. & Kertész, J. [2003] "Geometry of minimum spanning trees on scale-free networks," *Physica A* **330**, 31–36.

van der Hofstad, R., Hooghienstra, G. & van Mieghem, P. [2001] "First passage percolation on the random graph," *Prob. Eng. Inf. Sci.* **15**, 225–237.

Watts, D. J. [2003] *Six Degrees*: *The Science of a Connected Age* (W. W. Norton, NY).

Wu, Z. *et al.* [2005] "Current flow in random resistor networks: The role of percolation in weak and strong disorder," *Phys. Rev. E* **71**, 045101-1–4(R).

Wu, Z., Braunstein, L. A., Havlin, S. & Stanley, H. E. [2006] "Transport in weighted networks: Partition into superhighways and roads," *Phys. Rev. Lett.* **96**, 148702-1–4.